Role of Sodium Chloride in Low Temperature Hot Corrosion of Superalloys

by

Shaik Palur Akbar Hussain

A Thesis Presented to the

FACULTY OF THE COLLEGE OF GRADUATE STUDIES

KING FAHD UNIVERSITY OF PETROLEUM & MINERALS

DHAHRAN, SAUDI ARABIA

In Partial Fulfillment of the
Requirements for the Degree of

MASTER OF SCIENCE

In

MECHANICAL ENGINEERING

June, 1997

INFORMATION TO USERS

This manuscript has been reproduced from the microfilm master. UMI films the text directly from the original or copy submitted. Thus, some thesis and dissertation copies are in typewriter face, while others may be from any type of computer printer.

The quality of this reproduction is dependent upon the quality of the copy submitted. Broken or indistinct print, colored or poor quality illustrations and photographs, print bleedthrough, substandard margins, and improper alignment can adversely affect reproduction.

In the unlikely event that the author did not send UMI a complete manuscript and there are missing pages, these will be noted. Also, if unauthorized copyright material had to be removed, a note will indicate the deletion.

Oversize materials (e.g., maps, drawings, charts) are reproduced by sectioning the original, beginning at the upper left-hand corner and continuing from left to right in equal sections with small overlaps. Each original is also photographed in one exposure and is included in reduced form at the back of the book.

Photographs included in the original manuscript have been reproduced xerographically in this copy. Higher quality 6" x 9" black and white photographic prints are available for any photographs or illustrations appearing in this copy for an additional charge. Contact UMI directly to order.

UMI

A Bell & Howell Information Company
300 North Zeeb Road, Ann Arbor MI 48106-1346 USA
313/761-4700 800/521-0600

ROLE OF SODIUM CHLORIDE IN LOW TEMPERATURE HOT CORROSION OF SUPERALLOYS

BY

SHAIK PALUR AKBAR HUSSAIN

A Thesis Presented to the

FACULTY OF THE COLLEGE OF GRADUATE STUDIES

KING FAHD UNIVERSITY OF PETROLEUM & MINERALS

DHAHRAN, SAUDI ARABIA

In Partial Fulfillment of the
Requirements for the Degree of

MASTER OF SCIENCE

In

MECHANICAL ENGINEERING

JUNE 1997

KING FAHD UNIVERSITY OF PETROLEUM AND MINERALS
DHAHRAN, SAUDI ARABIA

COLLEGE OF GRADUATE STUDIES

This thesis, written by

Shaik Palur Akbar Hussain

under the direction of his Thesis Advisor and approved by his Thesis Committee, has been presented to and accepted by the Dean of the College of Graduate Studies, in partial fulfillment of the requirements for the degree of **MASTER OF SCIENCE** in **MECHANICAL ENGINEERING.**

THESIS COMMITTEE

Dr. Ibrahim M. Allam (Chairman)

Dr. Zafarullah Khan (Co – Chairman)

Dr. Abdulghani A. Al Farayedhi (Member)

Dr. Zaki Ahmed (Member)

Dr. Mohammed O. Budair
(Department Chairman)

Dr. Abdallah M. Al – Shehri
(Dean, College of Graduate Studies)

5-7 97
Date

Dedicated to

My

PARENTS

and

FAMILY MEMBERS

whose love, patience and perseverance

led me to this accomplishment.

Acknowledgments

First of all I thank Almighty **ALLAH (SWT)**, the only **LORD** and **CREATOR** for His Eternal Blessings and Guidance.

I am extremely thankful and deeply indebted to my thesis advisor and committee chariman, Dr. Ibrahim M. Allam, for his guidance and advice. I acknowledge him for his efforts, constant encouragement, support, concern, patience, guidence and valuable time during all stages of this work and above all having complete faith in me. I wish to express my sincere appreciation and gratitude to my thesis committee co-chairman Dr. Zafarullah Khan and committee members Dr. Abdulgani A. Al Farayedhi, who provided facilities in heat engine lab and Dr. Zaki Ahmed for their interest, constructive criticism and personal understanding. I acknowledge them for their useful and valuable comments and suggestions.

Acknowledgements are due King Fahd University of Petroleum and Minerals and particularly Dr. Mohammed O. Budair, chairman, Mechanical Engineering Department, for providing me all the facilities and requirements for achieving my masters degree.

My appreciations are also due to Mr. Karam and Mr. Yunus, fitting shop, who helped me lot during my experimental work. I am also thankful to Mr. B.J. Aleem

and Mr. Latif and Mr. Riaz Ahmed for their extreme help in SEM analysis and Metallography.

I am also thankful to RI officials (KFUPM), Mr. Rasheed, Mr. Sridhar, Mr. Januoa, Dr. John shirkoff and Dr. Mohammad for their help and support during micro-analytical analysis.

I am also thankful to other faculty members and secretaries of the department, Mr. Jameel, Mr. Abdul Latif and Mr. Thomas for their co-operation and help during my stay.

I also express thanks to my friends Ilias, Yunus (elect), Sadath, Razzaq, Aizaz, Nehru Chowdary, Murali, Karnaker, Murali krishna, Khalid, Kareem, Samad, Mukarram, Adeeb, Tareeq, Kaleem, Haleem, Aleem and Imran for standing by me at all times and for making my stay at KFUPM a memorable one. A word of appreciation is also due to my friends and all Research Assistants whose moral support and patronage provided an impetus for the completion of this work.

Finally, I am very grateful to my Parents, Uncle, Aunt, Sister, Brothers and other family members for their sacrifices, constant support, patience, love and prayers.

Contents

List of Figures

List of Tables

Abstract

Name: Shaik Palur Akbar Hussain

Title: Role of Sodium chloride in Low Temperature Hot Corrosion of Superalloys

Major Field: Mechanical Engineering

Date of Degree: June, 1997.

In this thesis, the influence of $NaCl$ on hot corrosion behaviour of IN 738 and Mar-M 509 at 750° C in static air, under thermal cyclic conditions has been studied. Salt-coating technique was employed, in which alloy samples were coated with approx. 2.5 mg/cm^2 of salt. Hot corroded samples of IN 738 and Mar-M 509 have been analysed using SEM, Point EDS, X-ray mapping, ESCA and XRD techniques and correlated with corrosion kinetics. The results indicated that Na_2SO_4+25%$NaCl$ was very aggressive compared to that of either pure Na_2SO_4 or $Na_2SO_4 + 1\%NaCl$. All samples exhibited enhanced internal sulfidation in the presence of sulfate/chloride salt mixture. It has been concluded that continuous replenishment of Na_2SO_4 + 25%$NaCl$ mixture on both Ni-base and Co-base alloys resulted in a typical LTHC morphological features during the propagation stage. Basic fluxing model has been proposed for low temperature hot corrosion of IN 738 in Na_2SO_4+25%$NaCl$ mixture during the propagation stage. The intiation and propagation stage of Mar-M 509 is attributed to the attack along W-rich phase and sulfidation/oxidation of Cr. The role of NaCl on hot corrosion behaviour of IN 738 and Mar-M 509 has been discussed in the light of the above experimental study.

Master of Science Degree

King Fahd University of Petroleum and Minerals

Dhahran, Saudi Arabia

June, 1997.

ملخص الرسالة

الاســـم : شيخ بالور أكبر حسين

العنوان : دور كلوريد الصوديوم في التآكل الساخن عند درجات الحراره المنخفضه للسبائك القويه .

التخصص الرئيسي : الهندسه الميكانيكيه

تـاريــخ الدرجـــه : يونيو ١٩٩٧ م

في هذه الرساله تم دراسة تأثير كلوريد الصوديوم على التآكل الساخن لسبيكتى أ ى ن ٧٣٨ IN 738 و مار ٢-٩٠٥٠ Mar-M 509 عند درجة حراره ٧٥٠ درجه مئويه في الهواء الساكن . وتحت تاثير حالات دوريه . وتم تطبيق تقنيه التقطيه بالملح حيث تمت تقنيه عينات من السبائك بحوالي ٢ر٥ ملجرام لكل سنتمتر مربع من الملح . وتم تحليل العينات المتآكله على الساخن باستخدام SEM نقطة ، واشعة اكس وكذلك تقني على ESCAصور الأشعه السينيه XRD . وقد أوضحت النتائج ان Na2SO4 مع ٢٥٪ من كلوريد الصوديوم أكثر شدة من Na2SO4 النفى أو Na2SO4 مع ١٪ من كلوريد الصوديوم . وقد لوحظ تحسن في التصلد الداخلي بجميع العينات في وجود خليط من كبريتات وكلوريد الصوديوم . وقد استخلص من الرساله أن التزويد المستمر لـ Na2SO4 مع ٢٥٪ من كلوريد الصوديوم لكل من السبائك المعتمده على النيكل والكوبلت يؤدي الى خصائص تشكل معين اثناء مرحلة الانتشاء . وقد تم اقتراح نموذج اساسى حتّى للتآكل الساخن عند درجات حراره منخفضه لسبيكه أ ى ن ٧٣٨ IN 738 من مخلوط من كبريتات الصوديوم Na2SO4مع ٢٥٪ كلوريد صوديوم وقد استخلص ايضا أن مرحلتى البدايه والانتشاء لسبيكة و Mar-M 509 هما نتيجة لتعرضه اثناء مرحلة W-rich وكذلك تصلب اكسدة الكروم . وقد نوقش دور كلوريد الصوديوم على سلوك السبيكتين المذكورتين في حالة التآكل الساخن على ضوء الدراسه المعمليه المذكوره .

درجة الماجستير في العلوم

جامعة الملك فهد للبترول والمعادن

الظهران - المملكه العربيه السعوديه

يونيو ١٩٩٧ م

Chapter 1

Introduction

In a general sense, hot corrosion has been defined as the degradation of materials caused by the presence of a deposit or ash. In a more restrictive sense, hot corrosion is the degradation of a metal and/or an alloy owing to the oxidation processes which are affected by liquid salt deposits, predominantly Na_2SO_4. The primary source of sodium sulfate, in marine and aircraft engines, is due to the reaction between $NaCl$ in ingested air and sulfur in fuel according to the following reactions:

$$2NaCl + SO_2 + \frac{1}{2}O_2 + H_2O \rightarrow Na_2SO_4 + 2HCl \tag{1.1}$$

$$2NaCl + SO_3 + H_2O \rightarrow Na_2SO_4 + 2HCl \tag{1.2}$$

It is assumed that the sulfation of sodium chloride may take place in the hot section of a gas turbine according to equation (1.1) or (1.2) and then a thin liquid sulfate film may be deposited on the hot components either by condensation or by direct

impingement of liquid droplets from the hot gas stream. The main components that are subjected to severe attack by the salt deposit are the turbine blades and vanes (Figure 1.1).

Historically, the first incidence of hot corrosion was reported in an aero-type engine installed in a patrol boat in 1959 [2] although similar type of attack was reported in boiler tubes during 1940's [3]. However, turbine manufacturers and users became aware of hot corrosion in late 1960's, when severe corrosion attack occurred during vietnam war. At that time several investigators [4] to [9], [11] have conducted experimental as well as field tests to identify the nature of attack and explained its temperature dependence and the corresponding morphologies.

Depending on the melting point of the salt deposit (which can be either solid or liquid), the hot corrosion phenomena has been divided into two categories. One is high temperature hot corrosion i.e., "type I hot corrosion", that occurs usually above the m.p of Na_2SO_4 ($884°C$) where the salt is clearly a liquid. The other is low temperature hot corrosion i.e., "type II hot corrosion", which occurs below the m.p of Na_2SO_4 and where the salt is solid.

Hot corrosion process, generally, involves two distinct stages of metal attack. An initiation stage, during which the attack is not too severe and involves the formation of a more protective oxide scale, and a propagation stage where a less protective oxide layer is formed. The duration of the initial incubation period depends on several parameters [16], such as thermal cycling, salt composition, salt amount and

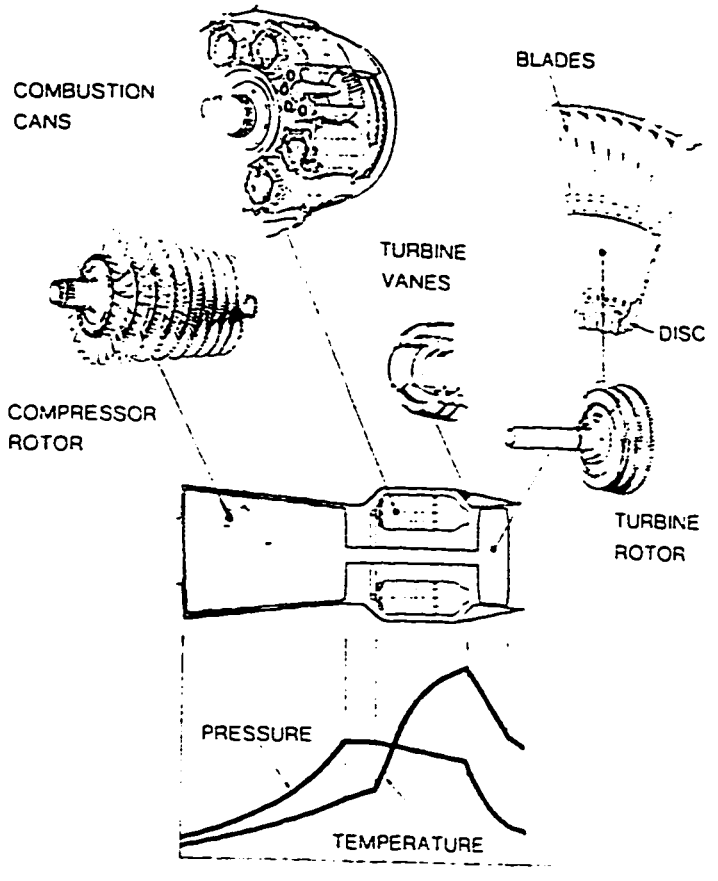

Figure 1.1: Hot section of a gas turbine engine with relative temperature and pressure profiles [1]

deposition rate. alloy chemistry, gas composition and gas velocity, as illustrated in Figure 1.2. Generally, the increase in salt amount ($1mg/cm^2$ to $5\ mg/cm^2$) increases the hot corrosion attack. The effect of Mo in $Ni-$ base alloys is detrimental because the Na_2SO_4 on the alloy surface becomes acidified due to the formation of sodium molybdate, which can flux Al_2O_3. The presence of SO_3 in the gas environment at lower temperatures leads to low temperature form of hot corrosion in $CoCrAlY$ coatings and the effect of thermal cycling or $NaCl$ is to reduce the incubation period.

Several mechanism have been put forward to explain the propagation stage in type I hot corrosion. Most notable of these mechanisms is the "salt-fluxing model" [6], [8] to [12]. In this model the destruction of the protective oxide scale occurs either by dissolution in a basic salt as an anion (basic fluxing) or the dissolution in an acidified Na_2SO_4 (low Na_2O activity) as a cation (acidic fluxing). Other mechanisms include:

1. Breakdown of protective oxide scale due to accelerated oxidation of $Ni - Ni_3S_2$ eutectic melt (m.p is $645°C$) [4].

2. Oxidation of the $Cr-$ depleted alloy followed by preferential internal sulfidation of Cr may render oxide scale non-protective (sulfidation-oxidation) [5].

3. The impacting particles of $NaCl$ may reach pre-existing Na_2SO_4 deposit and form volatile metal chlorides, creating local reducing conditions. These conditions may reduce oxide scale adhesion and incorporate sulfur to render oxide scale non-protective [9].

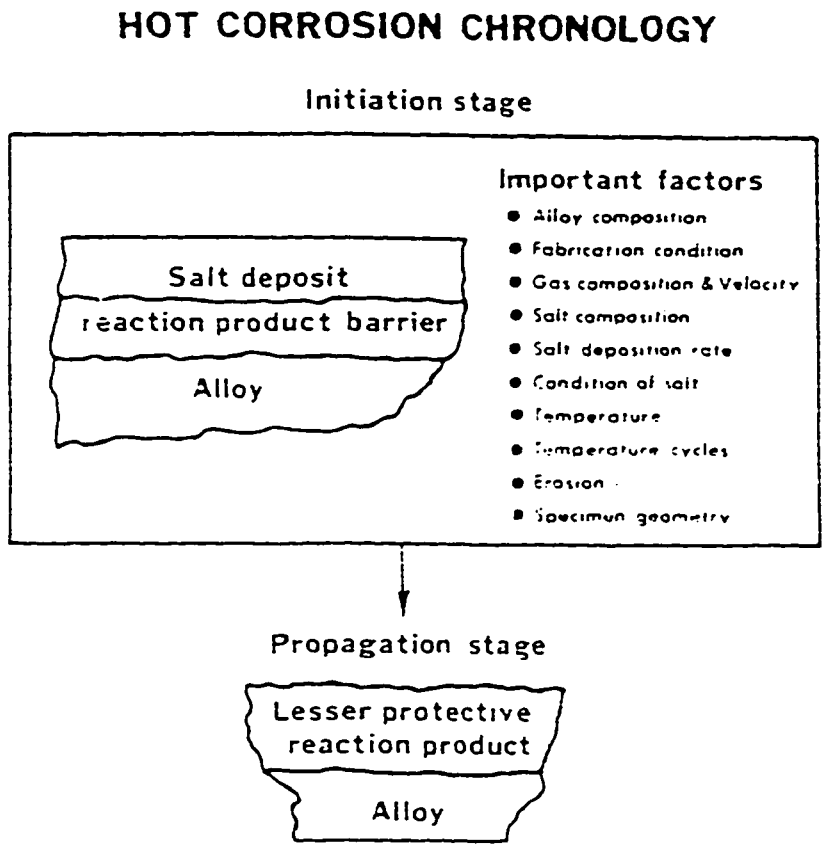

Figure 1.2: Schematic diagram showing the initiation and propagation stage of hot corrosion [16]

Type II hot corrosion (Low Temperature Hot Corrosion, LTHC) usually occurs in marine gas turbines, which tend to operate at somewhat low temperatures (600 – 800°C) and involves higher levels of sea-salt contamination. The initiation stage in LTHC is related to the formation of low-melting eutectic sulfates [17]-[21] on the alloy or coating surfaces. The formation of eutectic melts of Na_2SO_4 with $NiSO_4$ or $CoSO_4$ or iron sulfate is attributed to the oxidation of Ni or Co or Fe in the alloy and a subsequent sulfation reaction of oxide with SO_3 in the atmosphere. For example, in $Co-$ base alloys or coatings, cobalt oxide dissolution and its sulfation as $CoSO_4$ are the major processes at initial stages [17]. Once the liquid phase is stabilized and saturated with the salt, further corrosion occurs by counter transport of Co^{2+}/Co^{3+} ions to the salt/gas interface and precipitation of Co_3O_4 and/or $CoSO_4$ at salt-gas interface, depending on P_{SO_3} and temperature [17]. This process prevents the development of protective Cr_2O_3 and/or Al_2O_3 by formation of shallow pits in the alloy. It has been demonstrated that the presence of SO_3 is imperative [17]-[21] for the beginning and subsequent development of LTHC type of attack.

Several other mechanism have been proposed for the propagation of LTHC in $Ni-$ and $Co-$ base alloys. These include decomposition of molten salts [19] and sulfidation-oxidation [20], reduction of sulfate or sulfate dissociation mechanism [20] and formation of duplex scale ($NiO + Ni_3S_2$) above the scale/metal interface [21].

1.1 Outline of the Problem

It is very well established that sodium sulfate alone causes accelerated oxidation of superalloys and coatings at high temperatures, where Na_2SO_4 ($m.p = 884°C$) is in the liquid form. Many researchers [4]-[8] have studied the mechanism of Na_2SO_4-induced hot corrosion at high temperatures (type I hot corrosion) for $Ni-$ base and $Co-$ base alloys. In high temperature regime, the attack results in destruction of protective oxide scale by scale exfoliation or oxide dissolution and precipitation reaction in the salt film. This is usually accompanied by depletion of the alloy substrate from key elements for protection, typically aluminum (in Al_2O_3 formers) and chromium (in Cr_2O_3 formers) .

In marine environments, where low power operation maintains the alloys at relatively lower temperature (below m.p of Na_2SO_4), the predominant form of attack of first stage blades and vanes of gas turbines is due to type II hot corrosion. The surfaces of most cobalt base superalloy and coatings suffer a non-uniform form attack which manifested the formation of shallow pits, accompanied by the presence of a thin layer of sulfide at the attack front with little or no depletion of Al or Cr in the substrate and formation of Co-rich mound at the salt/gas interface.

Since marine and industrial turbines which are often situated near the coastal regions operate most of the time at part load conditions, and at lower blade temperatures there is likelihood for the deposition and longer survival of $NaCl$ on first

stage blades . Conde [9] has shown that the short residence of combustion gases (5 milli seconds) in the turbine may not convert $NaCl$ completely to sodium sulfate at low blade temperatures. Hence, the primary question that arises is, "whether SO_3 alone is responsible for LTHC type of attack or other species, such as $NaCl$ play a significant role ?". Earlier work [13]-[18], especially by Luthra and Shores [18] reports that the characteristic morphology of LTHC is reproduced only when sufficient SO_3 is employed in an oxydising environment. During the service operation of gas turbine engines, the equilibrium partial pressure between SO_3 and SO_2 is never achieved. The exhaust gas streams in the turbines show equilibrium SO_3/SO_2 ratios only about 0.1 despite their high air-to-fuel ratios, whereas 3.08 is required for the occurance of LTHC [19] in laboratory studies. Jones [19] showed that the catalytic activity of CoO or decomposition reaction of mixed sulfates may increase the P_{SO_3} near the salt-metal interface, which is considered to be important for the occurance of low temperature hot corrosion.

Several investigators [23]-[32] have studied the primary role of $NaCl$ on hot corrosion behavior of $Ni-$ and $Co-$ base alloys and attributed the failure mode of protective scales to the formation of volatile metal chlorides and/or oxychlorides. Barkalow and Pettit [28] indicated that the severe attack of $CoCrAlY$ coatings under LTHC environment may not be attributed exclusively due to $NaCl$. Mckee et al [45] attributed the degradation of Al_2O_3 forming alloy to the release of chlorine gas at initial stages and formation of metal chlorides and salt eutectics during propagation

stages. Later, Conde [29] and Hancock [31] proposed that the decomposition of $NaCl + Na_2SO_4$ under non-equilibrium conditions, such as high gas velocities or thermal cycling may be an important source of high SO_3 and localized attack in LTHC should be related to either erosion of blade surfaces caused by salt particles or chloride attack rather than SO_3. Recently, Nichollis and Stephenson [32] showed that $NaCl$ on previously damaged samples of IN 738 at low temperatures initiated pitting type of attack.

Although it is well established that SO_3 is the principal pre-requisite for the occurance of LTHC in coatings or alloys [17], the role played by the $NaCl$ in LTHC is not well established. Inspite of the extensive research efforts in low temperature hot corrosion, there is very limited number of studies relating the role of $NaCl$ to LTHC behavior of $Ni-$ and $Co-$ base alloys.

The present study concerns the understanding of the effects of $NaCl$ on low temperature hot corrosion behavior of IN 738 and Mar-M 509 under thermal cyclic conditions. It is essential to consider thermal cycling near actual turbine conditions where blades and vanes may be subjected to thermal stresses, generated by temperature cycling or intermittent blade cooling . These conditions may yield a localized attack of a cooled rotor blade near the mid-chord region where the temperature represent that is required for the occurance of type II attack (Figure 1.3). Further, this study has a practical value in the region of Saudi Arabia as most industries utilizing gas turbines for power generation are situated near the coastal regions.

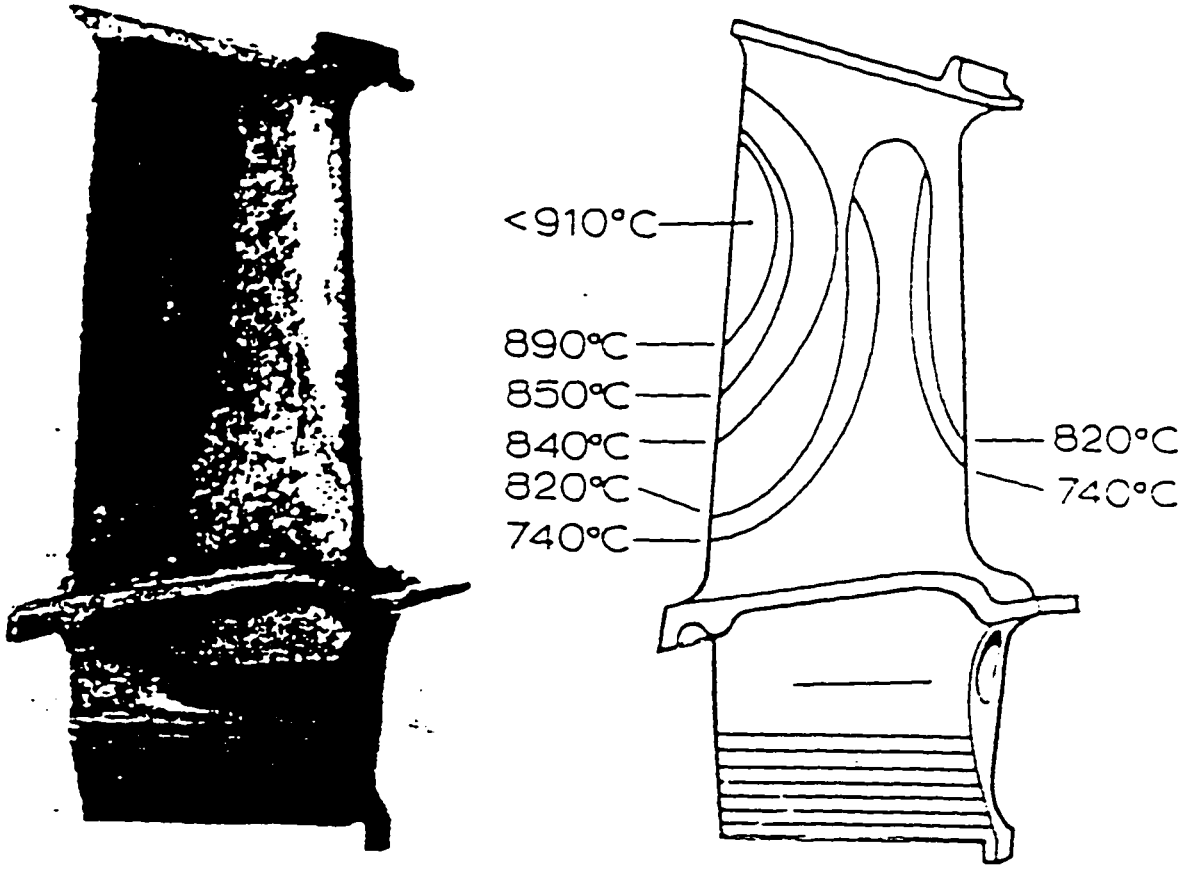

Figure 1.3: Corrosion of pressure surface of cooled HP (high pressure) rotor blade compared with temperature contours [52]

In addition to this, military planes, helicopters and rescue planes operating near coastal areas may be contaminated with chloride and sulfates.

In the next chapter, the literature related to the present study is briefly reviewed and discussed. The experimental setup, procedures and test techniques are presented in Chapter 3. The results of this investigation are then presented and discussed in Chapter 4. Finally, Chapter 5 presents conclusions and recommendations for future work.

Chapter 2

Literature Review

This chapter provides a review and a summary of the literature relevant to the present study.

In the first section, the mechanisms related to the high temperature hot corrosion are briefly described although an excellent summary of work upto 1970 [50] has been presented and then critically reviewed the work upto 1987 [49] by Stringer. Later, a detailed review of work related to low temperature hot corrosion has been presented. The literature on both types of hot corrosion also outlines the effect of $NaCl$ and other mixed sulfates on hot corrosion behavior of $Ni-$ and $Co-$ base alloys. Finally, previous studies addressing the role of $NaCl$ in low temperature hot corrosion has been reviewed.

2.1 High Temperature Hot Corrosion

High temperature hot corrosion (type I hot corrosion) is the form of hot corrosion that usually occurs above the melting point of sodium sulfate (884°C), where the salt is clearly a liquid.

The first technical publication on hot corrosion was contributed by Simons et al [4], who outlined a reaction mechanism involving metal sulfidation by Na_2SO_4, with emphasis on the accelerated oxidation of a sulfide-base eutectic ($Ni - Ni_3S_2$). Seybolt [5] emphasized the importance of chromium sulfide formation in Na_2SO_4 corrosion at high temperatures by illustrating the formation of similar phases for $Ni-$ base alloys reacted in H_2/H_2S gases and then showed that accelerated oxidation also occurs for an alloy depleted in chromium. This mechanism is now well known as sulfidation-oxidation model. Bronstein and Decresente [6] demonstrated that the degradation of an alloy at high temperatures does not depend on sulfidation/oxidation mechanism, but rather on dissolution of the normally protective oxide (Cr_2O_3/Al_2O_3). Specifically, the investigators showed that pre-sulfidizing three different superalloys ($B-1900$, Udimet 700 , and Waspalloy) at 900°C did not accelerate the attack during subsequent oxidation. However, thin coatings of Na_2CO_3 and $NaNO_3$ on the alloys produced hot corrosion kinetics similar to Na_2SO_4. From this, the researchers concluded that the formation of sulfides in hot corrosion is only incidental and did not play an important part in the reaction.

Geobel and Pettit [8] studied the hot corrosion of Ni and $Ni-$ base alloys beneath a fused Na_2SO_4 film at 1000°C and provided a semi-quantitative mechanism for the degradation of pure Ni. The authors concluded that the NiO formation increases the sulfur activity in molten sulfate and allows sulfur into the substrate to form nickel sulfide (if a pore or crevice is present during the growth of oxide). As the sulfur is removed from the salt, the local bascity increases to such an extent that reaction of salt with protective scale produces a basic solute (probably sodium nickelate), which may either precipitate within the salt or migrate to the salt-gas interface. The mechanism by which sulfur diffuses into the alloy has not been explained. Goebel et al [10] extended the fluxing theory to explain the acidic fluxing of protective scales in Cr_2O_3 and Al_2O_3 forming alloys which contain Mo, W and V. Figure 2.1b shows that Al_2O_3 can be fluxed as cationic species if the salt attached to the metal surface is acidified by refractory metal oxides, such as MoO_3, WO_3 and V_2O_5. It has been concluded that the acidic fluxing of alloys is self-sustaining as the refractory metal oxide is continuously produced rather than the basic fluxing of protective scale. Figure 2.2a shows a schematic diagram of fluxing model of hot corrosion at high temperatures [10]. For example, consider the $Ni - Al$ alloy for explaining the basic fluxing of Al_2O_3. Initially, the sulfur activity in the Na_2SO_4 is not sufficient to cause the reaction between the alloy and sodium sulfate to form sulfides in the substrate (see Figure 2.1a). A continuous layer of Al_2O_3 forms on the alloy surface by using the oxygen present in the salt. This increases the

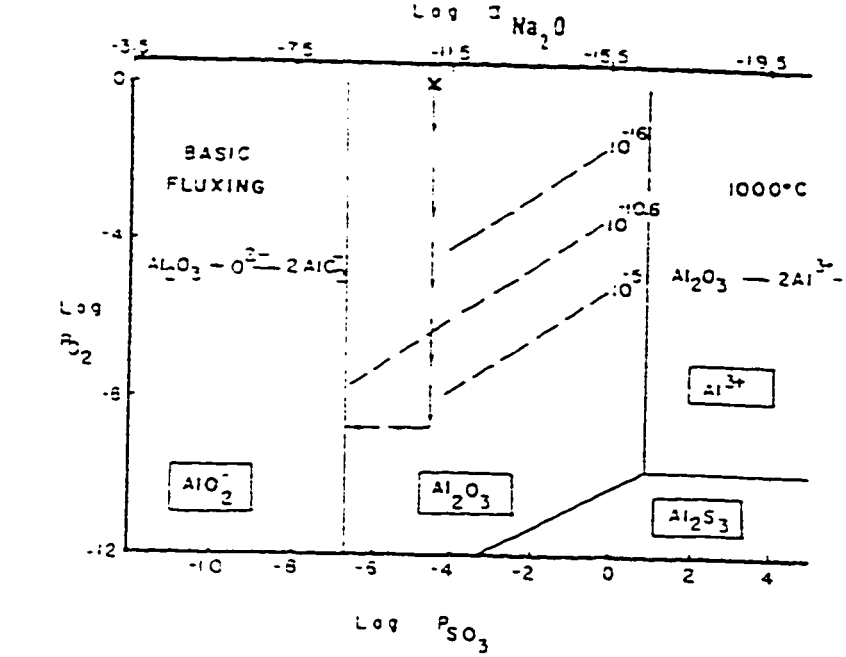

(a)

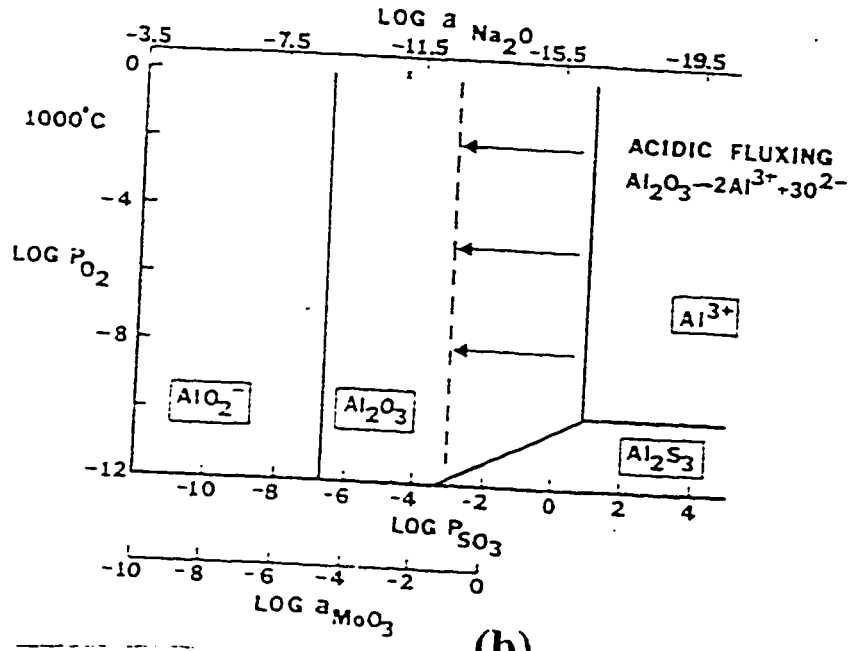

(b)

Figure 2.1: Stability diagram showing (a) the phases of aluminum that are stable in Na_2SO_4 (b) phases of Al that are stable in acidified salt at 1000°C [10]

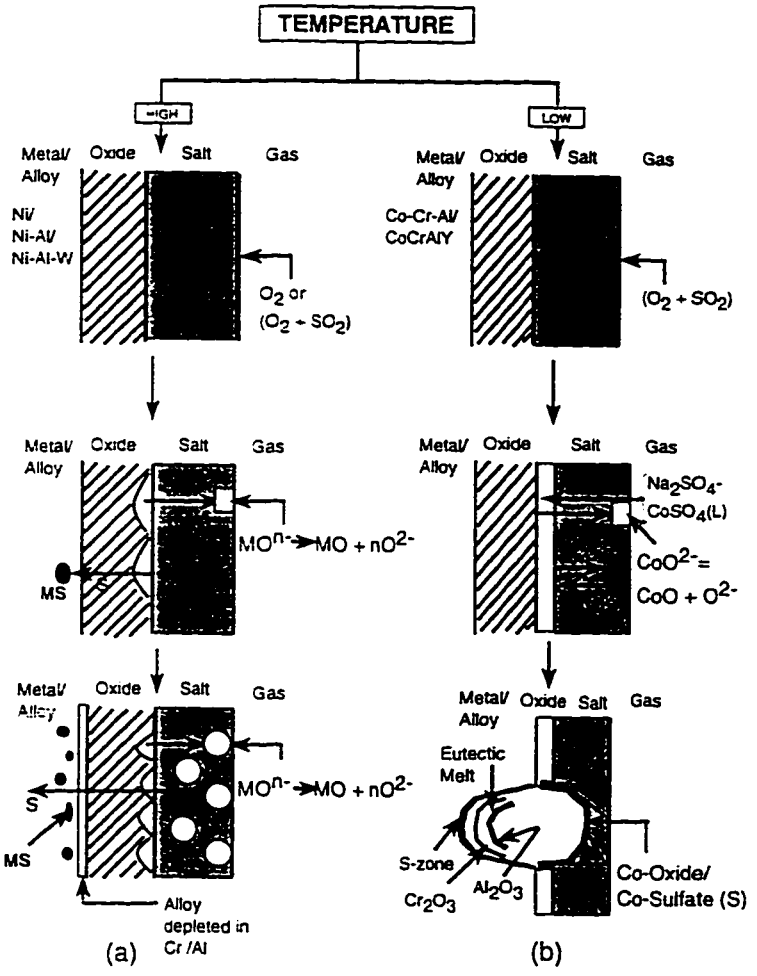

Figure 2.2: Schematic diagram to illustrate the mechanism of hot corrosion in (a) high temperature as well as (b) low temperature regimes.

sulfur activity in the salt as shown by the downward movement of the arrow in Figure 2.1a. The sulfur activity increases to such an extent that the sulfides of aluminum are formed as particles in the metal substrate. Due to the formation of sulfides of aluminum in the substrate, the key element (Al) for protecting the alloy surface gets depleted in the alloy. Once the sulfur is removed from the salt, the oxygen activity in the salt increases (as shown by the left horizontal arrow in Figure 2.1a), the local bascity of salt increases to such an extent that Al_2O_3 dissolves in the basic salt at the oxide/salt interface and get reprecipitated at the salt/gas interface, where the salt is nearly stoichiometric. This reaction continues until the sodium sulfate remains on the alloy surface and increases the rate of hot corrosion due to fluxing of protective oxide scale.

Rapp and Goto [12] proposed a more generalized fluxing model for the hot corrosion of superalloys, which demonstrates that a negative solubility gradient of oxide at scale-salt interface is required for a dissolution and precipitation sequence. They have shown that the reduction of oxygen or pyrosulfate ion ($S_2O_7^{2-}$) creates a high basic condition near the scale/salt interface and generate oxide ions as reaction products.

Johnson et al [25] studied the effect of $NaCl$ on Na_2SO_4-induced hot corrosion of $Co - 25w/oCr - 7.5w/oW$ alloy at 900°C. The accelerated oxidation in salt mixtures was related to scale cracking and internal sulfidation of the alloy. It has been concluded that morphological features didn't show acidic fluxing features of

Cr_2O_3 and the mechanism by which sulfur penetrates into the alloy is not clear. Stringer et al [26] proposed similar mechanism as suggested by Johnson et al [25] for the hot corrosion of Mo, Al, and Ta containing $Co-Cr$ alloys in sulfate/chloride mixtures at $900°C$ in O_2 alone. The authors depicted the principal role of $NaCl$ as to promote internal sulfidation by cracking of protective scales either by metal chloride formation or thermal cycling. The detection of Cr^{3+} ions and release of Cl_2 gas was considered as evidence for the breakdown of $NaCl$.

In summary, high temperature hot corrosion mechanisms include mainly the fluxing of protective oxide scale in $Ni-$ and $Co-$ base alloys containing high Cr and/or Al. The acidic fluxing of Cr_2O_3 in superalloys at high temperatures was not studied in detail.

2.2 Low Temperature Hot Corrosion

Low temperature hot corrosion (type II hot corrosion) is one of the forms of hot corrosion that occurs below the m.p of Na_2SO_4, where the salt is supposed to be a solid.

Umland and Voigt [33] showed high corrosion rate with high recovery of Ni and Co - sulphates for several Fe, Co and Ni - base alloys exposed to Na_2SO_4, K_2SO_4 and mixture in air or air containing SO_3 in the temperature range $650-900°C$. High Corrosion rates were related to the formation of soluble nickel, cobalt and chromate

ions. Jones and Godamski [15] explained the rapid corrosion of nickel and cobalt base alloys by the decomposition of sulphate melt (within the minute pores of the oxide scale), which contains mixtures of Na_2SO_4 and Fe, Co, Ni and Cu sulphate, accompanied by liberation of corrosive gas (SO_3) during melting of salt deposits.

Luthra and Shores [17] studied the mechanism of Na_2SO_4 - induced hot corrosion of $Ni-30Cr$ and $Co-30Cr$ at 750°C in O_2+SO_2 environment which correspond to the conditions required for LTHC. High corrosion rate during the initial stages were attributed to the rapid sulfation of cobalt oxide or Co (at scale/metal interface) which forms liquid eutectic melt followed by the dissolution and precipitation of cobalt oxide at salt-gas interface by counter transport of Co^{2+}/Co^{3+} ions during the propagation stage (Figure 2.2b). Thus, the fluxing of cobalt oxide prevents the formation of protective layer of Cr_2O_3. The effect of P_{SO_3} and temperature on LTHC has been presented in detail. As the temperature increases the partial pressure of SO_3 decreases, which is not sufficient to form liquid eutectic mixture. Hence, the corrosion rate at high temperature is much less than at low temperatures. The increase in P_{SO_3} in the environment, allows to form $CoSO_4$ (s) at the salt/gas interface in $CoCrAlY$ coatings. In this study, the mechanism by which Cr_2O_3 looses its ability to protect alloy substrate at the end of propagation stage is not well characterized and the LTHC mode of attack for Ni- base alloy was not outlined in detail.

Jones [19] demonstrated the role of catalytic activity of Co_3O_4 in increasing the

partial pressure of SO_3 at salt-gas interface on hot corrosion of $CoCrAlY$ coating alloys at $625°C$. It has been concluded that molten sulfates are formed at initial stages and further corrosion might have occurred by sulphate decomposition, which resulted in the formation of sulfur rich pits ahead of corrosion front. Chiang et al [20] related the loss of protecitivity of Cr_2O_3 and/or Al_2O_3 scales at the end of propagation stage to the high local reducing conditions generated by oxidation and sulfidation of Cr and/or Al ($Ni-15Cr-11Al$) and opposed the fluxing mechanism proposed by Luthra et al [17]. The mechanism by which the local reducing conditions are generated is not clear.

The effect of SO_2 and SO_3 on LTHC of pure Ni in the temperature range of $750-900°C$ was examined by Misra and Whittle [21]. A considerable effort has been done to explain the mechanistic model for the LTHC mode of attack for pure Ni. The model includes the formation of low melting eutectic of $Na_2SO_4 - NiSO_4$ at the initial stage as suggested by Luthra et al [17] and subsequent propagation stage have been proposed by a number of mechanisms including: sulphate decomposition, oxidation of sulfide-base eutectic ($Ni - Ni_3S_2$). The formation of duplex scale was proposed to be the primary reason for accelerated oxidation of Ni.

Luthra [18], [35]-[37] studied the hot corrosion behavior for several $Co-Cr$, $Co-Al$, $Co-Cr-Al$ alloys at 750° in $O_2+0.15\%SO_2$ environment. It has been shown that $Co-Cr$ and/or $Co-Al$ alloys are more resistant to type II attack than $Co-Cr-Al$ alloys and proposed that the formation of spinels, such as $CoCr_2O_4$

and/or $CoAl_2O_4$ may prevent pitting mode of attack.

A consistent model of hot corrosion for Ni-base alloys has been presented by Misra [28] in $Na_2SO_4 - LiSO_4$ melt system at $750°C$ in $O_2 + 0.1\% SO_2$ atmospheres. The formation of duplex scale ($NiO + Ni_3S_2$) after liquid melt decomposition was considered as the primary cause of degradation. It has been shown [28] that without the melt system ($Na_2SO_4 - LiSO_4$) on the alloy surface the degradation of the protective scale is minimum, probably due to the absence of duplex scale.

Levy et al [39] used a technique similar to that reported by Jones [15] and Misra [38] to observe the characteristic morphology of three model $Ni-$base alloys containing refractory elements (Mo and W). The $Ni-$ base alloys were cyclically corroded in $Na_2SO_4 + 45\% MgSO_4$ melt in air alone at $700°C$. All alloys showed low temperature hot corrosion features without the presence of SO_3 in the gas phase, such as no depletion of Cr at the scale/metal interface and thin S-rich zone ahead of corrosion front .

The hot corrosion of pure iron and various $Fe - Cr$ and $Fe - Al$ alloys was studied by Buscaglia et al [40]. Zhang and Shih et al [41], [42] in SO_3 containing gas atmospheres at $923 - 1023°K$ using pure Na_2SO_4 and $Na_2SO_4 - K_2SO_4$ salt deposits. A maximum corrosion rate was observed at $973°K$ for all most all alloys which was attributed to the formation of a liquid eutectic of iron sulfate and sodium sulfate. The results were interpreted by dissolution/precipitation of iron oxide near scale/metal interface caused by counter transport of Fe^{2+}/Fe^{3+} from scale/metal

to salt/gas interface.

Recently, Amin [43] have investigated the effect of $Fe_2(SO_4)_3$ on hot corrosion of sodium sulfate coated specimens of AISI-304 steel in O_2 environment alone, under isothermal conditions. Weight change measurements showed heavy attack when the sample coated with the mixture of iron sulfate and sodium sulfate was exposed to $700°C$. It was concluded that the formation of liquid phases, namely, $Na_3(FeSO_4)_3$ and $Na(FeSO_4)_2$ may be the possible reason for heavy attack. This study has not provided detailed explanation for the protective scale breakdown but only indicated that the evolution of gases is responsible for cracking of oxide.

2.3 Role of NaCl in LTHC

The influence of solid contaminants including $NaCl$, Na_2SO_4 and $Na_2SO_4 + NaCl$ on iron and nickel- base alloys was examined by Hurst et al [24] using hot stage microscopy. All alloys showed extensive attack in the presence of salt mixtures and this was related to the mechanical failure of the surface protective scales. It has been proposed that direct access of contaminant ($NaCl$ or salt mixture) to the metal and formation of volatile oxychlorides may be the possible mode of attack. Conde [44] showed that $Na_2SO_4 + 25\% NaCl$ is very aggressive than $1\% NaCl$ enriched salt for Cr_2O_3 formers and attributed the cracking of surface scales to the formation of volatile oxychlorides rather than metal chlorides, which do not require

very low oxygen partial pressures. Mc Kee et al [45] showed that Al_2O_3 formers are also susceptible to sulfate/chloride mixtures at low temperatures and outlined the synergetic effect of SO_2 and $NaCl$ in accelerating the attack. The breakdown of protective scales were related to the release of Cl_2 gas and formation of low-melting eutectics of $NaCl - NiCl_2$ or $NaCl - CoCl_2$. As the isothermal tests were of short duration. the propagation stage of samples corroded in condensed salt mixtures, exposed to O_2 alone was not studied in detail.

Barkalow and Pettit [28] tried to explain the important species that is responsible for LTHC of $CoCrAlY$ coatings. Preferential removal of Al and the formation of internal network of pores in an alloy depleted in Al has been observed in sulfate/chloride mixtures. However, samples corroded in $Na_2SO_4 + SO_3$ without chloride did not reveal depletion of Al at the scale/metal interface. The alloy samples corroded in sulfate/chloride mixtures showed broad frontal attack compared to pitting type of attack in $Na_2SO_4 + SO_3$ environments. Hence, it has been concluded that SO_3 is responsible for LTHC of coatings than $NaCl$.

Conde [29] suggested that low temperature hot corrosion should occur in the presence of $NaCl + Na_2SO_4$ mixtures by sulfate decomposition, if local non-equilibrium conditions are considered, because the seasalt is the SO_2 and SO_3 generator. Chiang et al [20] showed LTHC morphology for Na_2SO_4-coated $Ni - Cr - Al$ alloys in $O_2 + NaCl(v)$ environment at 750°C. A pitting type of morphology was observed. which consists of Cr_2O_3 at the salt/gas interface and a thin S-rich zone at

the scale/metal interface. The mechanism by which pitting attack occurs was not clear. Kameshwari [30], [46] observed preferential removal of Cr, Co, Al, and Ti and a network of voids in the substrate, as proposed by Barkalow and Pettit [28], for $Ni-$ base alloys. The author concluded that the corrosion rate is high when the specimens were corroded in sulfate/chloride mixtures, consisting of low concentration of (1w/o-5w/o)$NaCl$ (solid+liquid) compared to that of either 25w/o$NaCl$ + Na_2SO_4 (completely liquid) or pure sodium sulfate (solid).

Hancock [31] opposed considering of fluxing of oxide scales in type II hot corrosion because the $NaCl$ is constantly replenished in marine turbines with contaminant flux rate (contaminant flux rate is defined as the amount of salt that deposits on the blades and vanes of gas turbine per unit hour and surface area) 0.27 $\frac{mg}{cm^2}$, which can continuously re-initiate the localized attack. Surayanaraynan [48] attributed the propagation of pure Ni in $Na_2SO_4 + 25\%NaCl$ mixtures to the oxidation of $Ni-Ni_3S_2$ and due to oxidation of chlorides. Recently, Nicholis and Stephenson [32] showed that the previously damaged samples of IN 738 exhibited localized attack in sulfate/chloride mixtures when gas environments contains sufficient SO_3 only.

Inspite of extensive efforts spent in attempting to elaborate the mechanism of low temperature hot corrosion, the effect of $NaCl$ on Na_2SO_4-induced hot corrosion of $Ni-$ and $Co-$ base alloys is still controversial. Nevertheless, it has been widely accepted investigators [7, 9], [17]-[18], [20, 30, 38] that $NaCl$ induces attack on Na_2SO_4- coated specimens of Ni and $Co-$ base alloys at low temperatures in air

or O_2. Most of these investigators concluded that the presence of $NaCl$ along with SO_3 in the atmosphere incur damaging effect even on highly resistant alloy, such as IN 738. The influence of $NaCl$ on Na_2SO_4- coated specimens is less severe when O_2 or air alone is used. There is no detail information about the LTHC behavior of superalloys in sulfate/chloride mixtures. Therefore, it would be useful to investigate further the effect of $NaCl$ under thermal cyclic conditions at intermediate temperatures in order to come up with a suitable hot corrosion mechanism.

2.4 Objectives

The following are the specific objectives of the present study.

1. To understand the effect of $NaCl$ on low temperature hot corrosion behavior of Na_2SO_4 coated specimens of IN 738 and Mar-M 509 at 750°C in Air, under thermal cyclic conditions.

2. To understand the low temperature hot corrosion mechanism of $Ni-$ and $Co-$ base alloys at oxide/metal interface and at the oxide/salt interface in samples exposed to $Na_2SO_4 + NaCl$ mixtures, under thermal cyclic conditions.

Chapter 3

Experimental Setup and Procedures

3.1 Materials

During the course of this study, two conventional superalloys have been investigated, namely, IN 738 and Mar-M 509, whose nominal composition is shown in Table 3.1 and Table 3.2. These superalloys were perticulary chosen because of their extensive use as blade and vane materials in gas turbines. Reagent grade $NaCl$ and Na_2SO_4 used in the present study were prepared by Johnson Matthey Chemicals [28].

Table 3.1: Nominal Composition of IN 738 in weight percent

Ni	Cr	Al	Ti	Co	W	Mo	Ta	B	C	Zr	Fe
Bal	16.1	3.68	3.42	8.37	2.68	1.83	1.84	0.009	0.155	0.08	0.24

Table 3.2: Nominal Composition of Mar-M 509 in weight percent

Co	Cr	Ti	Ni	W	Si	Ta	B	C	Zr	Fe
Bal	22.7	0.20	10.6	7.24	0.18	3.30	0.009	0.61	0.49	0.37

3.2 Experimental Test System

A schematic diagram of the high temperature test system used in this study is shown in Figure 3.1. The test system consists of Lindberg horizontal tube furnace (Model 5534) with a maximum usable 3 inch outer diameter tube and which can be operated to a maximum temperature of $1200°C$. A one-end closed ceramic tube of 2 inch internal diameter is inserted into the tube furnace supported by tube-adapters at both ends of the furnace. Two insulating blankets of alumina sponge were provided at the two-ends of furnace to minimize heat loss and/or temperature gradients within the furnace. The test temperature used in this study is $750°C$, which can be precisely controlled with a control consol with $\pm 1°C$ error. The test temperature in the reaction chamber is continuously checked with a chromel-alumate thermocouple. In the 24 inch hot zone, 12 to 15 samples can be corroded at the same time and approximately 5 inch cold zone ($150 - 200°C$) to cool the specimens during the process of thermal cycling.

3.3 Experimental Test Runs

Table 3.3 shows the total number of test runs conducted in the present investigation. The following conditions were used to all test runs:

1. Environment = Static air (room)

Table 3.3: Total test runs conducted for IN 738 and Mar-M 509

Run #	Test condition
1	100%Na_2SO_4 coated IN 738 corroded cyclically upto 20 cycles
2	100%Na_2SO_4 coated IN 738 corroded cyclically upto150 cycles
3	75%Na_2SO_4 + 25%$NaCl$ coated IN 738 corroded cyclically upto 1cycle
4	75%Na_2SO_4 + 25%$NaCl$ coated IN 738 corroded cyclically upto 20 cycles
5	75%Na_2SO_4 + 25%$NaCl$ coated IN 738 corroded cyclically upto 150 cycles
6	99%Na_2SO_4 + 1% coated IN 738 corroded cyclically upto 20 cycles
7	99%Na_2SO_4 + 1% coated IN 738 corroded cyclically upto 150 cycles
8	75%Na_2SO_4 + 25%$NaCl$ coated IN 738 after 150 hr isothermal corrosion
9	100%Na_2SO_4 coated Mar-M 509 corroded cyclically upto 20 cycles
10	100%Na_2SO_4 coated Mar-M 509 corroded cyclically upto 150 cycles
11	75%Na_2SO_4 + 25%$NaCl$ coated Mar-M 509 corroded cyclically upto 1cycle
12	75%Na_2SO_4 + 25%$NaCl$ coated Mar-M 509 corroded cyclically upto 20 cycles
13	75% Na_2SO_4 + 25%$NaCl$ coated Mar-M 509 corroded cyclically upto 150 cycles
14	99% Na_2SO_4 + 1% coated Mar-M 509 corroded cyclically upto 150 cycles
15	Na_2SO_4 + 52%$CoSO_4$ coated Mar-M 509 corroded cyclically upto 150 cycles

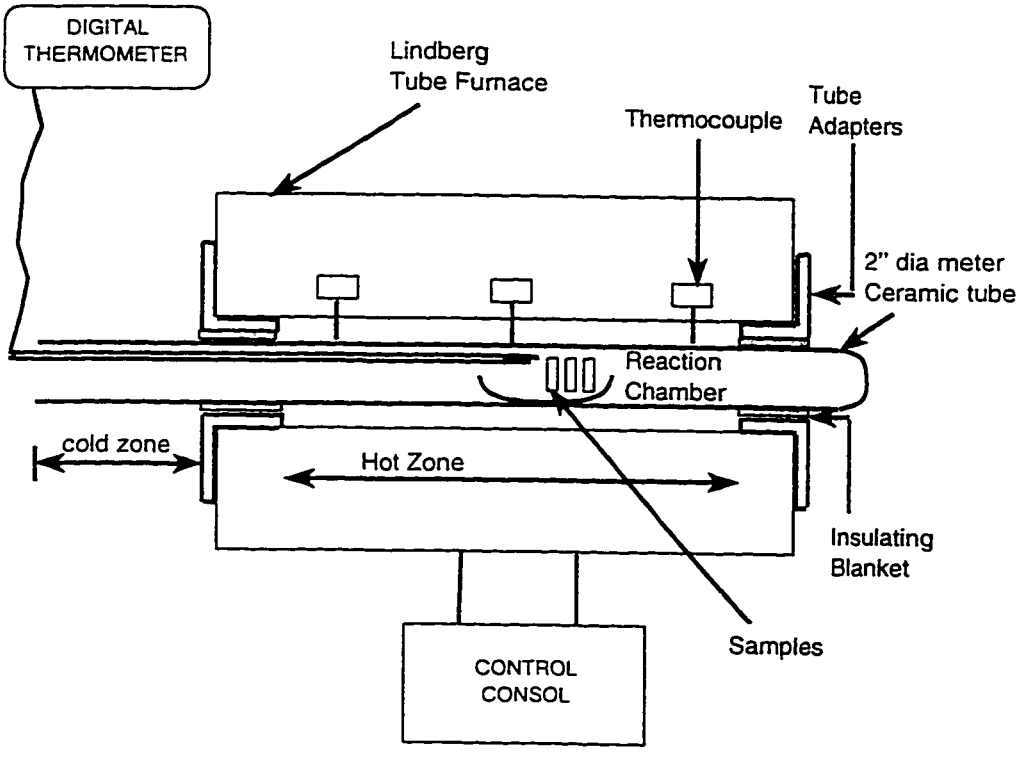

Figure 3.1: Schematic diagram of high temperature test system

2. Test temperature = $750°C$

3. Total amount of salt = $2.5mg/cm^2$

4. One thermal cycle equals to 1 hour in hot zone and 5 minutes in cold zone.

The graphical representation of thermal cycling exerted on alloy specimens during hot corrosion is shown in Figure 3.2. The samples were corroded for 1 hr at $750°C$ and then brought to the cold zone and held there for 5 minutes. The total duration consistues one thermal cycle. The total time duration of each thermal cycle is 1 hour 5 minutes. however it is ususally represented by 1 hour (hot zone) time for convience. The one hour and fifteen minute cycle was considered because to accelarate the rate of hot corrosion. as proposed by Goebel and Pettit for high temperature hot corrosion of superalloys [16].

For each test run two samples were used to perfom SEM and XRD analysis. Short duration tests of one cycle or 20 cycles were conducted to see the corrosion kinetics and morphology of the corroded samples at intial stages. Long duration tests of 150 cycles were done to observe the corrosion morphology of corroded samples at the propagation stage.

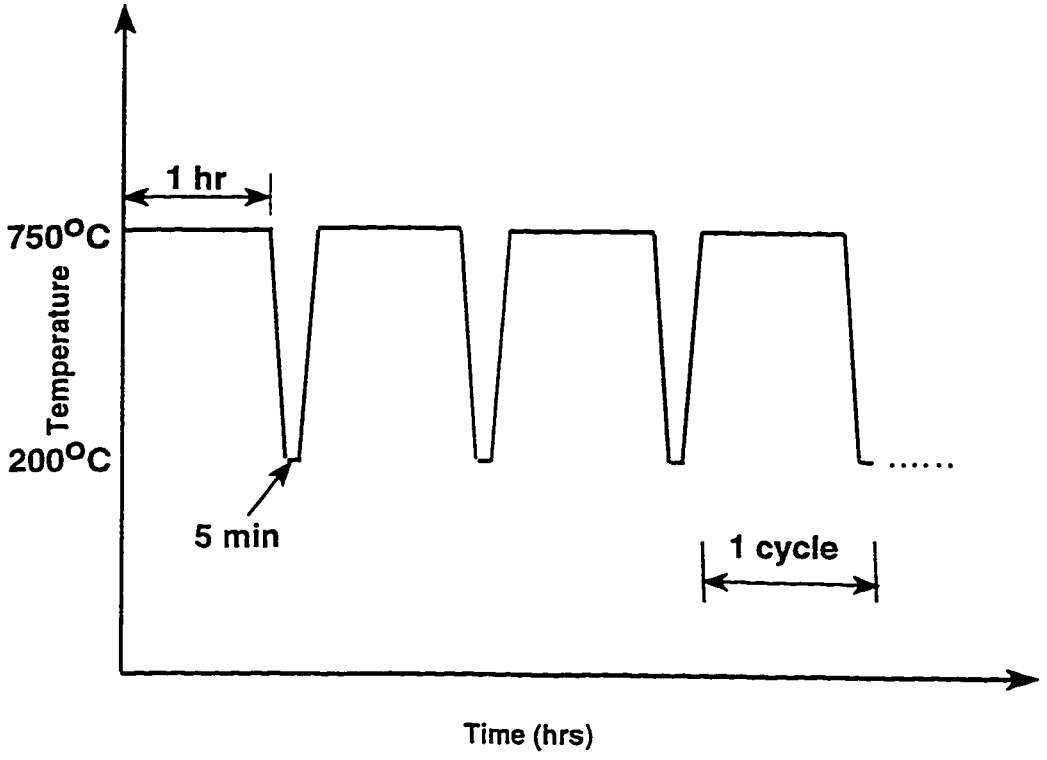

Figure 3.2: Schematic diagram illustrating the thermal cycling during hot corrosion

3.4 Procedures

3.4.1 Specimen Preparation

Samples of IN 738 and Mar-M 509 were cut into thin platlets of approximately equal size (1.25 cm × 1.1 cm × 0.3 cm), polished sequentially with 110, 240, 340, 600 grit size SiC paper and then cleaned in warm distilled water, kerosene and finally degreased with acetone.

3.4.2 Salt Coating Method

Intially, the weight of the cleaned sample before coating is recorded (W_1) using a microbalance with a sensivity of 0.01 mg. The amount of salt to be coated can be calculated as follows:

$$W_s = 2.5\ mg/cm^2 \times A \tag{3.1}$$

Where A is surface area in cm^2 and W_s is the amount of salt to be coated onto the sample.

The salt solution is sprayed onto the heated samples until $W_1 + W_s$ is read on a semi-micro balance within the range of ±10%.

In the present study, an aqueous saturated solution (44 gm of sulfate dissolve in 100 ml water) of pure Na_2SO_4, $Na_2SO_4 + 1wt\%NaCl$ and $Na_2SO_4 + 25wt\%NaCl$ was applied to the pre-warmed specimens with a spray gun (Figure 3.3) until the

desired coating weight i.e. 2.5 mg/cm^2 is achieved.

3.4.3 Hot Corrosion Experiments

Salt-coated specimens were placed in high purity Al_2O_3 ceramic boats and these boats were introduced into hot section of the reaction chamber very slowly (5 cm/min) after the desired temperature ($750°C$) is reached in the furnace. Then, the samples were corroded in static air for 1 hr, then slowly withdrawn to the cold zone within 5 minutes. The weight of the corroded sample was recorded after every 5 cycles intially and for every 10 cycles after 20 cycles of hot corrosion test. The desired salt is re-coated after every 20 cycles for Run #2, #5, #7, #10, #13, #14 and #15.

Weight Change of the sample is calculated as follows:

$$\Delta m = \frac{W_a - W_b}{A_b} \tag{3.2}$$

W_b = intial weight of the sample before coating, mg

W_a = weight of the sample after hot corrosion testing, mg

A_b = surface area of the sample before testing, cm^2

Δm = weight change, mg/ cm^2

3.5 Analysis of Corroded Samples

Corroded samples were cross-sectioned at important regions and mounted in epoxy. The sectioned samples were then polished sequentially with 240, 340, 600 grit size papers, followed by fine polishing with $1\mu m$ diamond finish paste. All polishing and cleaning operations were done using methonal and heptane to prevent dissolution of water soluble corrosion products. Figure 3.4 shows the cross-sectioned sample after mount preparation.

Corroded samples were analysed using micro-analytical techniques, including Scanning Electron Microscopy (SEM), Energy dispersive spectroscopy (EDS) and X-ray mapping. X-ray diffraction technique (XRD) and Electron spectroscopy for chemical analysis (ESCA) has been used to identify the chemical phases present in corroded samples. In the case of XRD analysis, the corrosion product was scrapped off about 0.5 mm (approximately) deep into the substrate to remove even traces of oxides and sulfides attach to the underlying metal. The powder was then analysed using powder diffractometer technique.

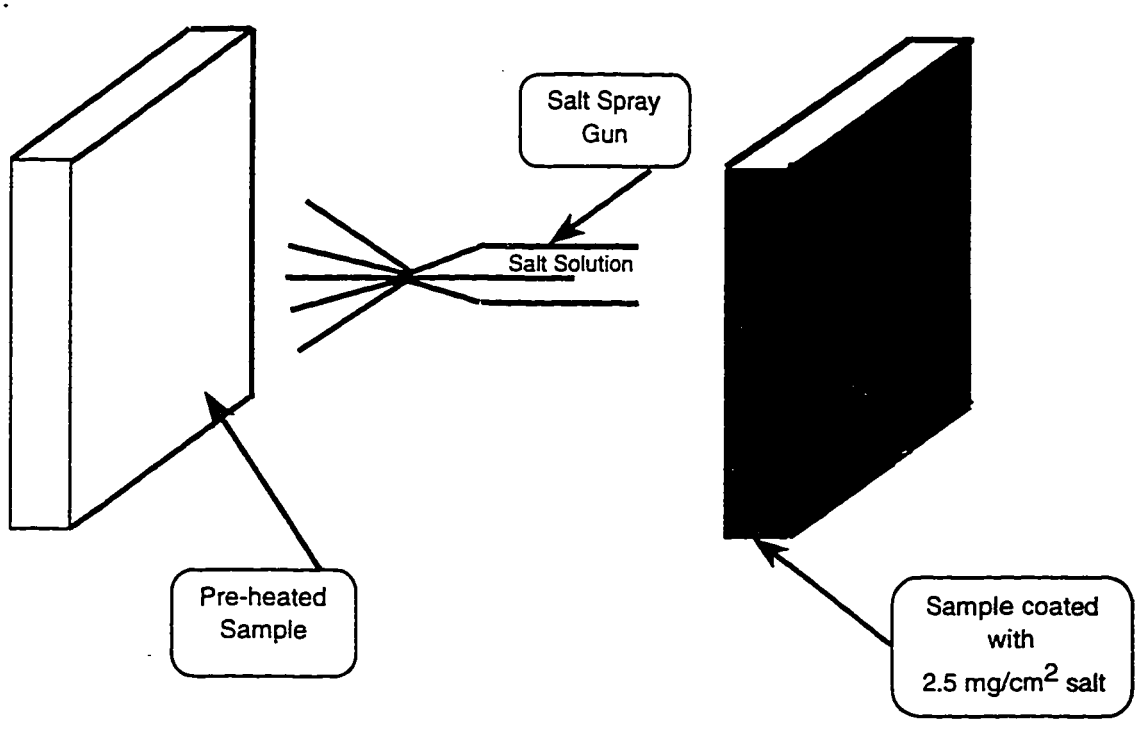

Figure 3.3: Schematic diagram illustrating the coated and uncoated test specimens

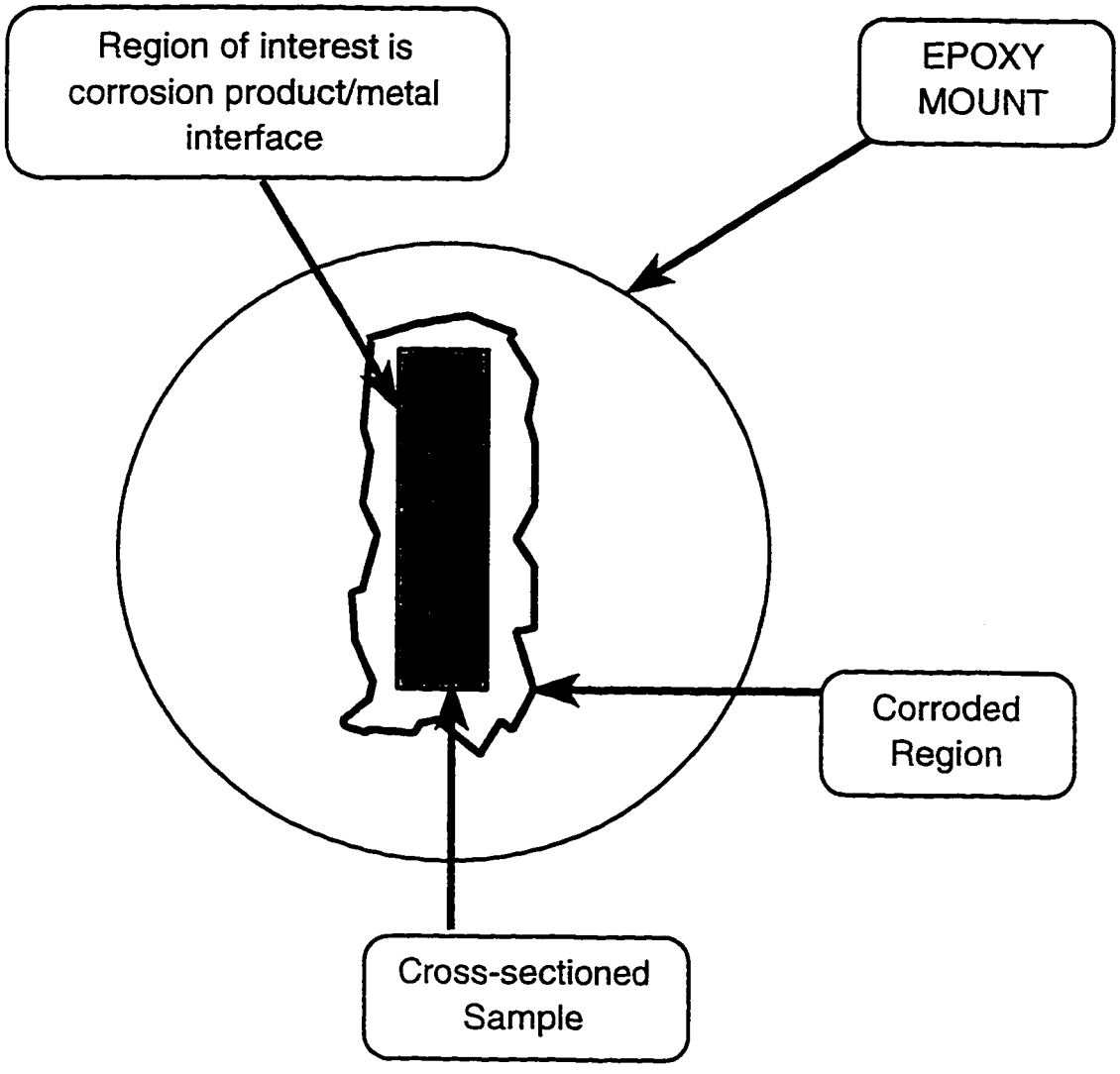

Figure 3.4: Schematic diagram showing the mounted sample after cross-sectioning for SEM analysis

Chapter 4

Results and Discussion

In this chapter, the morphological aspects of hot corrosion of IN 738 and Mar-M 509 coated in pure Na_2SO_4, $75\%Na_2SO_4 + 25\%NaCl$ and $99\%Na_2SO_4 + 1\%NaCl$ are discussed. This is followed by discussing the effects of $NaCl$ on the corrosion morphologies of exposed alloys both in the initial and propagation stages and correlating then with corrosion kinetics. Finally, suitable hot corrosion mechanisms for low temperature hot corrosion behavior of IN 738 and Mar-M 509 in salt mixture conditions have been proposed.

4.1 Results

4.1.1 IN 738

Figure 4.1 shows the kinetic data during the exposure of IN 738 to LTHC environment under thermal cyclic conditions. In pure Na_2SO_4, the results indicate a slight increase in weight gain upto 20 hrs, ensued by steady but slight weight loss after the breakdown of the protective scale. A dramatic loss in weight has been produced during both initiation and propagation stages in $Na_2SO_4 + 25\% NaCl$ mixture when compared to those experienced in either pure Na_2SO_4 or $Na_2SO_4 + 1\% NaCl$ mixture under similar exposure conditions. This indicate that the rate of hot corrosion attack increases with the increasing concentration of $NaCl$ in Na_2SO_4.

Figure 4.2 shows the cross-sectioned morphology of corroded IN 738, coated with 2.5 mg/cm^2 of Na_2SO_4 after 20 cycles (1 hr each) at 750°C in static air (initial stage). During the initial stage of attack, the scale formed on the alloy surface is a uniform, compact and protective oxide layer, which consists primarily of a mixture of Cr_2O_3 and small amount of NiO (spot A). No internal oxide or sulfide particles have been observed in the substrate (spot D). Figure 4.3 shows XRD results of a powdered sample exposed to pure Na_2SO_4 for 20 cycles, which confirm the exclusive formation of these oxides and the absence of sulfides.

After exposure for 150 cycles (1 hr each) in pure Na_2SO_4, well into the propagation stage, the alloy surface was covered with a thick porous scale, which contains

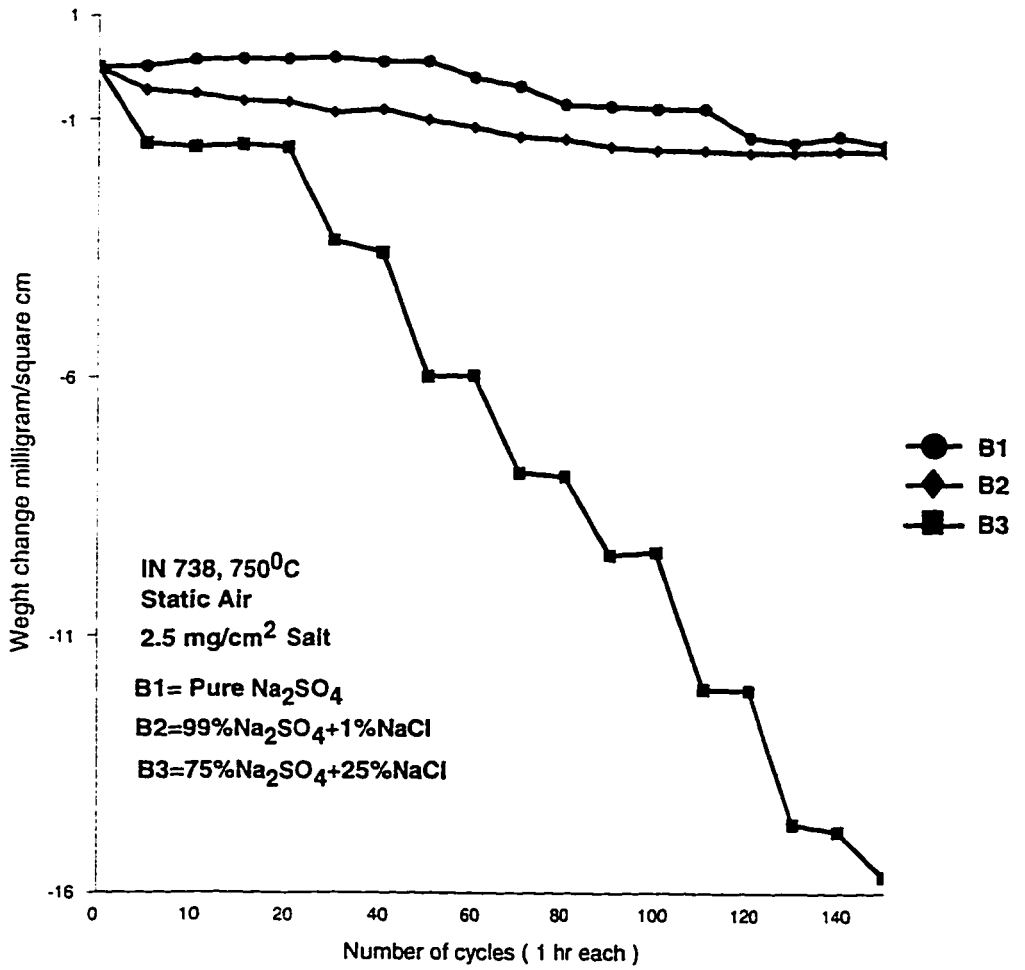

Figure 4.1: Rate of hot corrosion of IN 738 at 750°C

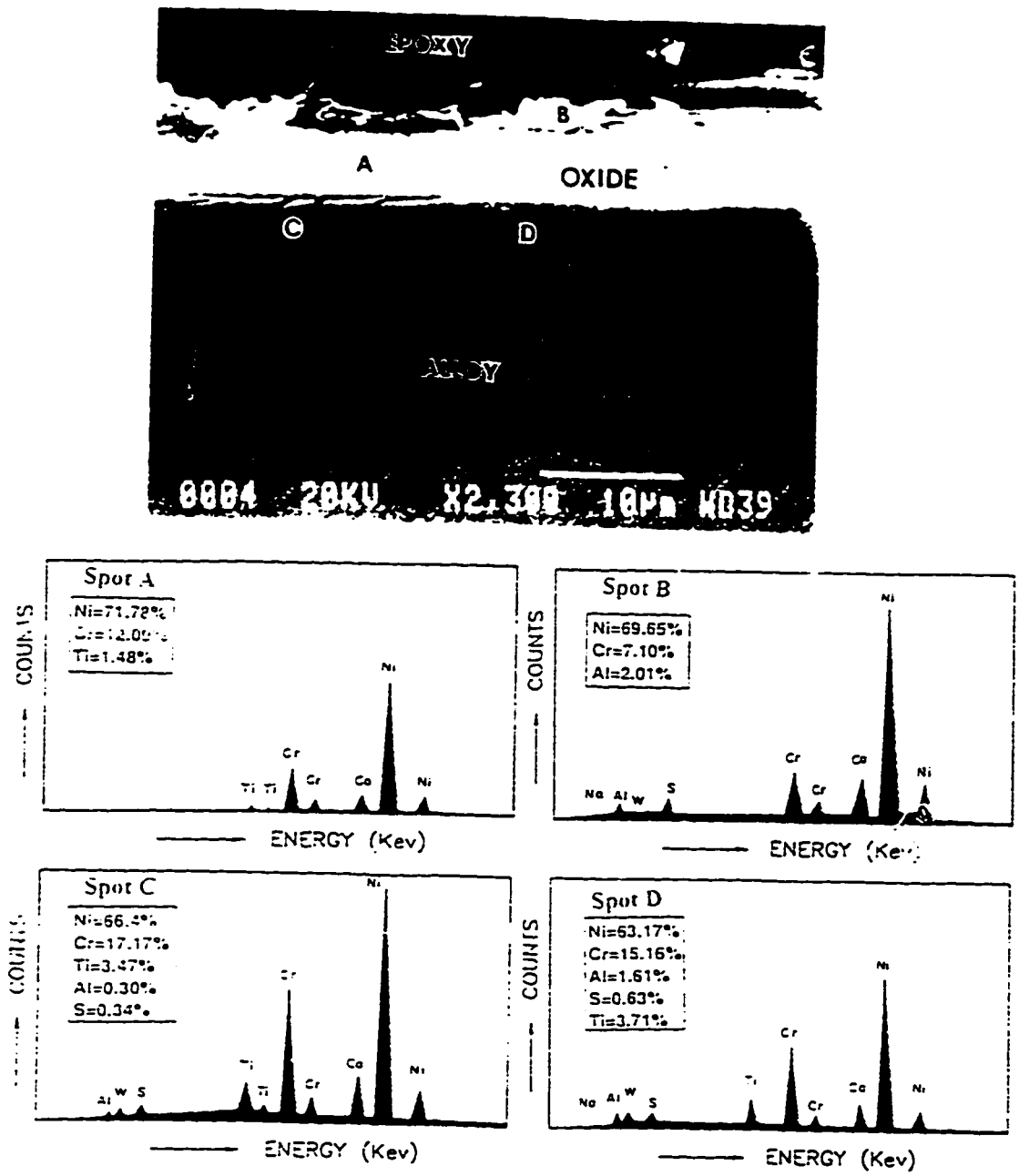

Figure 4.2: SEM micrograph and EDS spectra of pure Na_2SO_4-coated IN 738 after exposure for 20 cycles (1 hr each) in static air at $750°C$

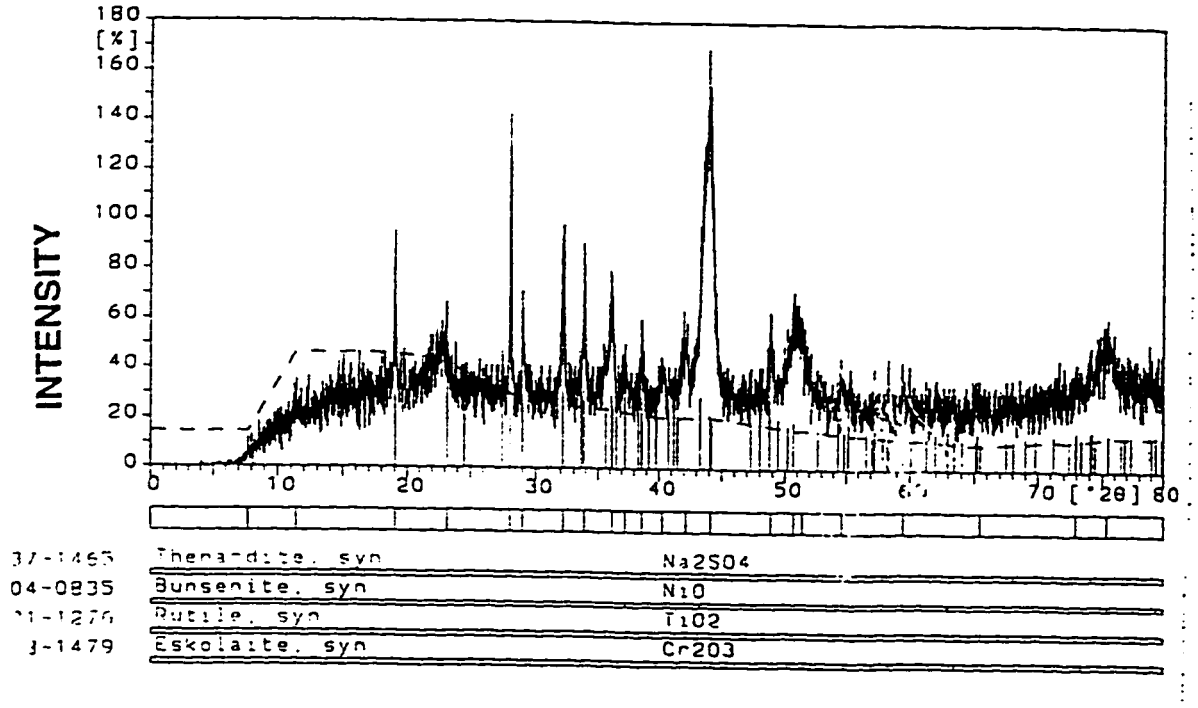

Figure 4.3: XRD pattern of pure Na_2SO_4-coated IN 738 after exposure for 20 cycles (1 hr each) in static air at 750°C

numerous voids and cracks (Figure 4.4).

The scale contains islands of unreacted Na_2SO_4, as it remains solid at the test temperature ($750°C$). Examination of the scale/alloy interface indicates the presence of a continuous dark layer, extending along the scale/alloy interface. Figure 4.5 shows the elemental distribution of corroded IN 738 coated with pure Na_2SO_4 after 150 cycles at $750°C$ in static air (inset of Figure 4.4). X-ray mapping (Figure 4.5) indicate that the dark layer attached to the scale/metal interface is enriched in Al and O indicating that it may consist of Al_2O_3. Below the alloy/scale interface in the metal side, there exists a subscale layer containing large number of internal particles which are rich in Al and O indicating that it consists primarily of Al_2O_3 particles embedded in the alloy matrix. On the other side the dark Al_2O_3 layer, another continuous intermixed grey layer is seen. This layer is enriched in Cr and Ti, indicating that it may consist of a mixture of TiO_2 and Cr_2O_3. However, XRD results (the corrosion product was scrapped off about 0.5 mm deep into the substrate and the powder was analysed using powder technique) (Figure 4.6) confirm the presence of Cr_2O_3, unreacted Na_2SO_4 and elemental Ni, along with Al_2O_3 which is probably picked from the underlying layer. The presence of TiO_2 was not confirmed because its concentration may be lower than the detection limit of XRD. It is also clear from the Ti and O x-ray maps that the TiO_2 is semi-continuous when compared to Cr_2O_3. The steady loss of weight (Figure 4.1) of sample in pure Na_2SO_4 after 150 cycles almost correlates with the observed degradation of IN 738, coated with pure

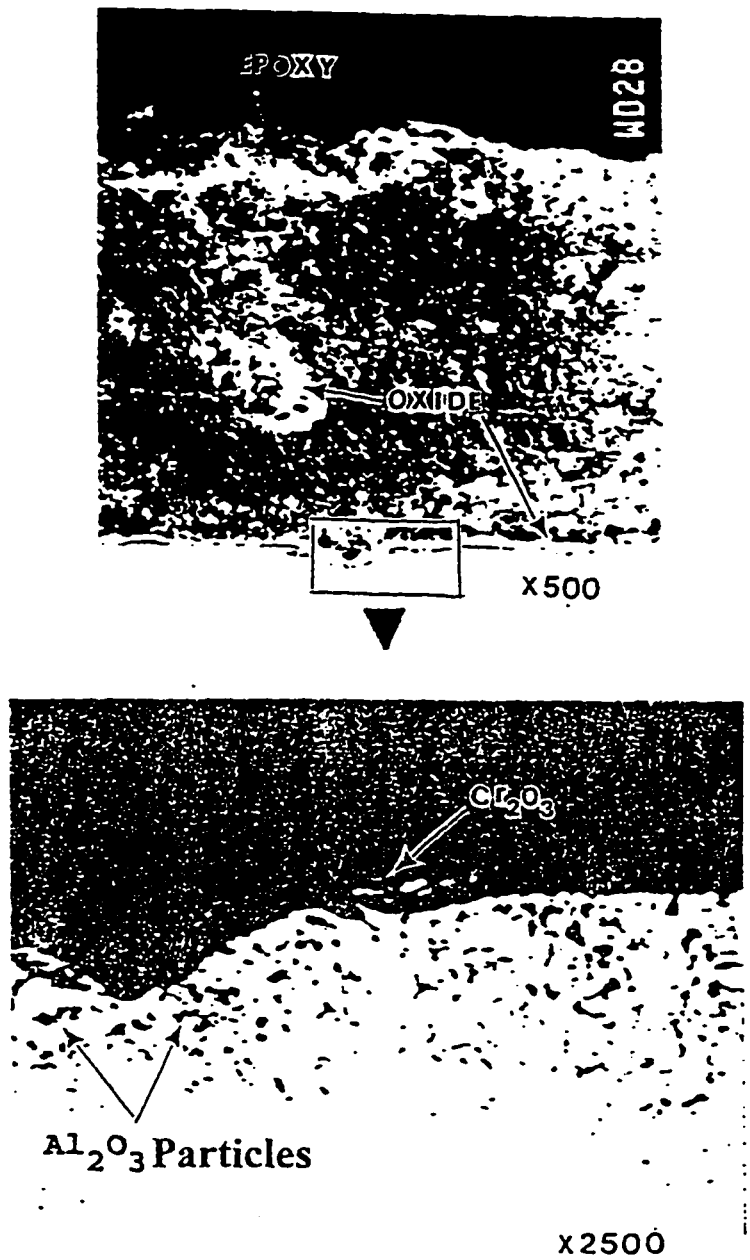

Figure 4.4: SEM micrograph of pure Na_2SO_4-coated IN 738 after exposure for 150 cycles (1 hr each) in static air at 750°C

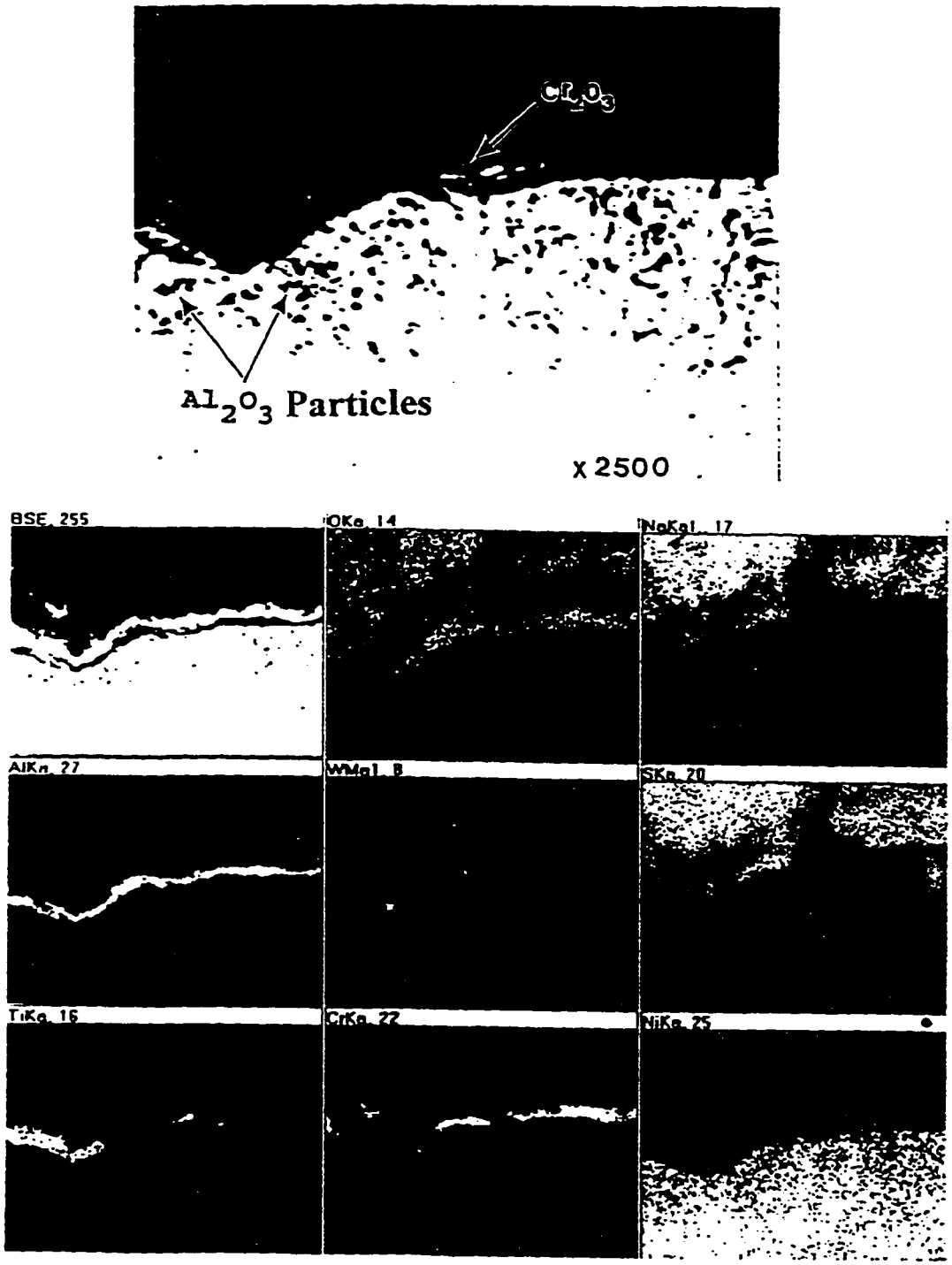

Figure 4.5: SEM micrograph (inset region of Figure 4.4) and elemental distribution of pure Na_2SO_4-coated IN 738 after exposure for 150 cycles (1hr each) in static air at 750°C

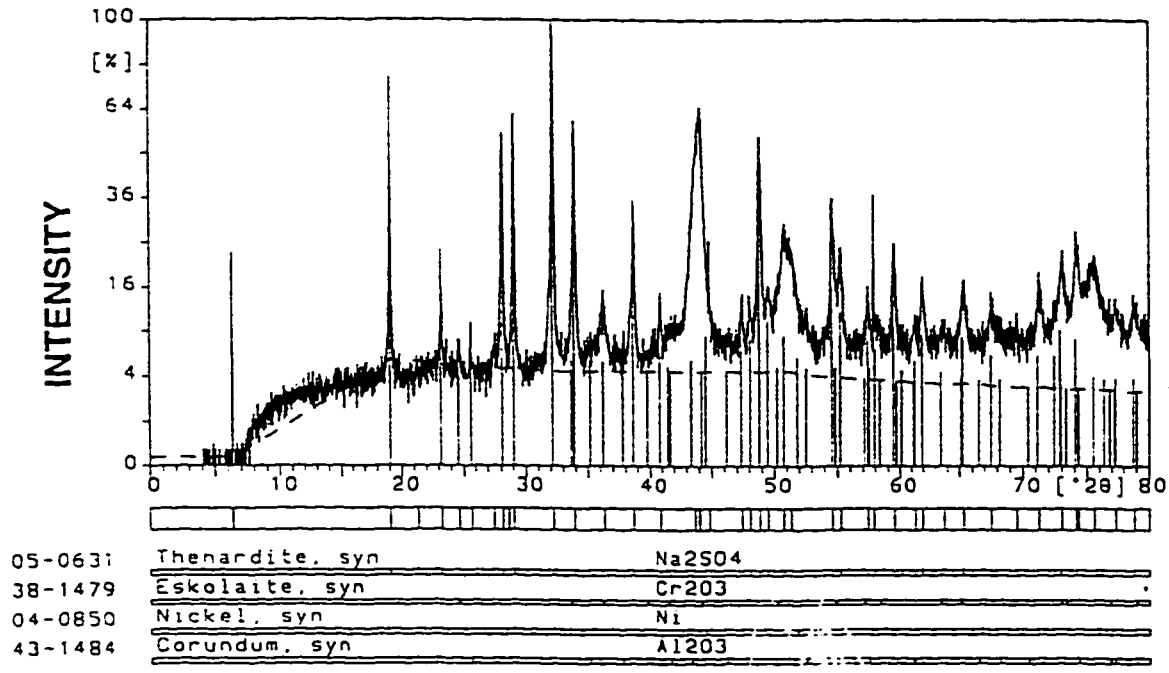

Figure 4.6: XRD pattern of pure Na_2SO_4-coated IN 738 after exposure for 150 cycles (1hr each) in static air at 750°C

Na_2SO_4 alone.

Figure 4.7 shows the cross-sectioned morphology of IN 738 alloy corroded in $99\%Na_2SO_4 + 1\%NaCl$ mixture after 20 cycles in air. The corrosion product/alloy interface is fairly irregular, and was detached from the substrate at numerous locations. The outermost region of the scale near the salt-air interface is enriched in Cr with almost no trace of sulfur (spot C in Figure 4.7) indicating that it consists of exclusively of Cr_2O_3. The semi-continuous intermediate thick grey scale is rich in Ti and Cr indicating that it may consist of intermixed oxides of Ti and Cr (spot F in Figure 4.7).

Below the alloy/oxide interface, the subscale may consists of large number of S-rich and Cr/Ti as well as W-rich particles indicating that they may consists of TiS, WC and CrS(spot B in Figure 4.7). At the alloy/scale interface Ni-rich islands are observed (spot D in Figure 4.7) which appears to be metal fragments dispersed in the intermediate scale. Figure 4.8 shows the XRD results, which confirm the presence of NiO, Cr_2O_3 and TiO_2. The analysis of the dark layer rich in Al, Ti and Ni extending along the scale/alloy interface indicates that it may consists of Al_2O_3, TiO_2 and NiO (spot E). The weak intensity of sulfur peak indicate that this layer contain no sulfides of Al, Ti or Ni.

Figure 4.9 shows similar type of morphology (which consists of outer porous Cr_2O_3 layer and intermediate layer of TiO_2 and Cr_2O_3) to that of shown in Figure 4.7, but at the corner of the IN 738 specimen. This confirms the reproducibility

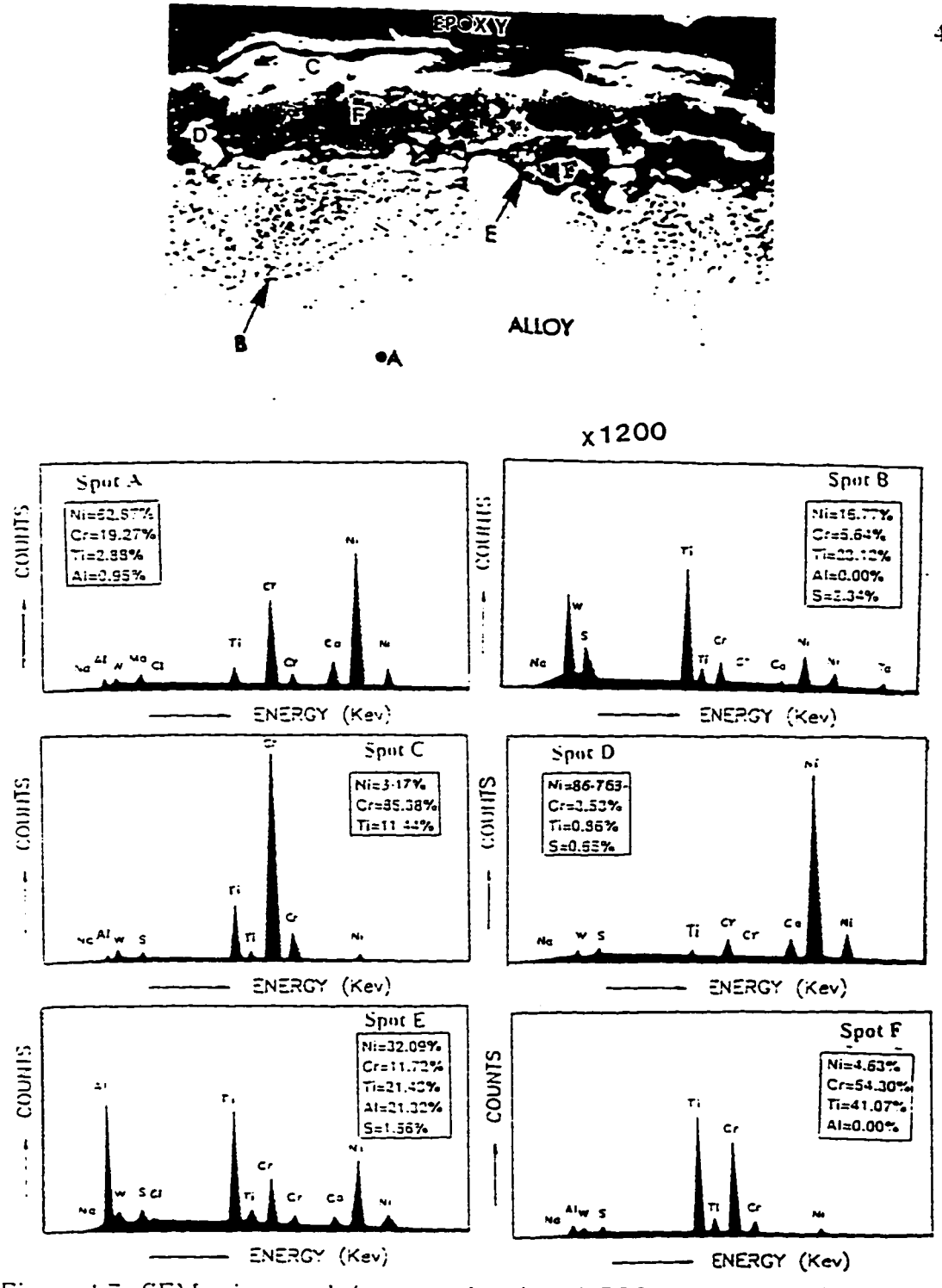

Figure 4.7: SEM micrograph (cross-sectioned) and EDS spectra of 99% Na_2SO_4 + 1% $NaCl$ coated IN 738 after exposure for 20 cycles (1hr each) in static air at 750°C

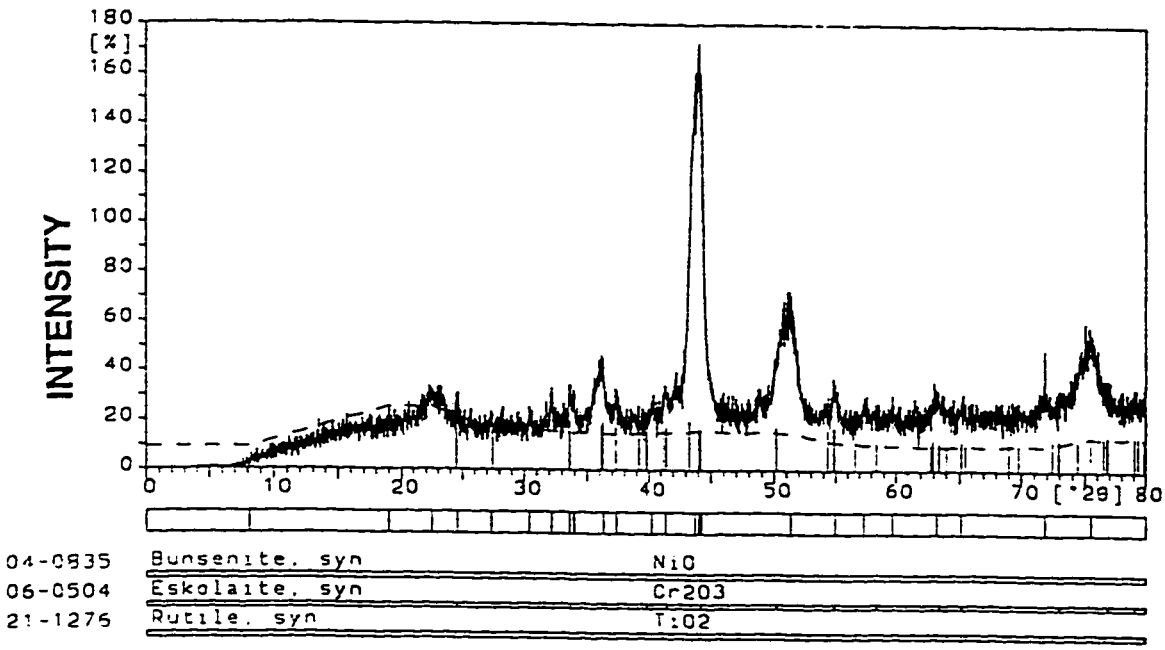

Figure 4.8: XRD pattern of 99% Na_2SO_4+1%$NaCl$ coated IN 738 after exposure for 20 cycles (1hr each) in static air at 750°C

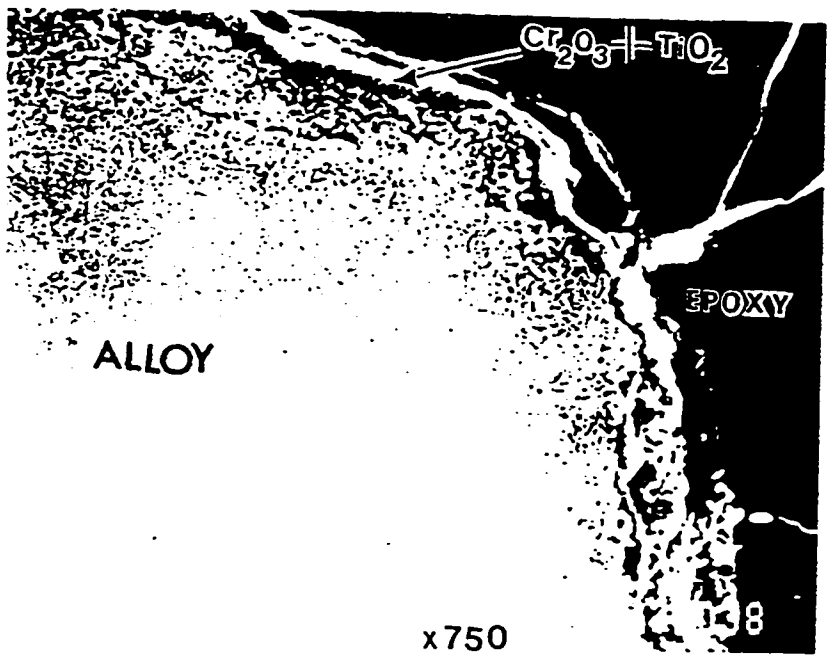

Figure 4.9: SEM micrograph (corner edge) of 99% Na_2SO_4+1%$NaCl$ coated IN 738 after exposure for 20 cycles (1hr each) in static air at 750°C

of the corrosion morphology of $99\%Na_2SO_4+1\%NaCl$ coated sample at $750°C$ after exposure for 20 cycles.

Figure 4.10 shows the morphology in cross-section of IN 738 sample coated with $99\%Na_2SO_4 + 1\%NaCl$ after exposure for 150 cycles in air at $750°C$. The scale formed on the surface of IN 738 alloy is thick and contain different corrosion products at various regions. The scale/alloy interface is fairly irregular and very thin dark layer rich in Al indicate that it consists primarily of Al_2O_3 (spot A-Figure 4.10). Because of the low intensity S peak, the presence of sulfides of Al cannot be presumed.

Above the alloy/scale interface, the presence of a thick, continuous grey layer rich in Cr and Ti indicate that it may be an intermixed oxide of Ti and Cr (spot B in Figure 4.10). The XRD results confirm the presence of only Cr_2O_3 (Figure 4.11), TiO_2 was not identified, probably, because of its low concentration in the powder sample. EDS analysis at spot C indicate a dark phase enriched in S indicating that it may consist of a mixture of Na_2SO_4 and probably some Cr and Ni sulfides.

EDS analysis at spot D (Figure 4.10) within the thin strip of dark phase, shows a fairly high levels of Ni, Cr and S. This dark phase may consists of sulfides of Ni and Cr (see spot D), which may be liquid at temperature. because the melting point of nickel sulfide ($690°C$) is lower than the test temperature ($750°C$). The formation of nickel sulfide (Ni_3S_2) was positively confirmed from XRD analysis shown in Figure 4.11. Just above the dark phase, a thin white layer is seen which is

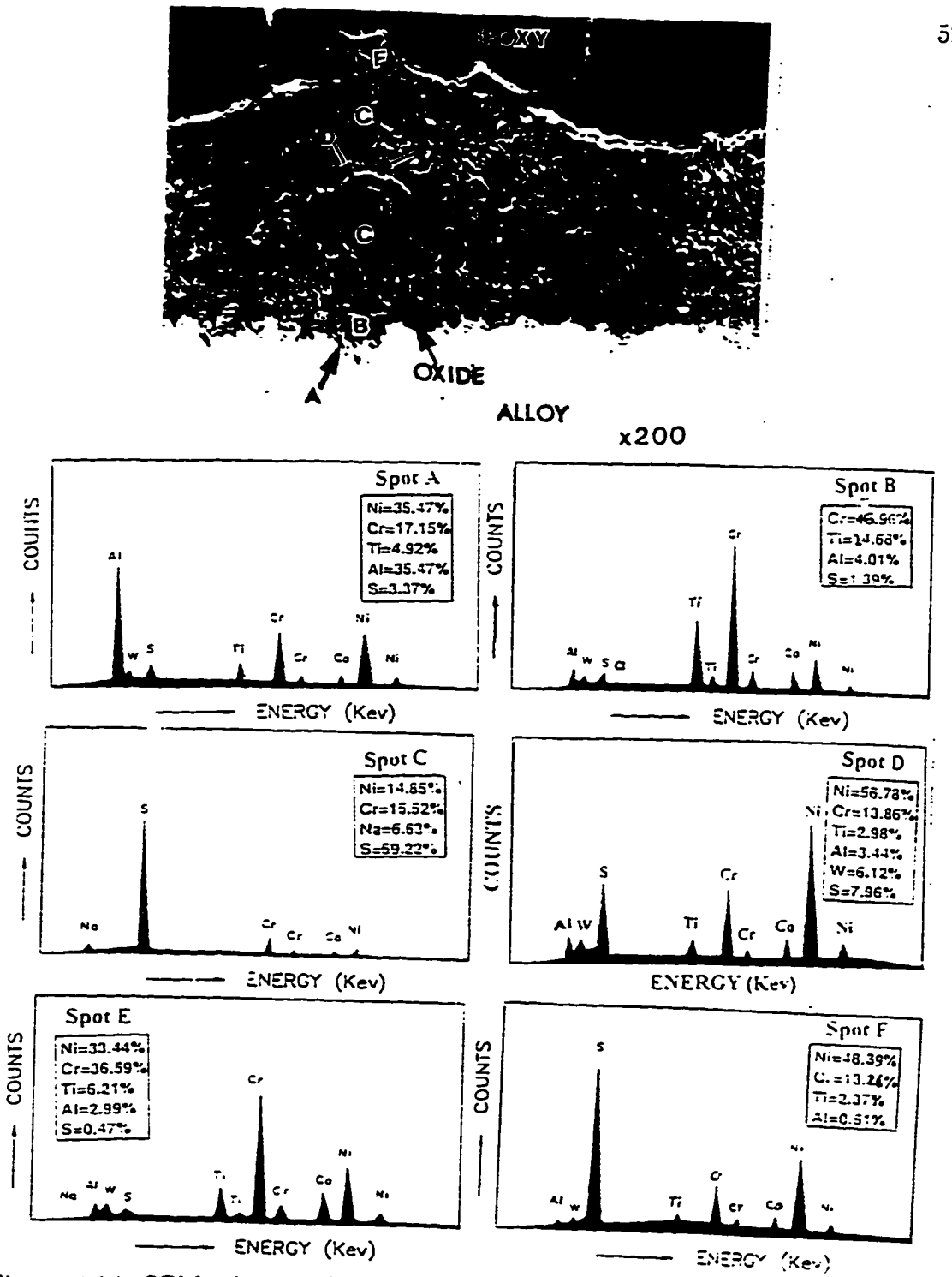

Figure 4.10: SEM micrograph and EDS spectra of 99% Na_2SO_4+1% $NaCl$ coated IN 738 after exposure for 150 cycles (1hr each) in static air at 750°C

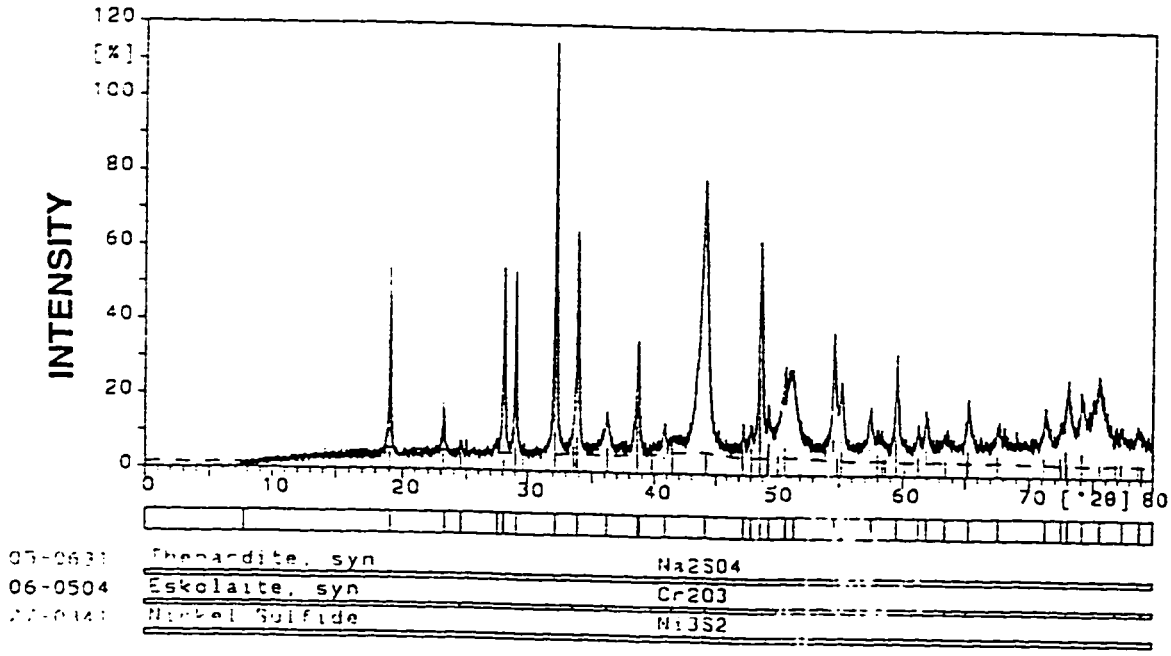

Figure 4.11: XRD pattern of 99% Na_2SO_4+1%$NaCl$ coated IN 738 after exposure for 150 cycle (1hr each) in static air at 750°C

rich in Cr/Ni indicating the presence of Cr_2O_3 and/or NiO (spot E in Figure 4.10). At the salt-gas interface, the scale is rich in Ni, S and Cr indicating the exclusive formation of nickel sulfide and probably chromium sulfide (spot F in Figure 4.10).

Figure 4.12 shows the cross-section morphology of a corroded sample of IN 738, coated with $75\%Na_2SO_4 + 25\%NaCl$ after 1 cycle at $750°C$ in air. The scale on the alloy surface is a thin, compact and protective layer of NiO (spot B in Figure 4.12). At the alloy/scale interface, a small pit enriched in Al is observed, which is probably due to the polishing powder used during sample polishing (spot A in Figure 4.12). Near the alloy/scale interface, undergrowing nodules rich in Cr and to some extent in Ti are formed discretely (spot C in Figure 4.12). This indicate that 1 hr of exposure at this high $NaCl$ concentration is too short to cause significant sulfidation in the alloy.

Figure 4.13 shows the corrosion morphology of $75\%Na_2SO_4 + 25\%NaCl$-coated specimen of IN 738 after exposure for 20 cycles at $750°C$. The morphological examination of the specimen cross-section shows the formation of Al-rich internal oxide layer within the alloy matrix below the interface (spot B). Such a layer was not present after the shorter 1 hr exposure (Figure 4.12) interface shows internal penetration of oxide (rich in Al) which frequently form at the alloy/scale interface. The island in the pit (spot C in Figure 4.13) is rich in Ni, Cr, and W and somewhat depleted in protective element (Al), indicating that it is probably a metal island.

EDS analysis at spot D (Figure 4.13) shows that the outer layer is rich in Al, Ti

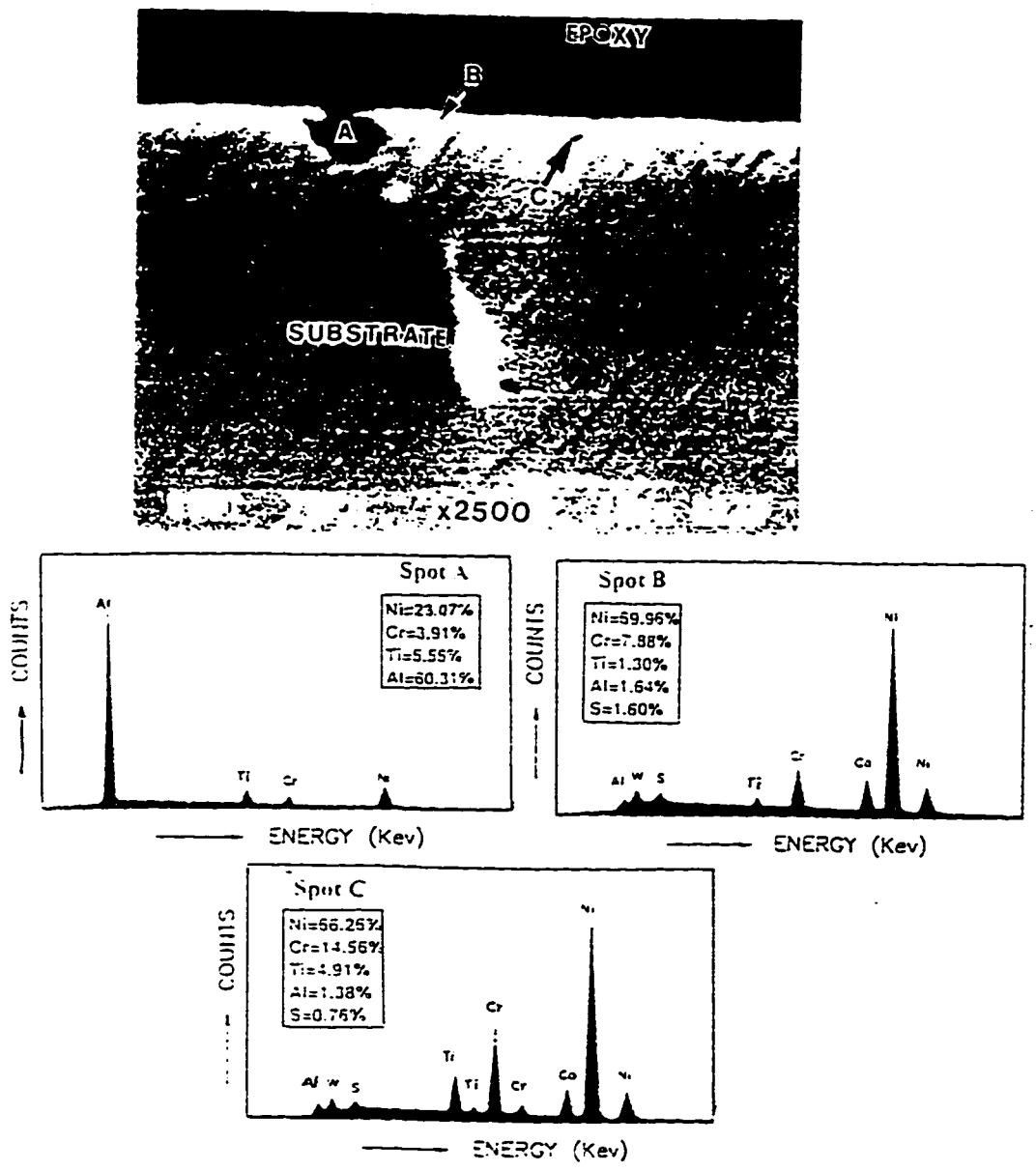

Figure 4.12: SEM micrograph of 75% Na_2SO_4+25%$NaCl$ coated IN 738 after exposure for 1 cycle (1hr each) in static air at 750°C

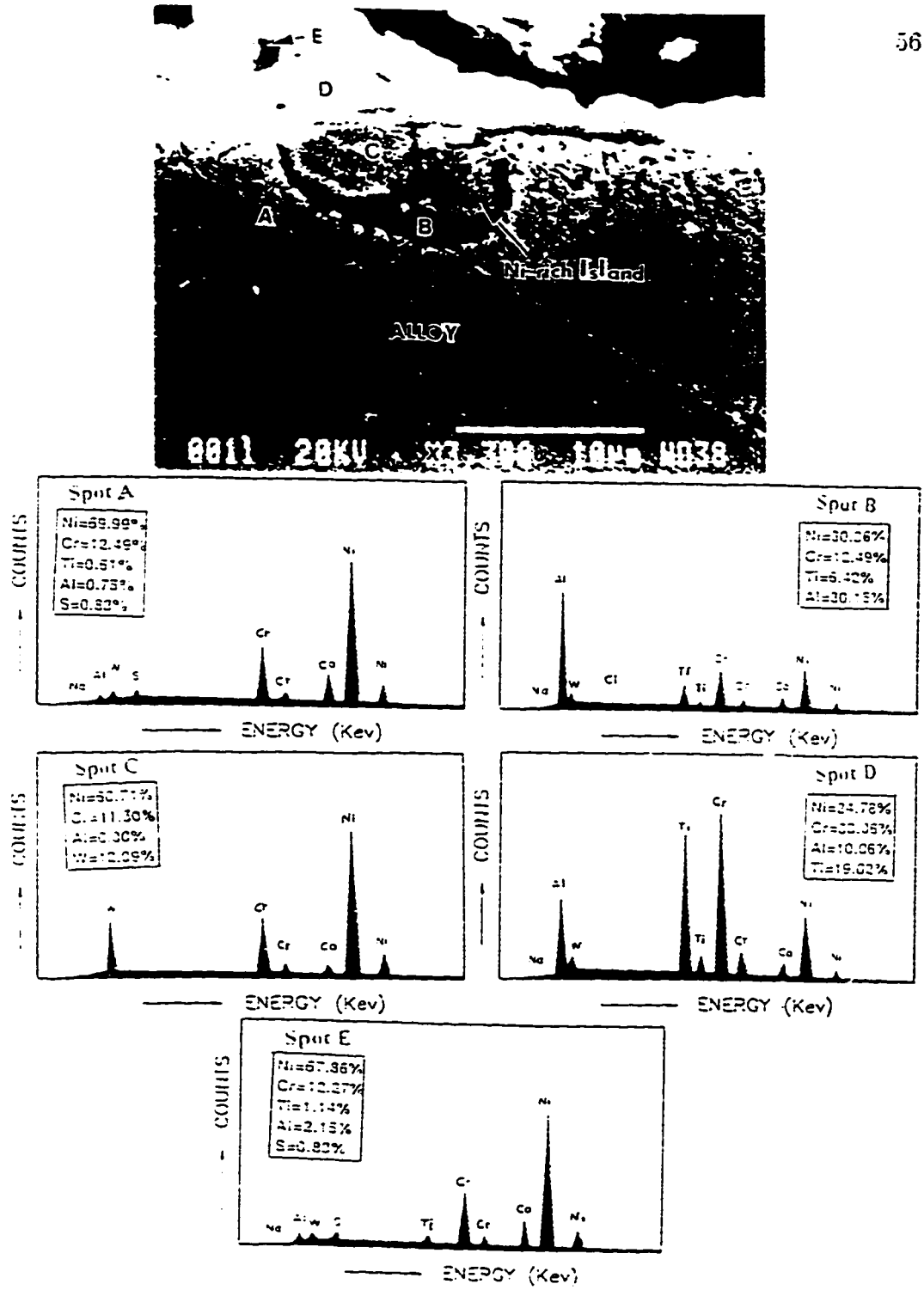

Figure 4.13: SEM micrograph and EDS spectra of $75\% Na_2SO_4 + 25\% NaCl$ coated IN 738 after exposure for 20 cycles (1hr each) in static air at $750^{\circ}C$

and Cr with no sulfur present in it, which indicate that it probably consists of a mixed oxide. XRD results (Figure 4.14) indicate that this layer consists primarily of Al_2O_3 and Cr_2O_3 and NiO. Below the alloy/scale interface, sulfide particles may be present in the zone of alloy depleted in Al (spot A in Figure 4.13). EDS analysis (spot B Figure 4.13) indicate that the dark layer enclosing the metal island consists primarily Al_2O_3, incorporating few white particles of NiO or Cr_2O_3. A dark spot in the outer scale layer (spot E) is rich in Ni and to some extent in Cr, indicating that it may consists of NiO and Cr_2O_3. Because of its dark color, it may be presumed that little sulfides formed in the outer scale might have oxidized, appearing as an oxidized sulfide.

Figure 4.15 shows the cross-sectioned morphology of the IN 738 specimen, coated with the salt mixture $75\%Na_2SO_4 + 25\%NaCl$, after extended cyclic exposure upto 150 cycles (1hr each) at $750°C$. The specimen surface contains numerous wide but shallow pits, typical of low temperature hot corrosion with a thick blister cover

Detailed examination of the x-ray maps shown in Figure 4.15 reveals the presence of a very thin continuous Al-rich layer at the metal/corrosion product interface (dark colour, Figure 4.16).

Above this layer, still at the pit bottom an almost continuous thick grey layer exist. This layer is rich in chromium, titanium as well as oxygen. Both layers are rich in sulfur towards the metal side indicating that the inner layer consist primarily of Al-oxide and outer thicker grey layer consists of a mixture of Cr and Ti oxides.

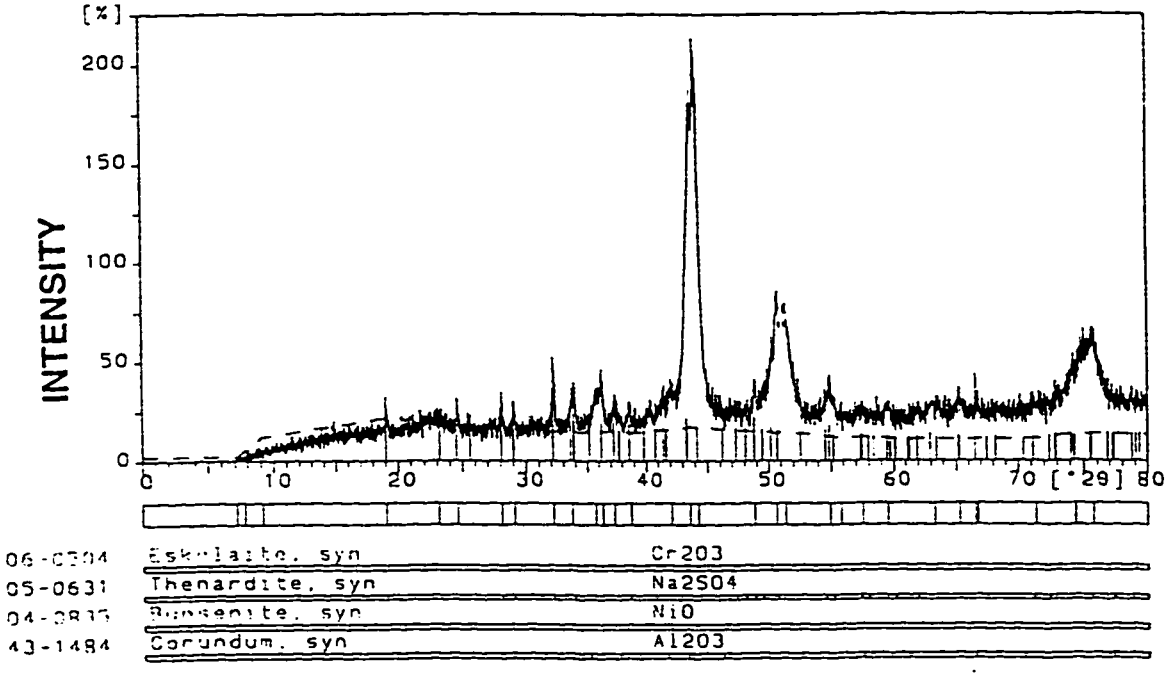

Figure 4.14: XRD pattern of $75\%Na_2SO_4$+$25\%NaCl$ coated IN 738 after exposure for 20 cycles (1hr each) in static air at $750°C$

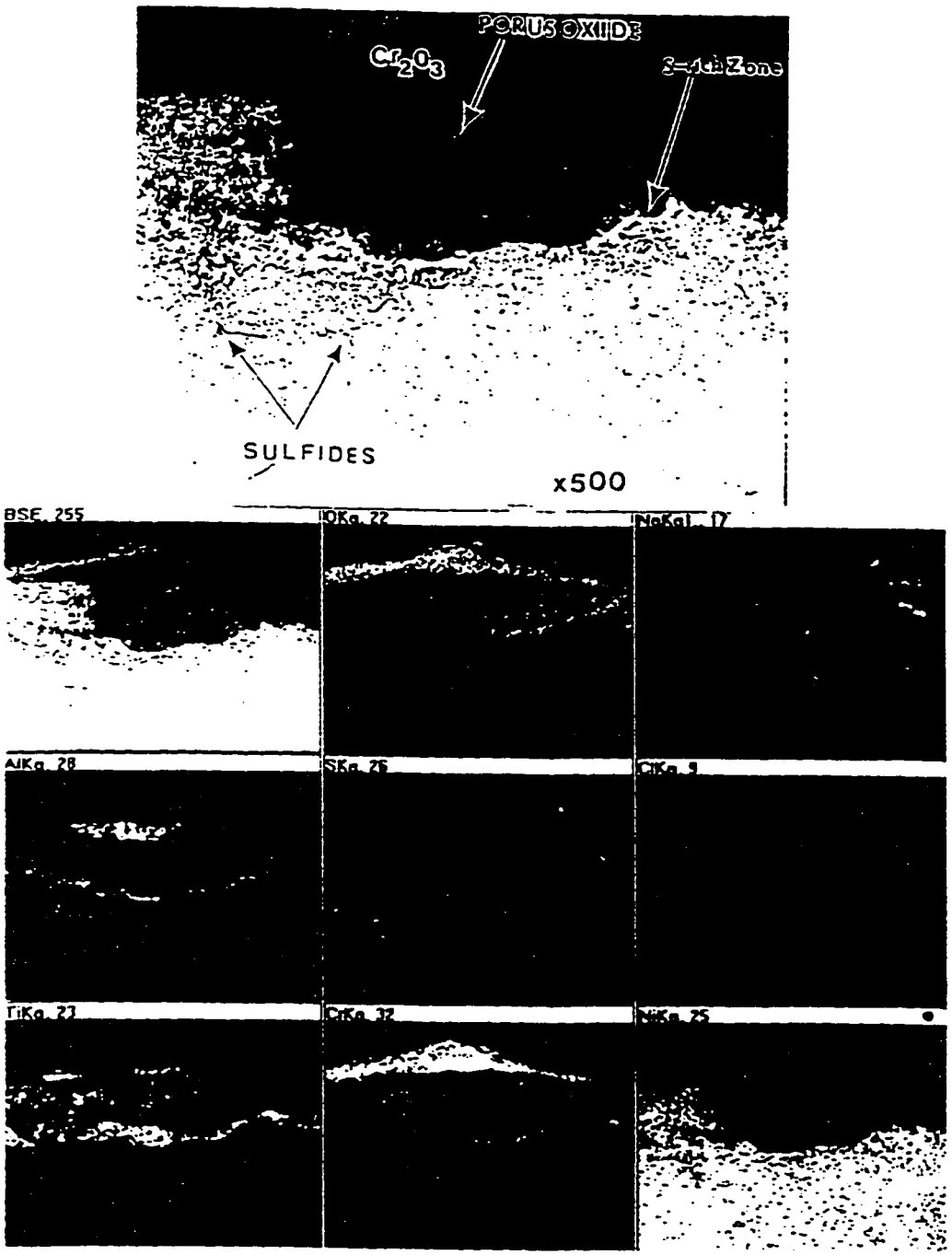

Figure 4.15: SEM micrograph and elemental distribution of 75% Na_2SO_4 + 25% $NaCl$ coated IN 738 after exposure for 150 cycles (1hr each) in static air at 750°C

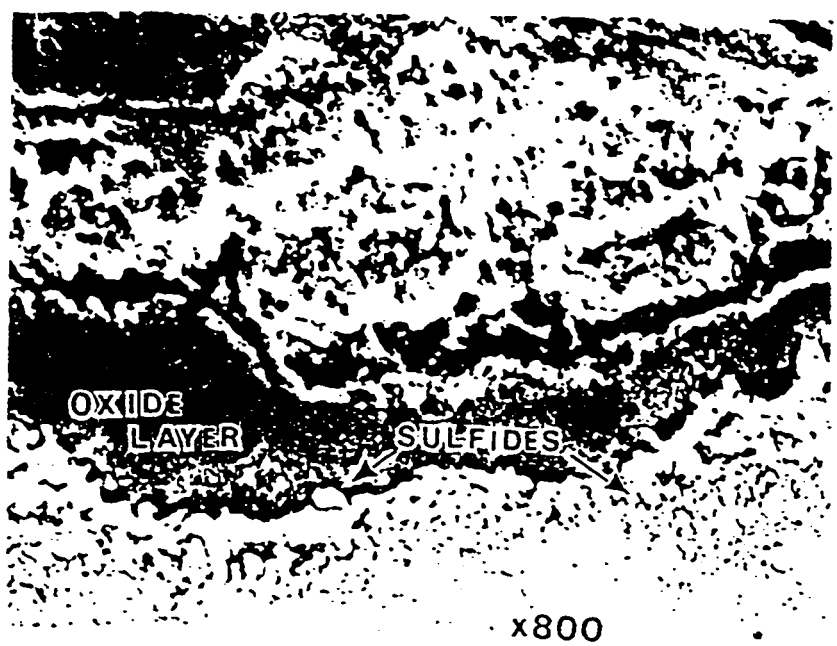

Figure 4.16: SEM micrograph showing details of Figure 4.15 at pit-alloy interface (inset of Figure 4.15)

The outer most scale above the pit is a chromium and oxygen rich mound, appears as a reprecipitated oxide above an Al_2O_3 layer. Titanium and sodium are distributed all over the pit region. Detailed observation of Na and S x-ray maps (Figure 4.15) reveals that Na is present at the outer region whereas sulfur is concentrated only at pit/alloy interface. This suggests penetration of sulfur into the alloy probably by a sulfate decomposition mechanism .

Well below the pit region, few particles of aluminum sulfides may also be seen below the rich sulfur zone suggesting sulfur penetration into the alloy. The presence of aluminium sulfide and probably chromium sulfide particles below the pit region is shown in enlarged view in Figure 4.16. XRD results of the powder sample (scrapped off upto about 0.55 mm deep in the substrate) show the presence of Al_2S_3 rather than CrS (Figure 4.17), since the intensity peak of CrS is not coinciding exactly with the diffraction peaks.

Figure 4.18 shows the cross-section morphology of isothermally exposed IN 738 specimen, coated with $75\%Na_2SO_4 + 25\%NaCl$ after continuous exposure (without thermal cycling) for 150 hrs. The scale formed on the alloy surface shows a broad frontal attack (no shallow pits), typical of high temperature hot corrosion. The scale consists of an outer porous oxide scale (spot D) and intermediate scale containing numerous $Ni-$ rich islands (spot D in Figure 4.18). Below the irregular alloy/scale interface, numerous sulfide particles, presumably Cr, Ni or Ti, are formed deep in the alloy (spot B).

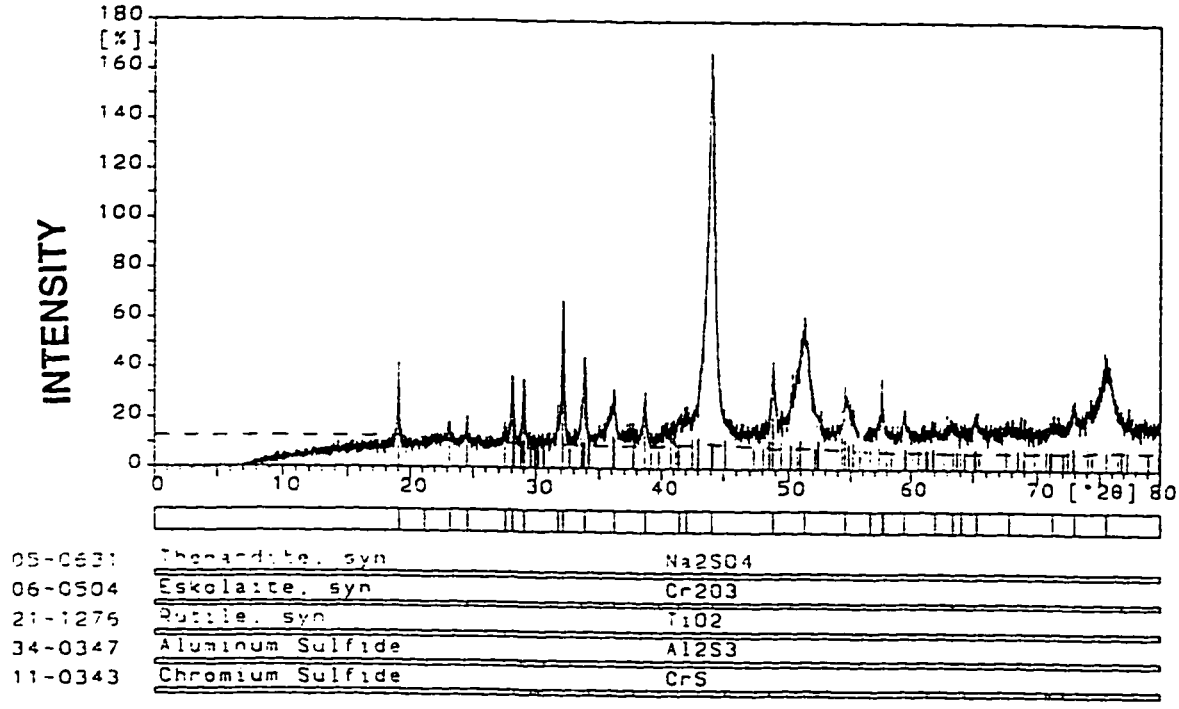

Figure 4.17: XRD pattern of $75\%Na_2SO_4$+$25\%NaCl$coated IN 738 after exposure for 150 cycles (1hr each) in static air at $750°C$

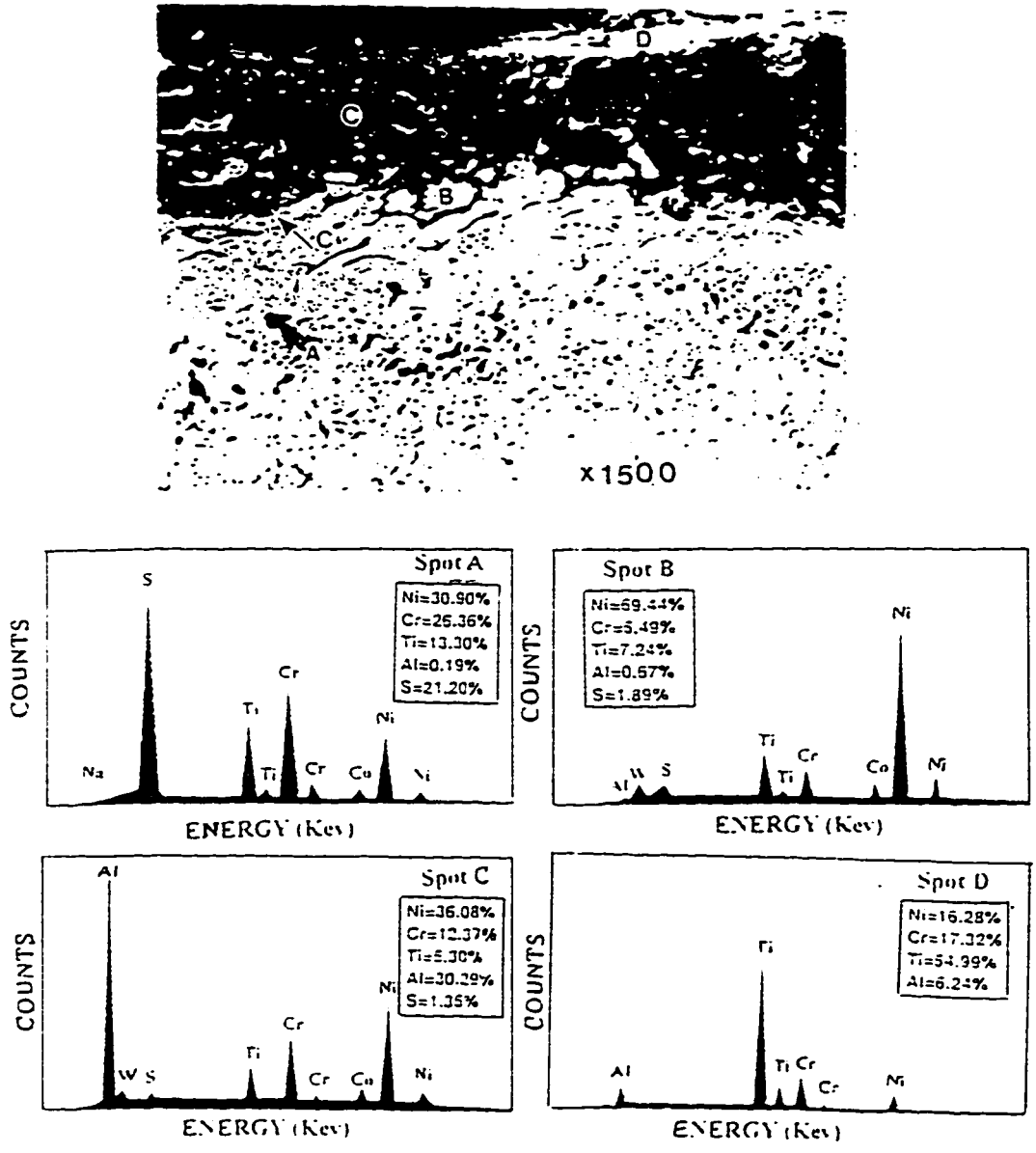

Figure 4.18: SEM micrograph and EDS spectra of $75\%Na_2SO_4$+$25\%NaCl$ coated IN 738 after continuous exposure (isothermal heating) for 150 hrs in static air at $750°C$

The effect of $25\%NaCl$ on corrosion morphology Na_2SO_4-coated IN 738 can be clearly demonstrated by comparing Figure 4.5 and Figure 4.15. Pure Na_2SO_4 did not accelerate the attack and the subscale contains only particles of oxide. No sulfide rich zone was seen in the sample corroded in pure sodium sulfate. However, a thin sulfur rich zone of either AlS or CrS is seen ahead of the oxidation front in Figure 4.15 (with $Na_2SO_4 + 25\%NaCl$). This suggests the rate of attack of the alloy exposed to $Na_2SO_4 + 25\%NaCl$ after 150 cycles is severe when compared to the sample exposed to pure Na_2SO_4, which is also clearly evident from the kinetic results (Figure 4.1).

In addition, the outer scale in Figure 4.5 shows enormous amount of unreacted Na_2SO_4, however, sulfate was totally consumed in sulfate/chloride mixture (Figure 4.15). Similar features are also observed on the surface of corroded samples in pure Na_2SO_4 and $75\%Na_2SO_4 + 25\%NaCl$ mixture (Figure 4.19 and Figure 4.20). The EDS analysis of outer surface of the sample exposed to pure Na_2SO_4 (Figure 4.19) shows high concentrations of Na and S, indicating the presence of large amount of unreacted sodium sulfate. The outer scale of the sample exposed to sulfate/chloride mixtures shows several dark nodules growing over the scale (spot 1 and spot 3 in Figure 4.20). These dark nodules are enriched in Cr, Ti and to some extent in Al, indicating the presence of oxide of Ti, Cr and Al. The outer scale in Figure 4.15 also shows Cr and Al oxides. Thus the results obtained from the cross-sectioned specimens correlates that of the results obtained from surface

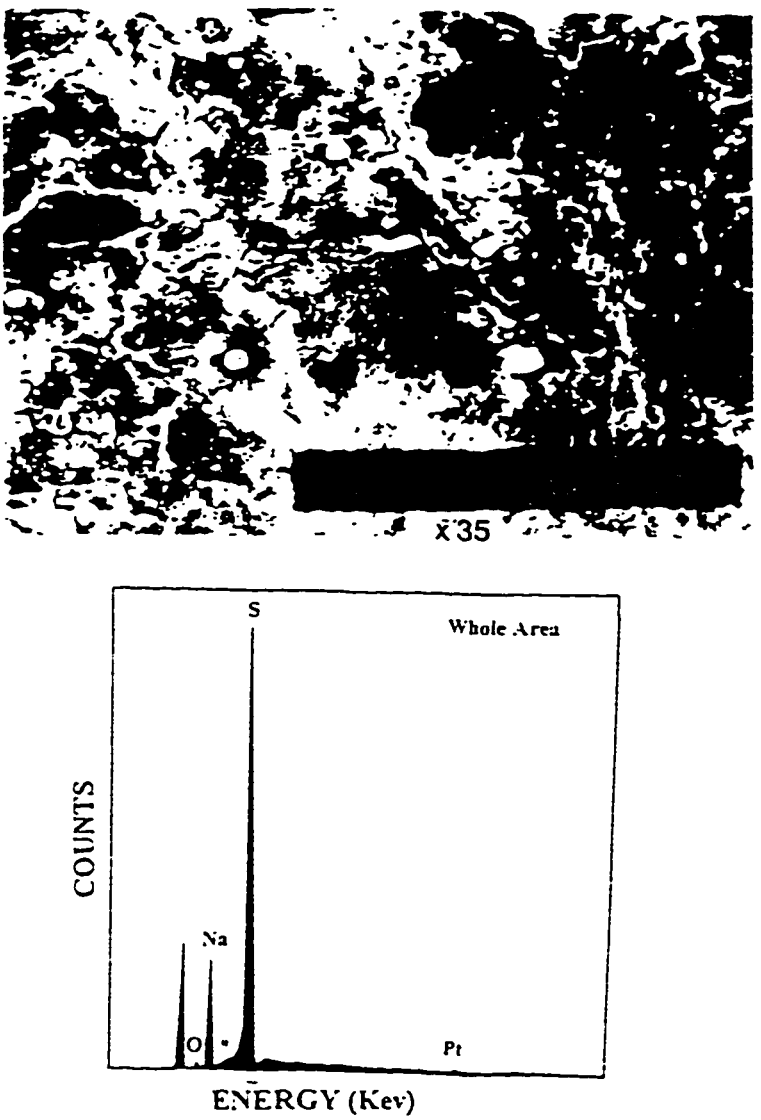

Figure 4.19: SEM micrograph (surface morphology) and EDS spectra of pure Na_2SO_4-coated IN 738 after exposure for 150 cycles (1 hr each) in static air at 750°C

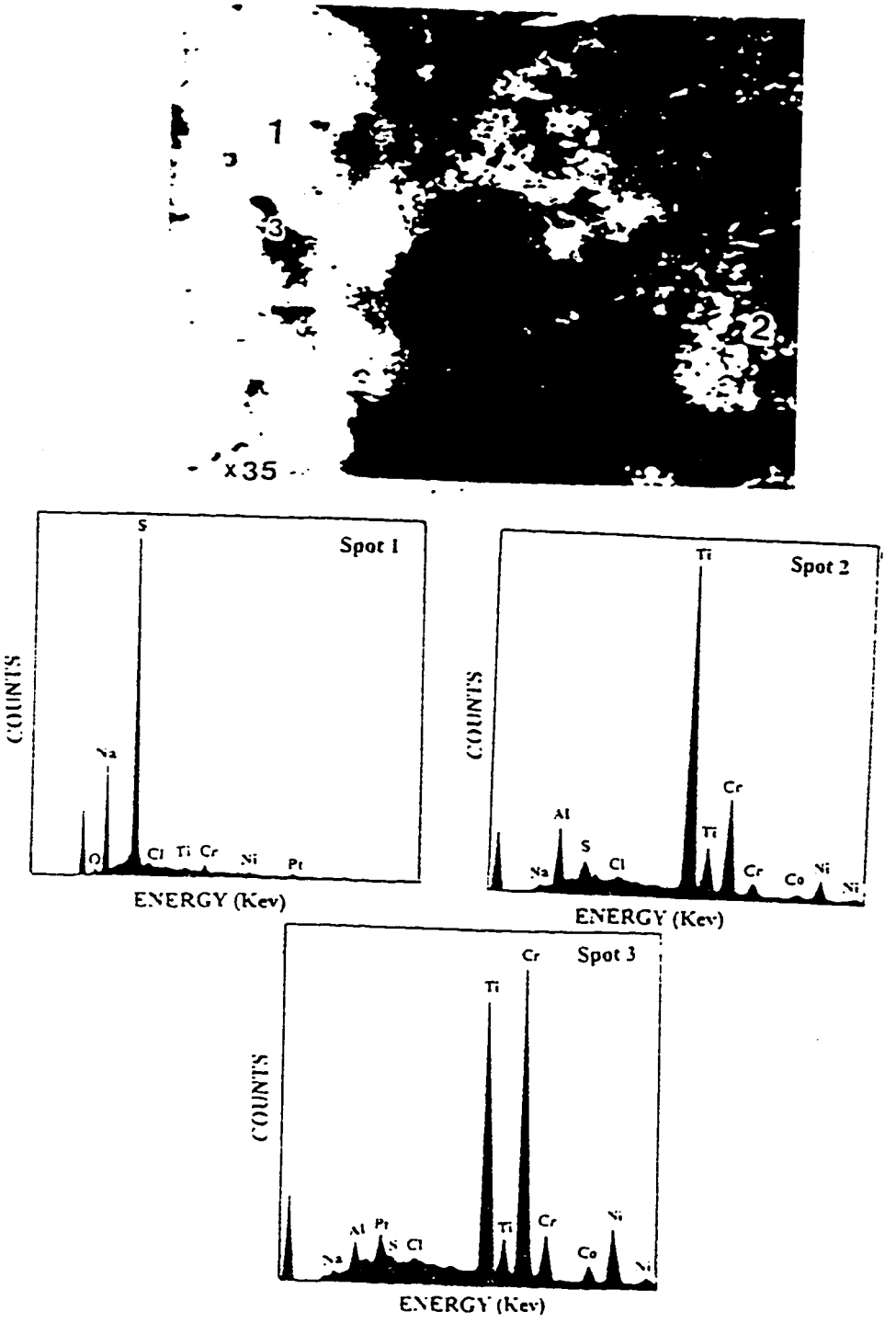

Figure 4.20: SEM micrograph (surface morphology) and EDS spectra of $75\% Na_2SO_4 + 25\% NaCl$-coated IN 738 after exposure for 150 cycles (1 hr each) in static air at $750^{\circ}C$

analysis.

A yellow deposit has been formed on the surface of the commercial Al_2O_3 ceramic boat containing $Na_2SO_4 + 25\%NaCl$ coated IN 738 sample after exposure for 20 cycles. Surface analysis of the yellow deposit has been performed using the technique of X-ray photoelectron Spectroscopy to identify the chemical species in the deposit on the boat. This analysis was conducted to observe which corrosion products were lost during the hot corrosion of IN 738 sample exposed to sulfate/chloride mixtures.

Figure 4.21a shows the XPS analysis of the ceramic base substrate, which mainly contain Al and Si. Figure 4.21b shows clearly the presence of significant amount of Na, Zn (probably an impurity) and Cr, and little amount of S and Cl . Chromium exists as $Cr^{+}6$ and $Cr^{+}3$ oxidation states. Because of high intensity peaks of sodium and chromium and chlorine, it appears that $CrCl_3$ and Na_2CrO_4 may be present in the yellow deposit. These results suggests that the sample exposed to sulfate/chloride mixture shows heavy loss of corrosion products as metal chlorides and spinels. No yellow deposit was observed on ceramic tube when alloy specimens were corroded in pure Na_2SO_4 coated conditions. Due to the loss of vapor species the corrosion rate is severe at initial stages for $Na_2SO_4 + 25\%NaCl$ coated sample compared to the sample exposed to pure Na_2SO_4 as shown in Figure 4.1.

In summary, the above results indicate that the effect of either $1\%NaCl$ or $25\%NaCl$ on pure Na_2SO_4 coated sample after exposure for 20 cycles (initial stages) is significant. In the case of sample exposed to pure Na_2SO_4, a protective oxide

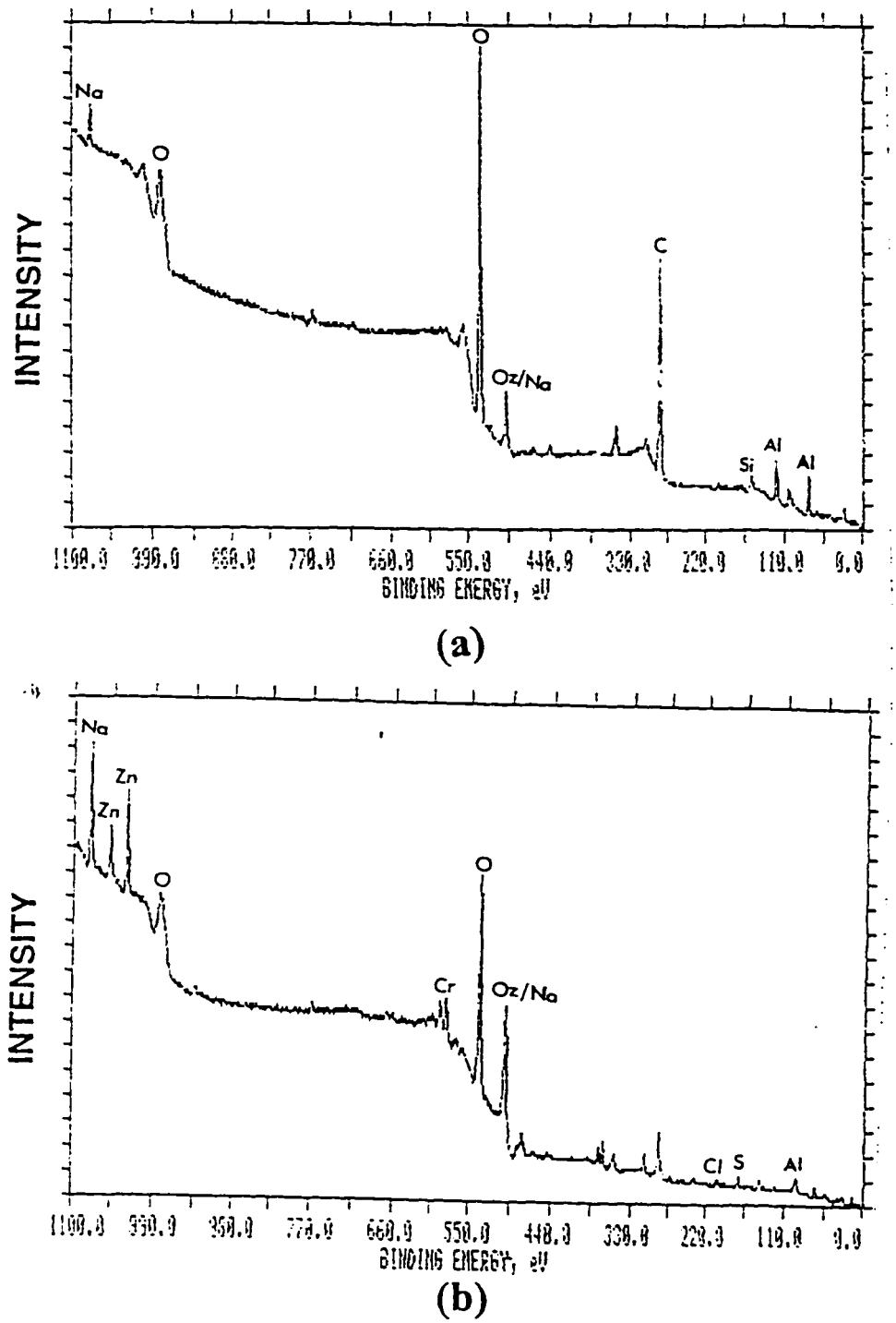

Figure 4.21: XPS spectra of (a) ceramic substrate (as-received) (b) yellow deposit on ceramic tube

layer was formed indicating no corrosion (Figure 4.2).

The sample exposed to either 1%$NaCl$ (Figure 4.7) or 25%$NaCl$(Figure 4.13) after 20 cycles shows the presence of internal dark particles below the alloy/scale interface and an alloy depleted in Al zone is also observed (Figure 4.13). This suggests that the corrosion rate in sulfate/chloride mixture was increased due to the depletion of a key element (Al) in the alloy right from the initial period of corrosion.

After prolonged exposure for 150 cycles, the sample corroded in Na_2SO_4 + 25%$NaCl$ shows a typical LTHC morphological features, consisting of a thin S-rich zone at the pit-alloy interface (Figure 4.15). Neither the sample corroded in pure Na_2SO_4 (Figure 4.5) nor in 1%$NaCl$ (Figure 4.10) showed a pitting type of morphology consisting of a thin S-rich zone at the pit/alloy interface. In addition to this, the sample exposed to 1%$NaCl$ (Figure4.10) shows the formation of sulfides in the outer scale when compared to the sulfide formation at the pit region for an alloy exposed to 75%Na_2SO_4 + 25%$NaCl$ mixture.

4.1.2 Mar-M 509

Figure 4.22 shows the kinetic results of thermally cycled Mar-M 509 specimen exposed under different hot corrosion conditions. The sample corroded in 75%Na_2SO_4+ 25%$NaCl$ mixture exhibited high corrosion rate than the specimen subjected to either pure Na_2SO_4 or 99%Na_2SO_4 + 1%$NaCl$ conditions after 150 cycles. The initiation of hot corrosion is faster for 25% $NaCl$ enriched salt. Because of faster

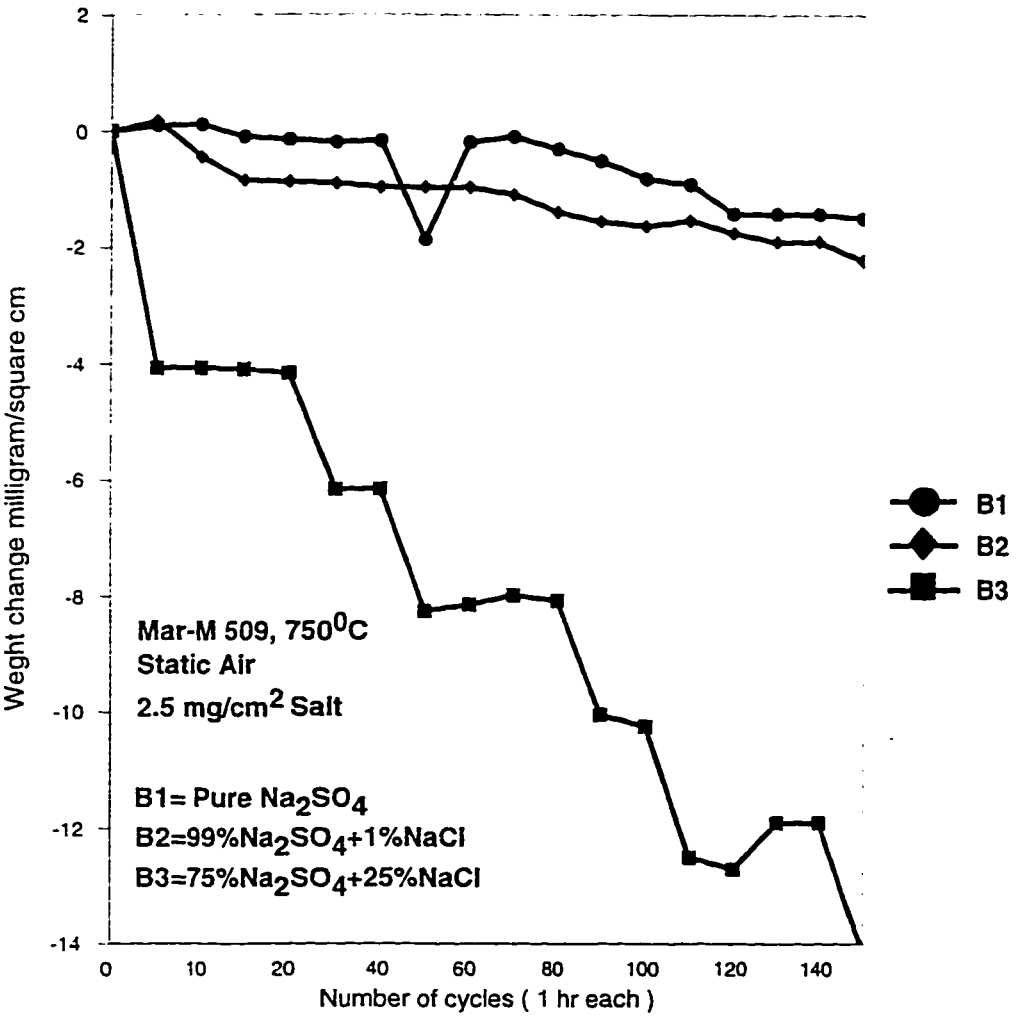

Figure 4.22: Rate of hot corrosion of Mar-M 509 at 750°C

growth rate of CoO than NiO, the sample exposed to pure sodium sulfate undergoes severe scale spalling after extended period of exposure (around 50 cycles). In the case of $Na_2SO_4 + 25\%NaCl$ mixture, the sample loses weight due to the formation of volatile products as long as $NaCl$ remains in the Na_2SO_4, which losts for 12 hrs and then the reformation of protective oxide scale continues due to the presence of solid Na_2SO_4. It is also clear from the kinetic results (Figure 4.22) that the weight loss due to thermal cylcing alone does not have significant effect when the $NaCl$ in Na_2SO_4 breaks down completely and hence the formation of oxide scale continues.

Figure 4.23 shows the morphology in cross-section of Mar-M 509 coated with pure Na_2SO_4, after exposure for 20 cycles (1 hr each) at $750°C$ in air. The scale formed on the alloy surface is primarily enriched in Cr indicating the presence of Cr_2O_3 (spot D in Figure 4.23). At the alloy/oxide interface, $Cr-$ depleted alloy islands (because the semi-quantitative results shown in the inlet box indicate only 16% Cr when compared to $27\%Cr$ in the alloy) were observed (spot A). A dark layer enclosing the metallic islands is rich in Co and Cr, indicating that it may consist of Cr_2O_3 and CoO or $CoCr_2O_4$ (spot C in Figure 4.23). It also appears from the EDS analysis at spot D that few Ni- sulfide particles may be present in the dark layer. XRD results confirm the presence of Cr_2O_3, CoO and NiS (Figure 4.24).

After exposure for 150 cycles, the outer scale is highly porous and appears to be exfoliated (spot D in Figure 4.25). EDS analysis at spot D show that the outer scale (white) is enriched in Cr, Co and S, which may consists of either Cr_2O_3 and

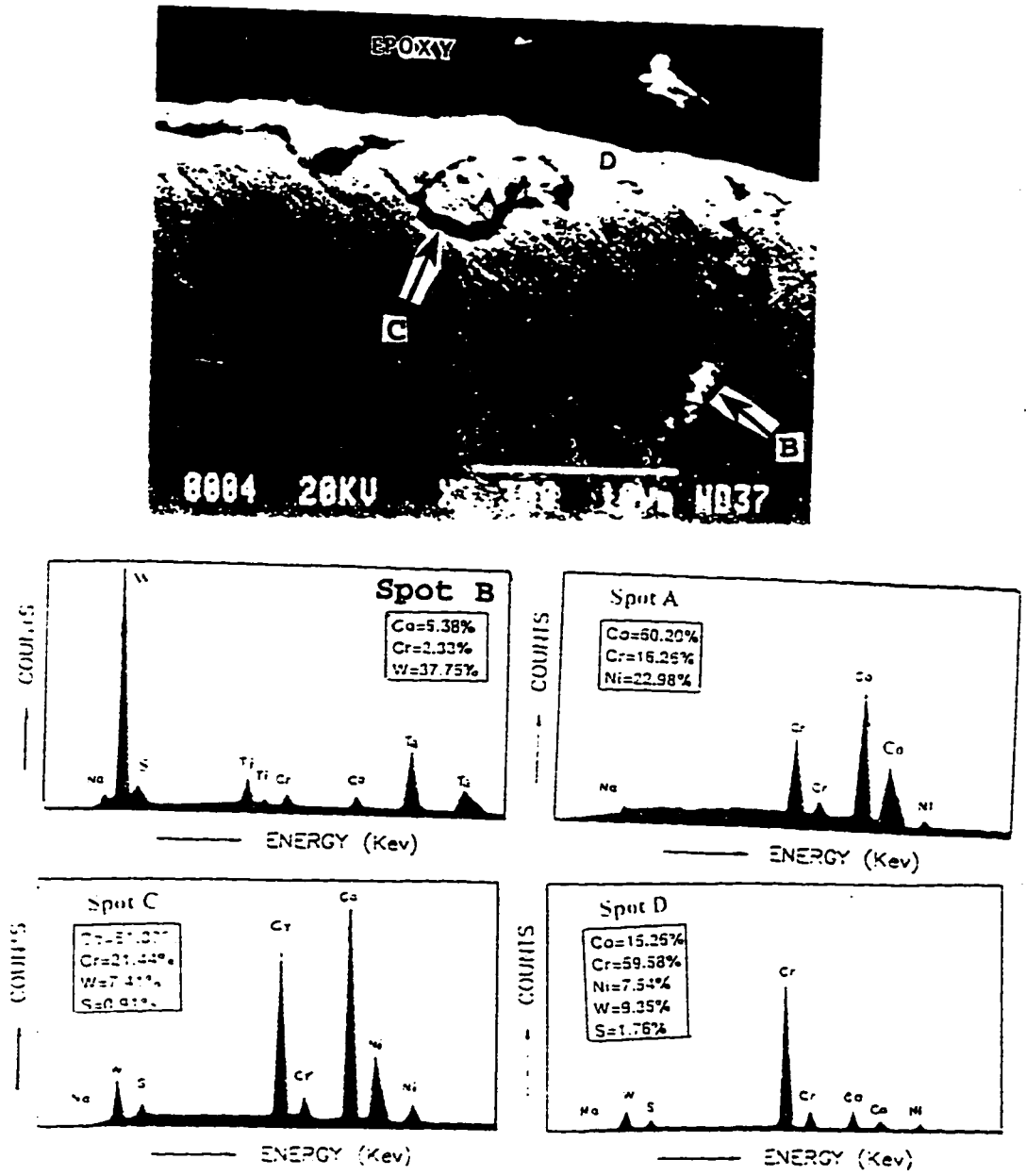

Figure 4.23: SEM micrograph and EDS spectra of pure Na_2SO_4 coated Mar-M 509 after exposure for 20 cycles (1hr each) in static air at $750°C$

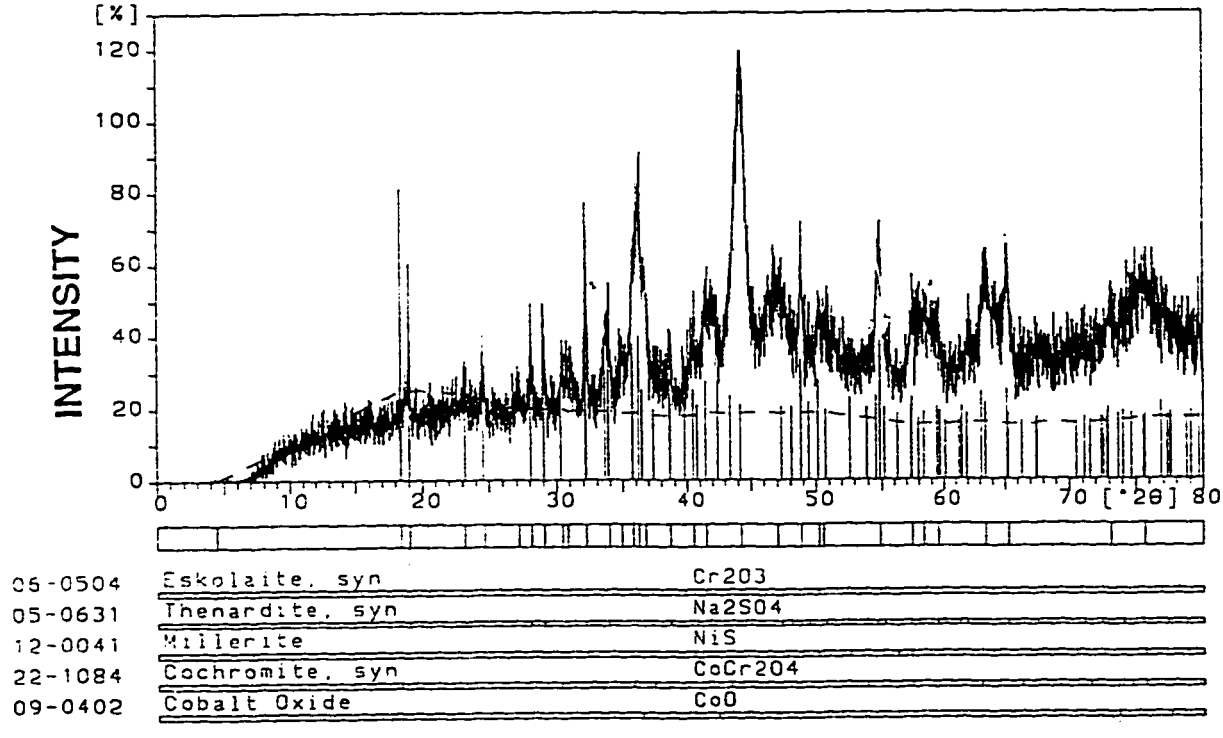

Figure 4.24: XRD pattern of pure Na_2SO_4 coated Mar-M 509 after exposure for 20 cycles (1hr each) in static air at $750°C$

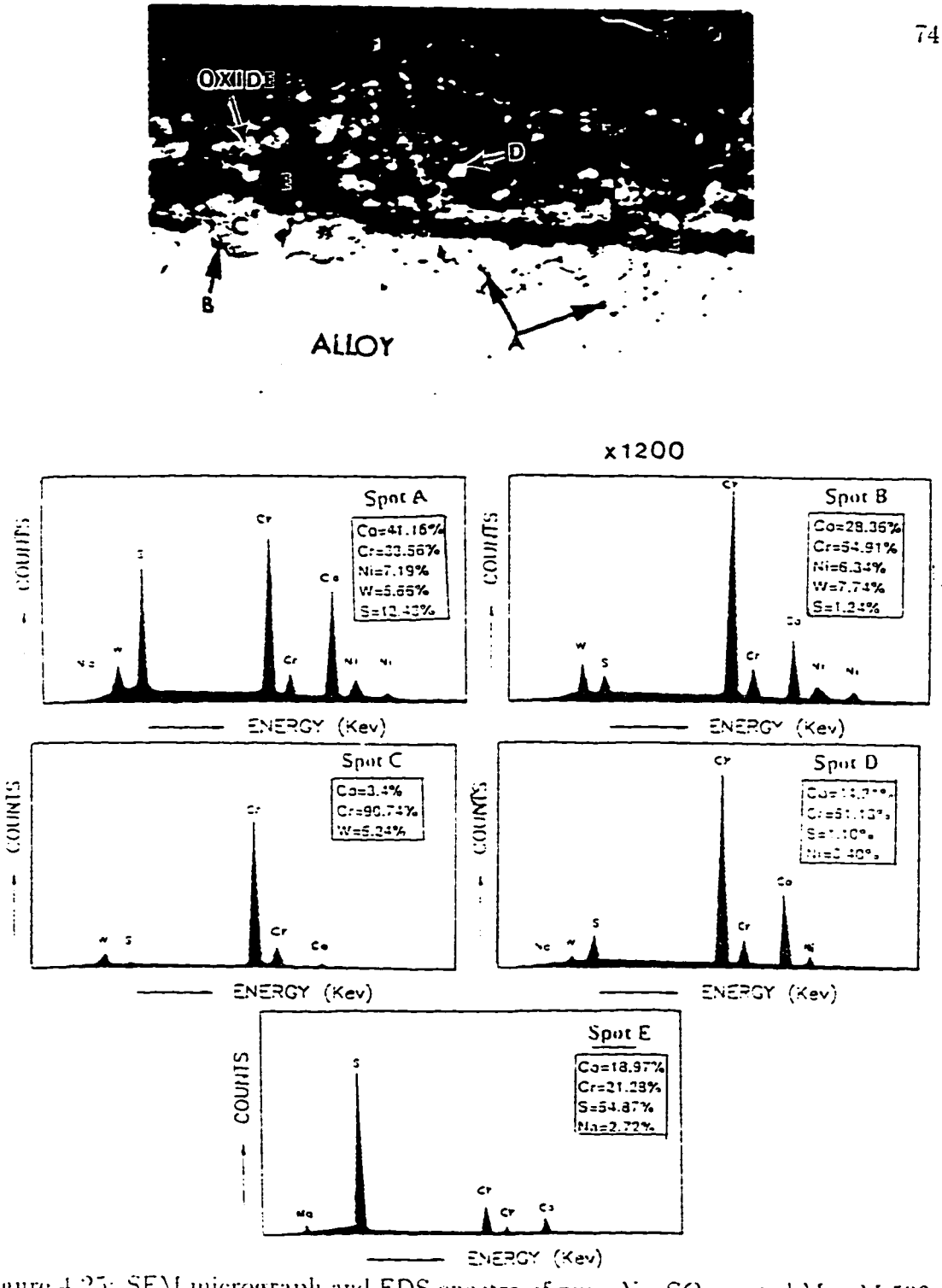

Figure 4.25: SEM micrograph and EDS spectra of pure Na_2SO_4 coated Mar-M 509 after exposure for 150 cycles (1hr each) in static air at 750°C

Co_3O_4 and few sulfides. XRD results also confirm the strong presence of these oxides in the outer scale (Figure 4.26). Near the alloy/oxide interface, an irregular alloy surface containing of small pits filled with Cr_2O_3 oxide is observed (spot C in Figure 4.25). A dark layer below the Cr_2O_3 at the pit/alloy interface is primarily enriched in Cr and Co (spot B in Figure 4.25) indicating the formation of mixed layer of CoO/Cr_2O_3. Just below the alloy/oxide interface, numerous sulfide particles are formed. EDS analysis at spot A (Figure 4.25) indicate that these particles may consist of either Cr or Co-sulfides. XRD results (Figure 4.26) indicate only the presence of oxides.

Figure 4.27 shows the morphology of Mar-M 509 coated with $75\%Na_2SO_4 + 25\%NaCl$ after exposure for 1 hr in air. The scale formed on the alloy surface is a thin, adherent and protective layer of cobalt oxide with little amount of Cr_2O_3 (spot A in Figure 4.27). EDS analysis at spot B shows few embedded particles are enriched in W indicating that it may be WC particles. Similar particles are observed deep in the alloy (spot C).

After exposure for 20 cycles, the outer scale formed on the alloy surface appearing light at the salt-gas interface is fairly porous, and enriched mainly in Co, Cr and S indicating that it may consist of sulfides of Co and Cr.(spot F in Figure 4.28). The intermediate grey layer is primarily enriched in Cr, indicating the presence of Cr_2O_3 (spot D in Figure 4.28). A dark phase in the matrix of grey oxide layer is enriched in Co and Cr, probably as $CoCr_2O_4$ (spot E in Figure 4.28).

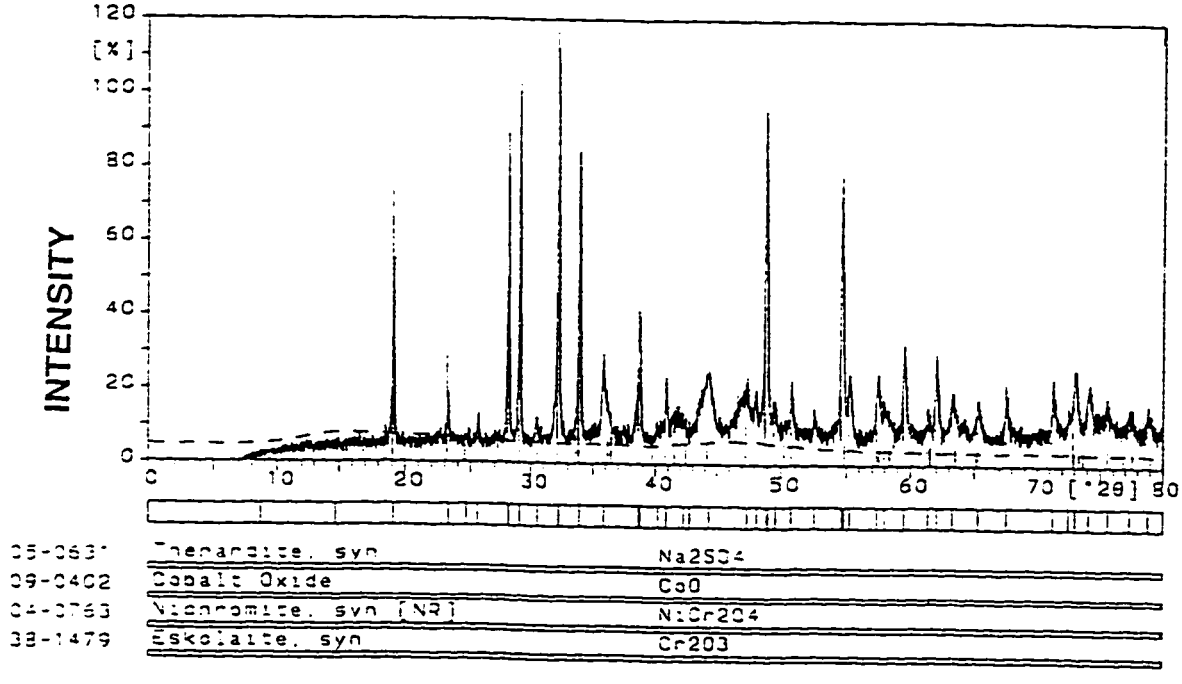

Figure 4.26: XRD pattern of pure Na_2SO_4 coated Mar-M 509 after exposure for 150 cycles (1hr each) in static air at 750°C

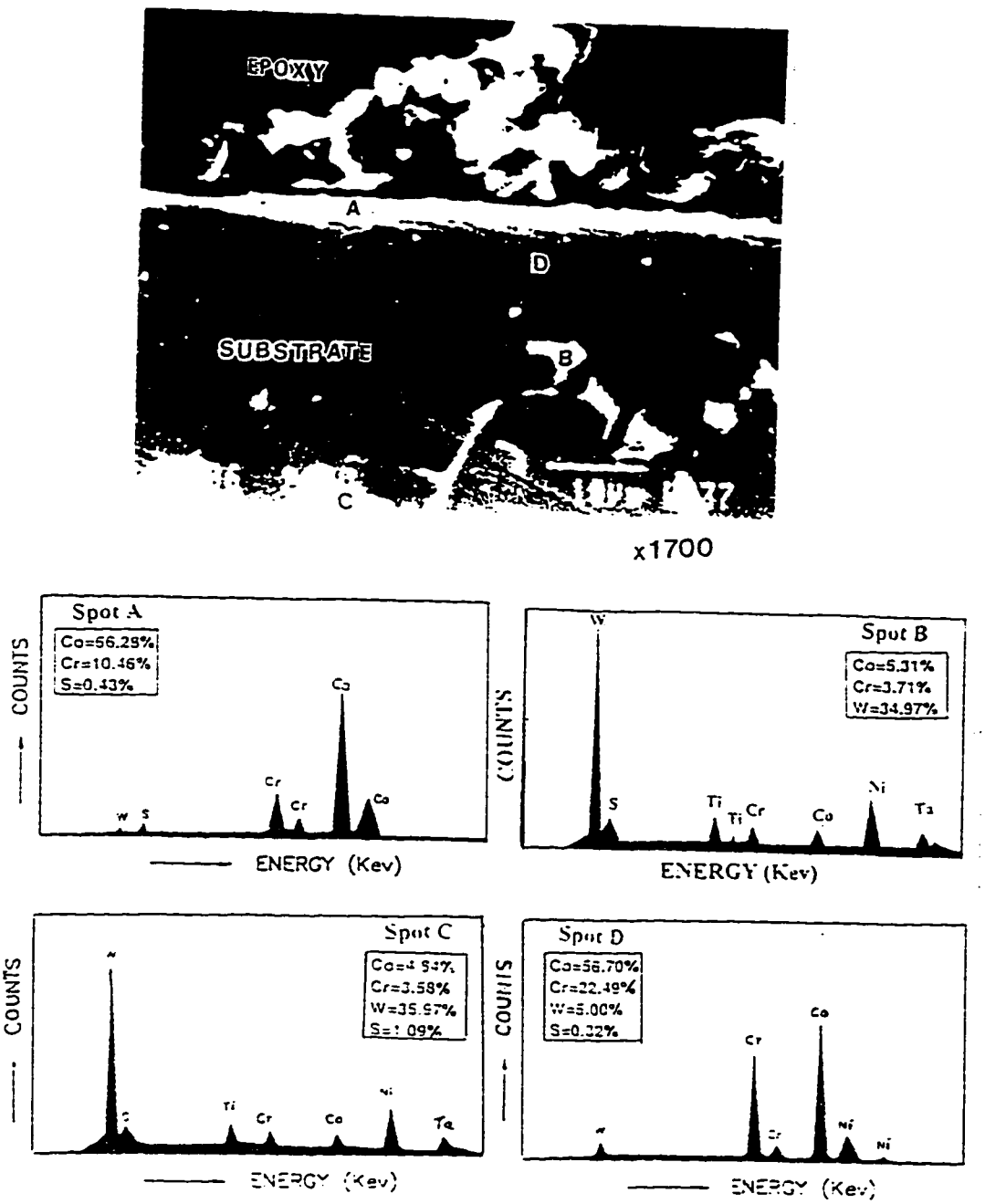

Figure 4.27: SEM micrograph and EDS spectra of $75\%Na_2SO_4+25\%NaCl$ coated Mar-M 509 after exposure for 1 cycle (1hr each) in static air at 750°C

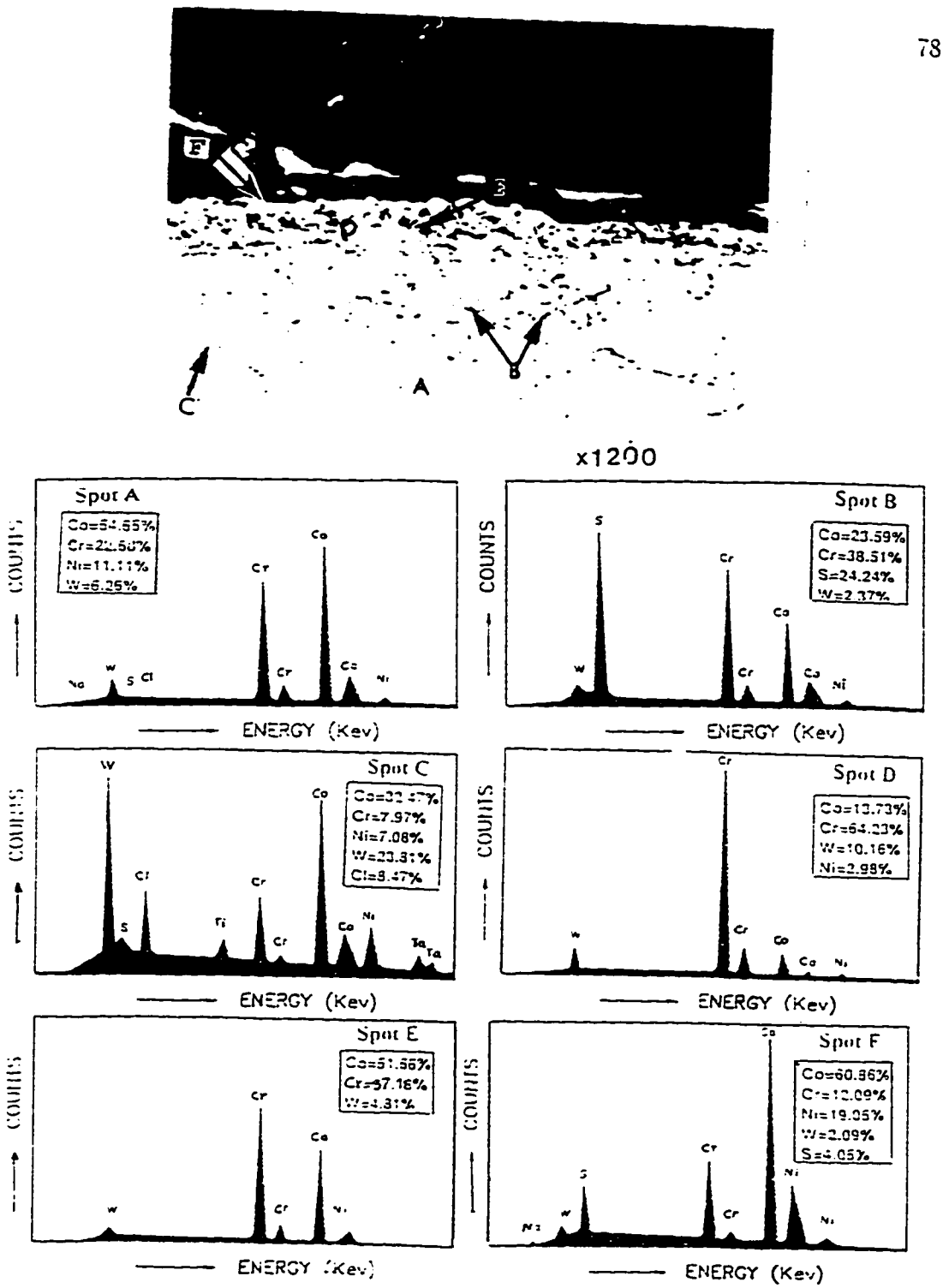

Figure 4.28: SEM micrograph and EDS spectra of $75\%Na_2SO_4$+$25\%NaCl$ coated Mar-M 509 after exposure for 20 cycles (1hr each) in static air at $750°C$

Below the alloy/oxide interface, the subscale consists of numerous particles of sulfides rich in which may probably be present as CrS (spot B in Figure 4.28). EDS analysis at spot C shows that the white particles are enriched in W, Co and Cl suggesting the presence of either W-carbides or oxychlorides of W. XRD results did not confirm the presence of chlorides (Figure 4.29)

Comparison of Figure 4.28 and Figure 4.23 indicates that the effect of 25% $NaCl$ on Na_2SO_4-coated samples after 20 cycles is significant with enhanced internal sulfidation in the substrate. Scale in pure sulfate consists of metal fragments whereas such feature is not evident in $NaCl$ enriched salt.

The microstructure of a corroded sample of Mar-M 509 in $Na_2SO_4 + 25\% NaCl$ mixture after prolonged exposure periods (after 150 cycles), Figure 4.30, shows type II hot corrosion morphology. X-ray mapping (Figure 4.30) indicates that a thin enriched zone of sulfur at the pit /metal interface may consists of CrS (see Cr and S x-ray maps). Below the pit/metal interface, there is no layer of alloy depleted in Cr because Cr x-ray does not show dark layer below the pit/metal interface. Chromium is enriched as Cr_2O_3 within the pit region. However, Co is depleted in the pit and probably reprecipitated as Co_3O_4 at the salt-gas interface (see Co x-ray map). The presence of Co_3O_4 has been confirmed by XRD (Figure 4.31). Tungsten is distributed all over the pit probably as oxide of W. Na and S x-ray map reveal that sulfate was consumed to a greater extent after prolonged exposure of the sample.

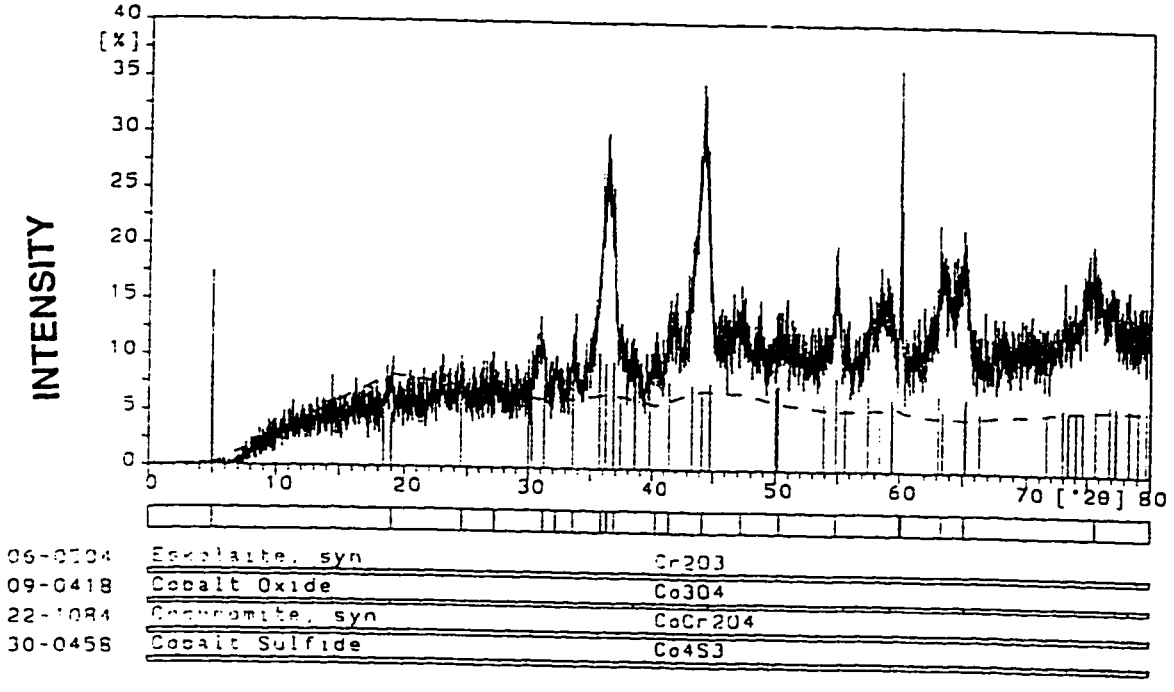

Figure 4.29: XRD pattern of $75\%Na_2SO_4+25\%NaCl$ coated Mar-M 509 after exposure for 20 cycles (1hr each) in static air at $750°C$

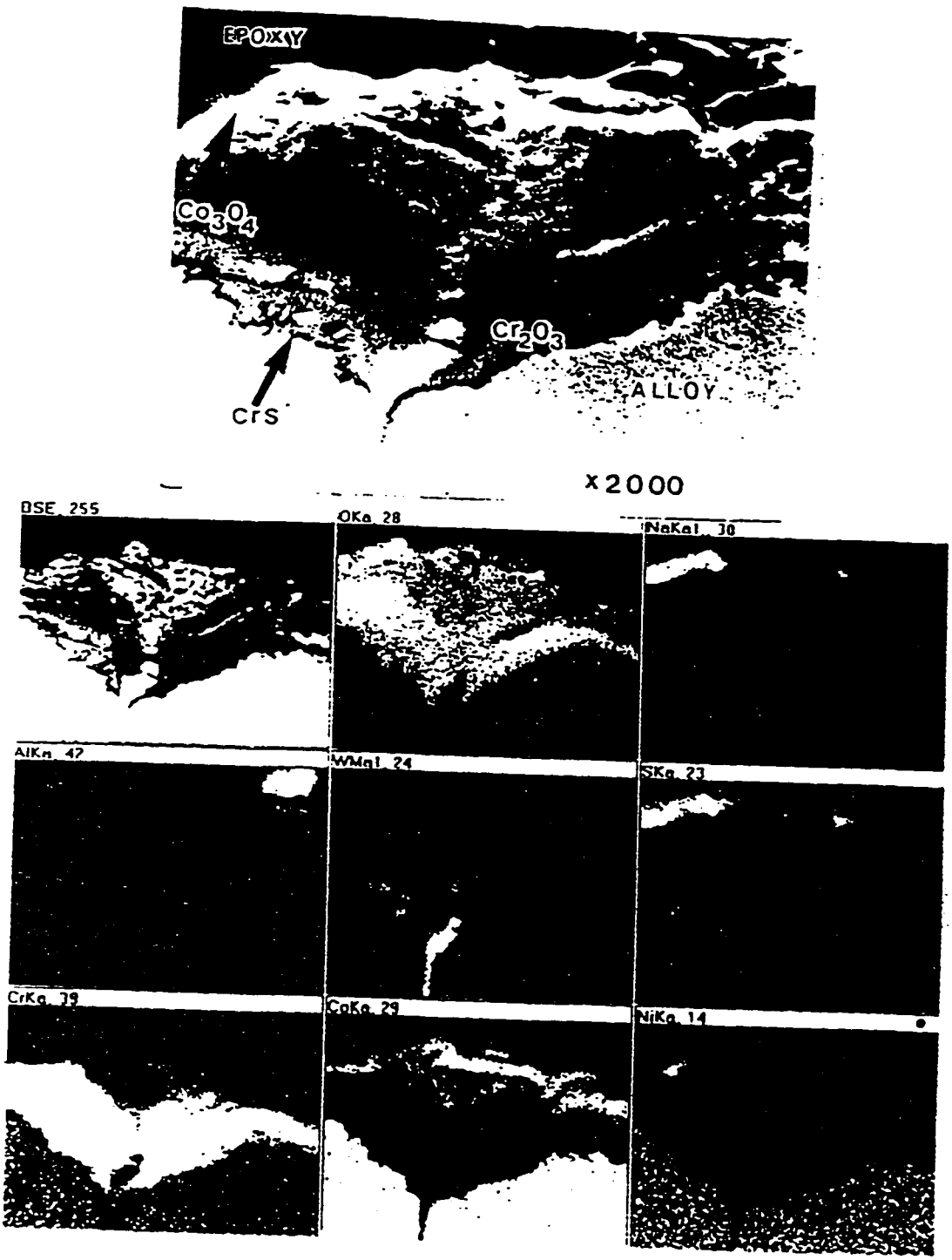

Figure 4.30: SEM micrograph and elemental distribution of $75\%Na_2SO_4+25\%NaCl$ coated Mar-M 509 after exposure for 150 cycles (1hr each) in static air at $750°C$

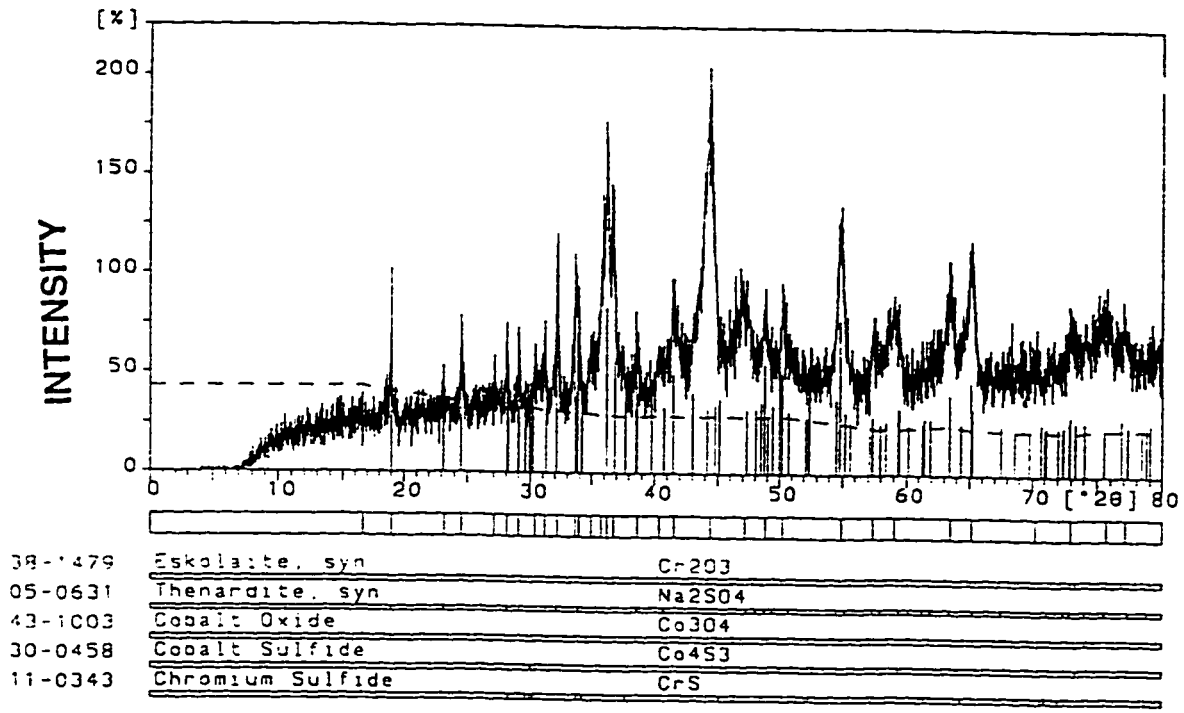

Figure 4.31: XRD pattern of $75\%Na_2SO_4$+$25\%NaCl$ coated Mar-M 509 after exposure for 150 cycles (1hr each) in static air at $750°C$

Figure 4.32 shows the morphology in cross-section of Mar-M 509 coated with $99\%Na_2SO_4 + 1\%NaCl$ after cyclic exposure for 150 hours. The outer scale is a compact layer of Cr_2O_3 (spot D in Figure 4.32) and intermediate scale is mixed Cr_2O_3 and cobalt oxide, CoO (spot C in Figure 4.32). Severe grain boundary attack along the carbide network is seen, which is the frequently observed in Co-base alloy. The presence of WC phase (in the form of M_7C_3) provides any easy path for the penetration of sulfur along the incoherent boundaries of W-carbides.

Figure 4.33 shows the cross-sectioned morphology of Mar-M 509 coated with $Na_2SO_4 + 52\%CoSO_4$ after cyclic exposure for 150 cycles. A thin layer rich in Cr and S is seen at the pit/alloy interface indicating that it may consists of CrS. There is depletion of Co between the scale/pit and pit/alloy interface and which appears as a reprecipitated oxide in the outer region (Co-x ray map). W-rich phase is observed all over the pit region, which seems to be not attacked during hot corrosion.

Comparing Figure 4.30, Figure 4.25 reveals that the sample exhibited localized form of attack only in $25\%NaCl$ enriched salt. Sulfide particles are observed in Figure 4.25 whereas a thin S-rich zone is seen in Figure 4.30.

In summary, the results obtained for a corroded sample of Mar-M 509 in three different salt conditions, such as pure Na_2SO_4, $Na_2SO_4 + 25\%NaCl$, $Na_2SO_4 + 1\%NaCl$ suggests that the $Na_2SO_4 + 25\%NaCl$ mixture was very aggressive and the corrosion rate was very high compared to that of either pure sodium sulfate or 1% $NaCl$ enriched salt. The results show extensive internal sulfidation in the alloy

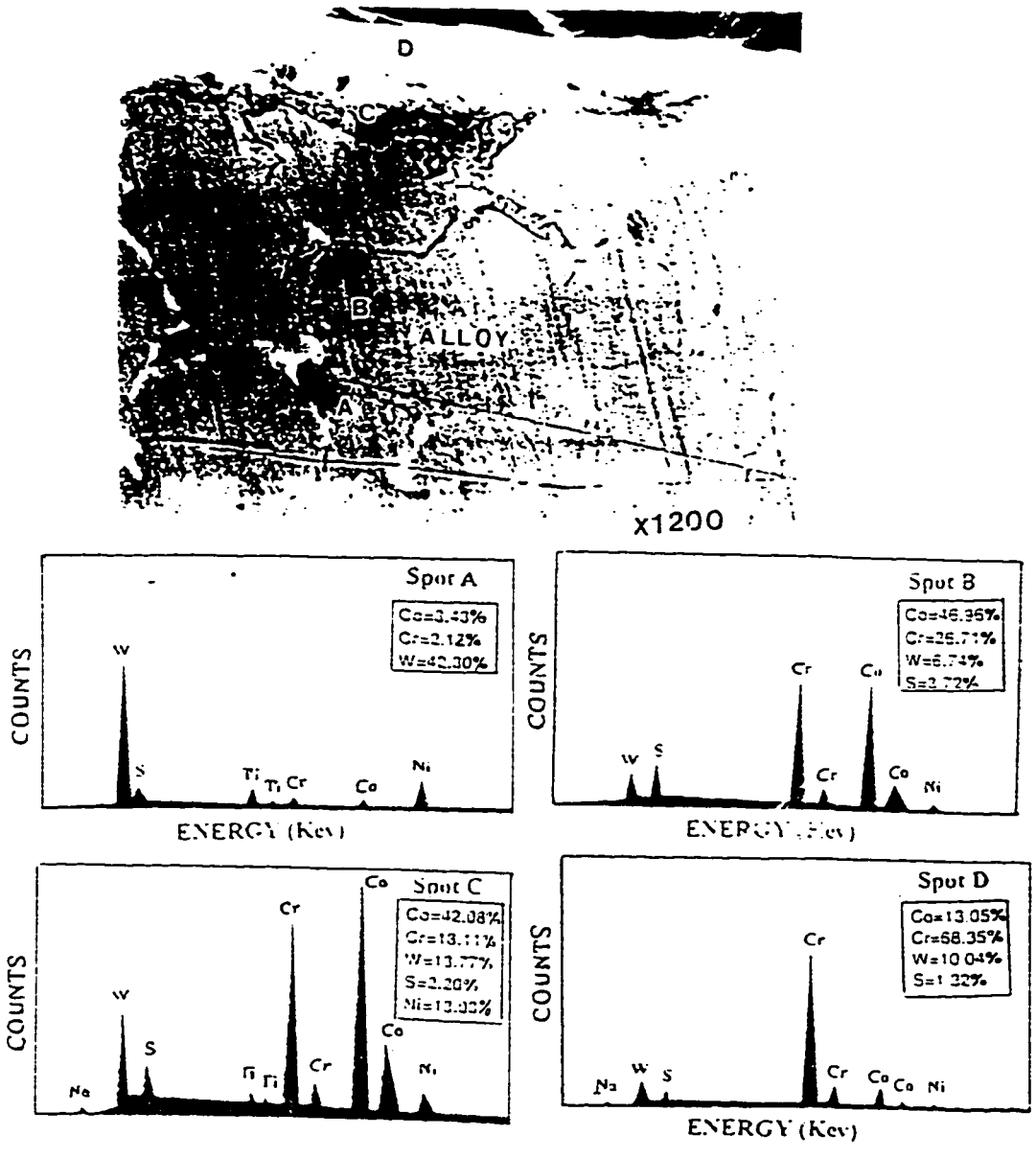

Figure 4.32: SEM micrograph and EDS spectra of $99\%Na_2SO_4+1\%NaCl$ coated Mar-M 509 after exposure for 150 cycles (1hr each) in static air at $750°C$

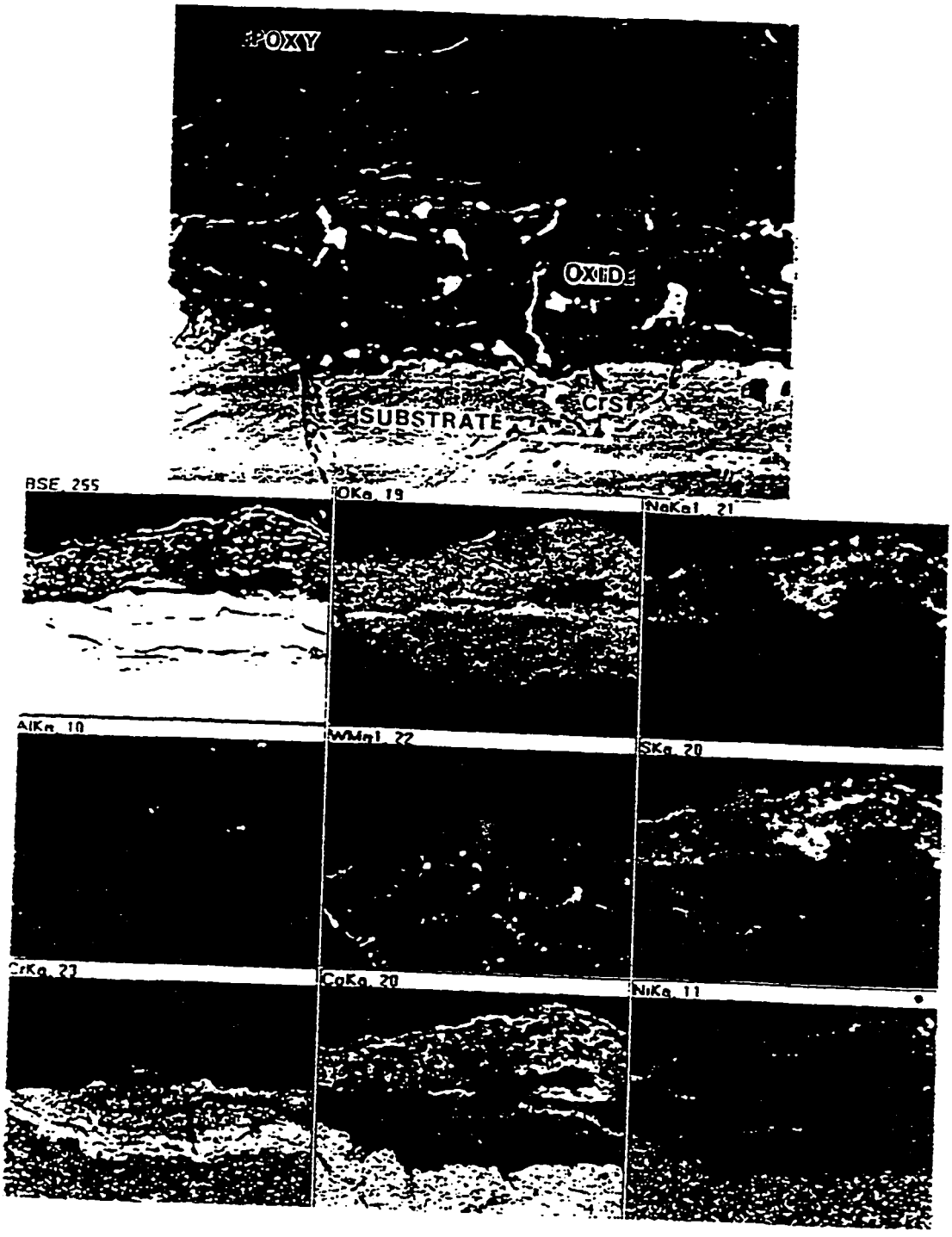

Figure 4.33: SEM micrograph and X-ray mapping of $Na_2SO_4 + 52\%CoSO_4$ coated Mar-M 509 after exposure for 150 cycles (1hr each) in static air at 750^oC

when the sample was exposed to $NaCl$ enriched salt right from the initial stage (Figure 4.28), however, such feature (internal particles) were not seen in the sample exposed to pure sodium sulfate (Figure 4.26). The important feature is internal penetration of chlorine as shown in spot C, Figure 4.28. In addition to this, a typical LTHC type of morphology was observed only at the propagation stage and that too for the sample exposed to $Na_2SO_4 + 25\% NaCl$ mixture alone (Figure 4.30).

4.2 Discussion

In the present study, the effect of $NaCl$ on low temperature hot corrosion of commercial superalloys (IN 738 and Mar-M 509) were considered without using SO_3 in the gas environment. The results clearly indicate that the presence of $NaCl$ in the Na_2SO_4 salt is responsible for the occurrence of low temperature hot corrosion in $Ni-$ and $Co-$base alloys.

4.2.1 Synopsis of Mechanisms

Several mechanism have been proposed for low temperature hot corrosion of Ni and Co-base alloys as well as $CoCrAlY$ and $NiCrAlY$ coatings. Most notable of these mechanisms is dissolution and precipitation mechanism. Basically, the type of hot corrosion mechanism depends on different test conditions, which also includes alloy composition, used during the investigation. The important one are briefly outlined as follows:

- The dissolution of a protective oxide scale (notably Cr_2O_3 and Al_2O_3) in an Na_2O rich Na_2SO_4 at the metal/corrosion product interface as cationic species (chromate/aluminate) and its re-precipitation at the salt/gas interface (where the Na_2SO_4 is nearly stoichiometric) as a porous oxide [58] and [8].

- When the Ni and Co-base alloys contain a refractory metal, such as Mo, W and V, the respective oxides formed at the metal/corrosion product interface

decreases the Na_2O activity of the Na_2SO_4. Then, the protective oxides (Cr_2O_3/Al_2O_3) will dissolve in an acidified Na_2SO_4 as cationic species at the metal/corrosion product interface and reprecipitates at lower solubility regions [16].

- A non-protective oxide scale may also form due to the oxidation of Cr/Al-depleted alloy. In this case, the formation of sulfides in the substrate depletes the alloy in Cr/Al whic h are key elements for hot corrosion resistance. Further, availability of oxygen from the environment oxidizes these sulfides [20].

- when the gas environment consists of SO_3 levels (the equilibrium is established by using Pt catalyst in the upstream of gases), the noble oxides (CoO/Co_3O_4 and/or NiO) formed on $CoCrAlY$ and $NiCrAlY$ coatings react with SO_3 to form $CoSO_4/NiSO_4$. Then the noble oxides dissolve in the eutectic melts of $Na_2SO_4 - CoSO_4$ at the metal/corrosion product interface and reprecipitates as oxide mount at the salt/gas interface. However, such a mechanism seems to be not possible for Ni-base alloys or $NiCrAlY$ coatings because the formation of $Na_2SO_4 - NiSO_4$ requires high partial pressures of SO_3 [35]-[37].

4.2.2 IN 738

Pure Na_2SO_4

First, let us consider the sequential stages during hot corrosion attack of IN 738 specimen coated with pure Na_2SO_4 (re-coated every 20 cycles). The results of this investigation indicate that during the early stages of exposure, only a thin protective intermixed oxide ($NiO + Cr_2O_3$) form on the alloy surface in pure Na_2SO_4 coated conditions (see Figure 4.2 and Figure 4.34a). This could be attributed to the availability of oxygen from air which permeate through the Na_2SO_4 coating layer which is solid at the test temperature. The morphology of this protective oxide scale correlates well with the corrosion kinetics, which indicates a very short incubation period followed by slight weight gain upto 20 cycles (Figure 4.1).

Due to the growth of a protective oxide layer ($NiO + Cr_2O_3$), the oxygen potential at the metal/corrosion product interface will be low when compared to that of P_{O_2} at salt/gas interface. This low oxygen potential is sufficient to form a semi-continuous layer of Cr_2O_3 and which may ultimately form as a protective layer (Figure 4.34b). Similarly, TiO_2 discretely grow under the continuous Cr_2O_3.

Further cyclic exposure for extended time eventually lead to local break down of the protective oxide layer and subsequent formation of discontinuous Al_2O_3

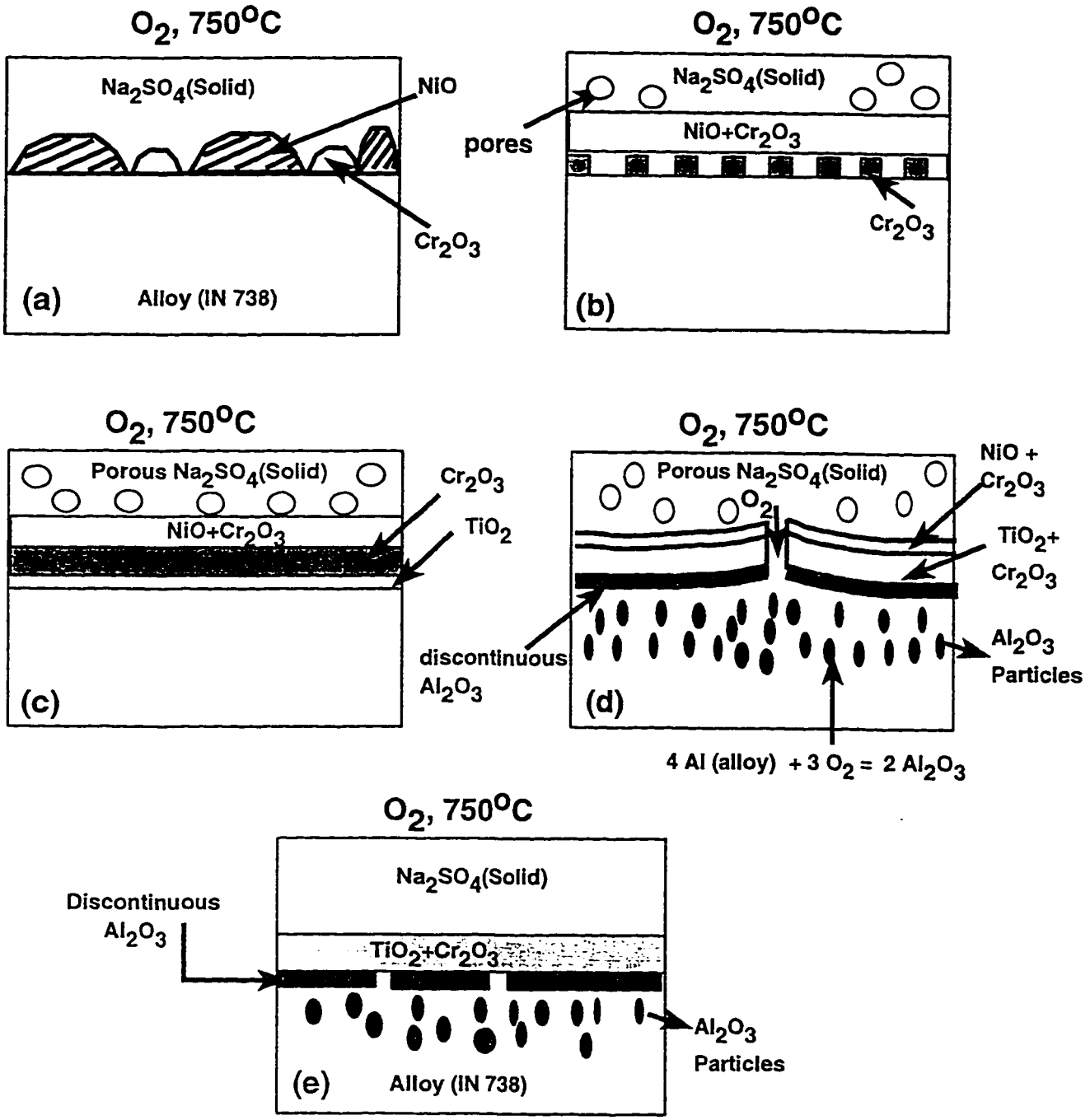

Figure 4.34: Schematic diagram illustrating the proposed mechanism of low temperature hot corrosion of IN 738 in pure Na_2SO_4 at 750°C.
Initiation stage is (a) to (b); propagation stage is (c) - (e).

layer below the protective oxide layer (Figure 4.34d). The presence of only 3.4%Al in the alloy is not sufficient to form an external continuous oxide layer and thus internal oxide particles form in the substrate as a subscale (Figure 4.34 e). Hence, cracking may lead to introduction of some oxygen in the alloy to form these internal oxide particles but the presence of Al, Cr and Ti always insure that the protectivity may be continuously re-established.

The formation of a multi-layered oxides at the alloy/corrosion product interface suggest that the oxygen penetrating the thick and porous outer corrosion product later arrive of the metal/corrosion product interface in a concentration high enough to allow the formation of the protective oxides (Figure 4.34 c), the bottom being internal Al_2O_3 subscale layer due to its higher thermodynamic stability than Cr_2O_3 and TiO_2 and thus it needs a lower oxygen potential to form.

Since no internal sulfide particles form inside the alloy ahead of the interface, then it can be assumed that the process is purely an oxidation reaction with oxygen arriving through the solid Na_2SO_4 layer to the alloy surface to form multi layer oxide (Figure 4.34 c). This layer undergo multiple cracking and healing with the result of allowing oxygen - at a lower concentration to dissolve into the outer alloy surface zone. Examination of the corrosion product/alloy interface in the vicinity of the multi layered oxide showed no sulfides exist

(Figure 4.6).

Effect of $NaCl$ on LTHC of IN 738

The present results indicate that during early stages of exposure of alloy specimen to $Na_2SO_4 + 1\%NaCl$ mixture, a non-protective corrosion product layer forms on the alloy surface, with a fairly irregular metal/corrosion product interface and numerous sulfide particles in the substrate, ahead of the corrosion front (Figure 4.7). A low melting eutectic ($Na_2SO_4 - NaCl$, m.p is 625°) forms on the specimen surface which is a liquid at the test temperature (750°C) [9]. Visual examination of samples coated with the $Na_2SO_4 + NaCl$ mixture showed the formation of a liquid phase on alloy surface, indicating that it is a molten eutectic mixture.

The formation of internal sulfide particles (TiS/CrS) in the substrate (spot B, Figure 4.7) could be a result of reaction between the sulfur from decomposition reaction of Na_2SO_4 with alloying elements. Cracking of oxide scale due to cycling may allow liquid eutectic mixture ($Na_2SO_4 - NaCl$) to come in direct contact with the metal. Then, Na_2SO_4 (in the form of liquid eutectic) decomposes upon contact with the metal since the O_2 potential at the metal/corrosion product interface is less than salt/gas interface [54]. The sulfur released after sodium sulfate decomposition, reacts with the alloying elements to form sulfides of Ti/Cr. Further intake of oxygen from the en-

vironment oxidizes these sulfides preferentially and incorporating some metal fragments in the intermediate corrosion product region (spot D in Figure 4.7) [51].

In the mean time, $NaCl$ in the liquid eutectic mixture interacts with Cr and Ti in the alloy to form volatile $CrCl_3$ and possibly $TiCl_4$ at the metal/corrosion product interface, which migrates outwardly to the salt/scale interface due to their high vapor pressures [20]. The volatile chlorides may either react with O_2 at salt/gas interface to form Cr-oxide (spot C, Figure 4.7) or lost to the atmosphere .

The formation of a mixed oxide layer (Cr_2O_3/TiO_2) in the intermediate corrosion product region (spot F. Figure 4.7) results from continuous oxidation of the metal during repeated cycling. After the build up of a mixed layer (Cr_2O_3/TiO_2) the oxygen potential at the metal/corrosion product interface may be low, which is sufficient to form Al_2O_3 and TiO_2 rich scale at the metal/corrosion product interface (spot E, Figure 4.7).

Examination of test specimens after prolonged exposures for 150 cycles in $Na_2SO_4 + 1\%NaCl$ (re-coated every 20 cycles) shows the formation of thick scale on the alloy surface (Figure 4.10). This thick scale contains regions of what seem to have been a liquid at temperature in the middle regions and at the outer regions . This could be attributed to the formation of molten salt

(presumably $Na_2SO_4 + NaCl$ mixture) at temperature. It appears that metal fragments rich in Ni and to some extent in Cr react with the Na_2SO_4 (in the liquid eutectic form) in the intermediate corrosion product itself and forms Ni_3S_2 and probably CrS. X-ray diffraction results indicated large amount of Ni_3S_2 (Figure 4.11). Further availability of oxygen from the environment oxidizes the Ni_3S_2 and CrS, which releases sulfur [21].

$$Ni_3S_2 + \frac{7}{2}O_2 \rightarrow 3NiO + 2SO_2(g) \tag{4.1}$$

$$2CrS + \frac{7}{2}O_2 \rightarrow Cr_2O_3 + 2SO_2 \tag{4.2}$$

Hence, the formation of light phase which is probably Cr_2O_3/NiO (spot E) is a result of oxidation of Ni_3S_2 and CrS as indicated by above equations . The sulfur released in the form of SO_2 escapes to atmosphere because the presence of thick outer scale may inhibit its penetration into the substrate. Therefore, internal attack of the alloy during the propagation stage is not quite significant.

Because of low concentration (1%) of $NaCl$ in Na_2SO_4, the eutectic mixture ($Na_2SO_4 - NaCl$) remains liquid on oxide surface only for short duration [30], which is also inferred from visual examination of the sample. As soon as the $NaCl$ breaks down due to the formation of metal chlorides, $CrCl_3$ and $TiCl_4$, the remaining salt consists of only Na_2SO_4 which may be solid at test

temperature. Thus the attack is reduced in the long duration as shown by corrosion kinetics (Figure 4.1).

When the concentration of $NaCl$ is increased to 25% in the salt mixture, the early stages of corrosion (1 hr) begins with the formation of a thin continuous layer of intermixed oxide ($NiO + Cr_2O_3$) on the alloy surface (see Figure 4.12 and Figure 4.35 a). Simultaneously, a low melting eutectic of $Na_2SO_4 - NaCl$ (m.p 625°C) [9] and [23]-[25] forms above the oxide layer, which is liquid at the test temperature (750°C). Subsequent cracking of oxide scale, due to thermal cycling may allow the liquid eutectic to come in direct contact with the metal (Figure 4.35 b). Once this takes place then the molten salt becomes unstable thermodynamically because the O_2 potential at metal/corrosion product interface is lower than at the gas/salt interface [21] and decomposes according to the reaction:

$$Na_2SO_4 \rightarrow Na_2O + SO_3(g) \tag{4.3}$$

SO_3 may then decomposes according to the reaction:

$$2SO_3 \rightarrow 3O_2 + S_2(g) \tag{4.4}$$

The partial pressure of S_2 at the metal/corrosion product interface may reach high enough levels such that it reacts with alloying elements to form sulfides in the substrate (CrS/AlS). The presence of high amount of Na-rich phase

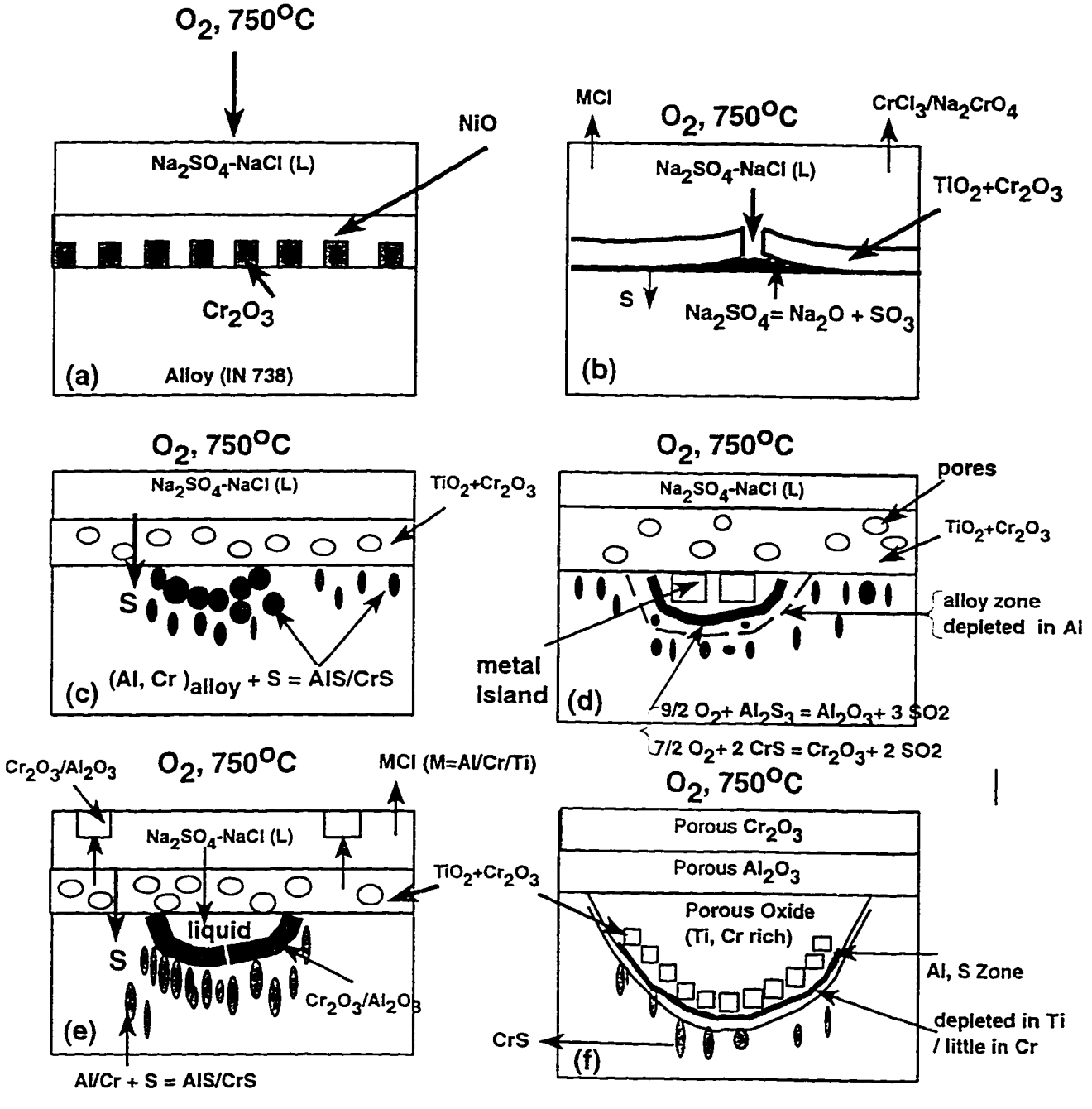

Figure 4.35: Schematic diagram illustrating the proposed mechanism of low temperature hot corrosion of IN 738 in $Na_2SO_4 - NaCl$ mixtures at 750°C. Initiation stage is (a) to (d): propagation stage is (e) - (f).

(possibly Na_2CrO_4) in the yellow deposit, observed on ceramic tube (Figure 4.21b) indicate that it is lost to atmosphere . Hence, the loss of Na_2O after sodium sulfate decomposition could be attributed to the formation of Na_2CrO_4.

The formation of volatile metal chlorides, such as $CrCl_3$, $TiCl_4$ and $AlCl_3$ may be common even in $Na_2SO_4 + 25\%NaCl$ mixture as described earlier for $Na_2SO_4 + 1\%NaCl$ mixture. These volatile metal chlorides may escape into atmosphere due to their high vapor pressures. Thus, the short initiation (within 1 hr) resulting in earlier beginning of propagation stage of hot corrosion may be partly due to the loss of corrosion products. It is possible that the volatile $CrCl_3$ [27] may form at very early exposures of the sample in $Na_2SO_4 + 25\%NaCl$ salt mixtures.

The decomposition of sodium sulfate (equation 4.1) allows sulfur to react with Al to form AlS/CrS (see Figure 4.13 and Figure 4.35 c). This results in Al-depletion from the alloy surface ahead of corrosion front. Further ingress of oxygen through the outer porous scale oxidizes these sulfides resulting in the formation of a semi-continuous Al_2O_3/Cr_2O_3 layer, separating metallic fragments [51] from the base metal (see spot D in Figure 4.13 and Figure 4.33 d). This morphology (Figure 4.13) indicate all the features, such as metal fragments above the scale/metal interface, Al-depletion ahead of oxidation front

and dark phase (Al_2O_3/Cr_2O_3) at metal/corrosion product interface are represented in Figure 4.33 d.

After extended exposure of IN 738 specimen (150 cycles), a non-protective oxide scale forms which contains numerous shallow pits (Figure 4.15), typical of LTHC morphology (formation of large shallow pits with a continuous S-rich layer at pit/alloy interface, little or no depletion of Al/Cr ahead of corrosion front and a thick blister cover on the top of pit) . The formation of a loose porous oxide could be attributed to the continuous dissolution/reprecipitation mechanism of Al_2O_3/Cr_2O_3, explained in the literature [10] and [58]. According to the fluxing mechanism, the protective oxides (Al_2O_3/Cr_2O_3) formed on the alloy surface dissolves in the basic Na_2SO_4 melt as aluminate and chromate ions at the scale/metal interface and reprecipitates as oxide precipitates at the salt/gas interface, where the salt is nearly stoichiometric.

Since the salt is replenished every 20 cycles, it is reasonable to suggest that a liquid $Na_2SO_4 - NaCl$ layer will be present at all times during the exposure tests for the entire duration of 150 hrs. The dark phase of oxide layer formed (spot D in Figure 4.13) during later steps in initial stages (20 cycles) may dissolve in the liquid melt as a basic component (chromate and aluminate ions) and reprecipitate as a porous outer oxide scale at salt/gas interface at later stages [10] (see Figure 4.35 e). This process is continuous until the salt

mixture is continuously available at the alloy surface and eventually results in the formation of large shallow pits (Figure 4.35 f). In addition, the formation of volatile chlorides ($CrCl_3/TiCl_4$ and $AlCl_3$) and their oxidation at the salt/gas interface may also be responsible for the development of a thick blister cover, as mentioned in earlier stages of corrosion.

The cross-section morphology (Figure 4.15) of test specimens corroded in the salt mixture after extended exposure (150 cycles) provides an excellent evidence of the occurrence of the above mentioned dissolution/precipitation mechanism.

To investigate whether typical LTHC morphology could be developed in isothermal conditions, a test run has been conducted without re-coating the salt mixture. The morphology shown in Figure 4.18 indicate a broad frontal attack, consisting of numerous metal fragments in the intermediate zone of the corrosion product layer. Although the conditions employed are of typical LTHC, the morphology did not the formation of large shallow pits, a thin S-rich zone at pit/alloy interface and a thick blister cover at the pit mouth. Hence, it is expected that dissolution/precipitation mechanism may not be the primary degradation of attack under isothermal conditions.

The most important features observed during the low temperature hot corrosion of IN 738 in sulfate/chloride mixture includes:

1. No depletion of Al ahead of the corrosion front.

2. Depletion of Ti (primarily) and Cr at the pit/alloy interface.

3. Formation of internal sulfides of Al/Cr.

The features observed in the present investigation are different from the study of Chiang et al [20]. In this study the depletion of Cr was observed because of the low concentration of Cr and Al which allowed to form particles of sulfides ahead of metal/corrosion product interface. This was also assisted by the formation of TiO_2 layer at the pit/metal interface. The dissolution and precipitation mechanism proposed in this study agrees well with the morphological features observed for IN 738 in $Na_2SO_4 + 25\%.NaCl$ mixtures during the propagation stage. This agrees well with the dissolution/precipitation of Fe_2O_3 proposed by Shi [58].The formation of non-protective oxide scale was related to dissolution of Fe_2O_3 rather than Cr_2O_3 because the $Fe-$ base alloy does not contain high concentration of Cr and Al. Similarily, the dissolution/precipitation of Cr_2O_3/Al_2O_3 proposed in this study is in agreement to that of one proposed by Amin for AISI 304 steel in sodium and iron sulfate mixtures at low temperatures.

From the above discussion. it is can be inferred that the LTHC morphology is developed only under condition $Na_2SO_4 + 25\%.NaCl$, when the salt mixture is periodically replenished. The LTHC morphology was not observed either

in $Na_2SO_4 + 1\%NaCl$ or under isothermal conditions. Because of low concentration of $NaCl$ in Na_2SO_4, very little amount of liquid eutectic mixture is formed on the alloy surface. The molten layer ultimately converts to solid Na_2SO_4 and this builds up on the alloy surface during extended period of exposure. Further recoating of $Na_2SO_4 + 1\%NaCl$ mixture may not penetrate deep (also because 1%NaCl in the salt stays for short duration only) into the alloy to react with alloying elements and lead to the formation of pits with thick blister cover (compare Figure 4.10 and Figure 4.15). In the case of isothermal conditions, the salt mixture is not continuously replenished and hence the liquid salt mixture is not continuously present on the alloy surface for dissolution/precipitation mechanism to occur. Based on this discussion it is concluded that the continuous replenishment of the salt mixture with high concentrations of $NaCl$ only resulted in the development of a typical LTHC morphology. The development of LTHC morphology during the propagation stage is primarily attributed to the sequence of dissolution/precipitation of protective oxide scales. Finally, LTHC does not occur in pure Na_2SO_4 when SO_3 is not present in gas phase. This is solely due to the absence of a liquid salt layer on the alloy surface as the test temperature is below the m.p. of sodium sulfate.

4.2.3 Mar-M 509

Pure Na_2SO_4

First, let us consider the sequential stages during the hot corrosion attack of Mar-M 509 in pure Na_2SO_4. The results obtained indicate that, like the case of IN 738, the behavior of Mar-M 509 during the early stages of exposure of some what similar to that observed for IN 738 exposure under similar conditions (Figure 4.36a). The formation of a continuous protective Cr_2O_3 layer during the early exposure of Mar-M 509 takes place much earlier than the case of IN 738 due to the presence of larger Cr concentration in former (see Figure 4.23 and Figure 4.36b). The growth of the protective oxide layer (Cr_2O_3) during the early stages is accompanied by a steady increase in specimen weight (Figure 4.22).

The formation of dark phase (spot C, Figure 4.23), indicate the existence of Cr and Co-oxide in the mixed or in the spinel form (probably $CoCr_2O_4$) at metal/corrosion product interface. Subsequently, cracking of oxide scale allows oxygen through the porous Na_2SO_4 (solid) layer to the metal/scale interface (Figure 4.36c). It seems that the incoming oxygen preferentially attack the W-carbide white phase (probably in the form of M_7C_3 [1]). In some case it may even encircle metallic fragments separating them from alloy or penetrate deeply into the alloy itself (see Figure 4.23 and Figure 4.36d). When the

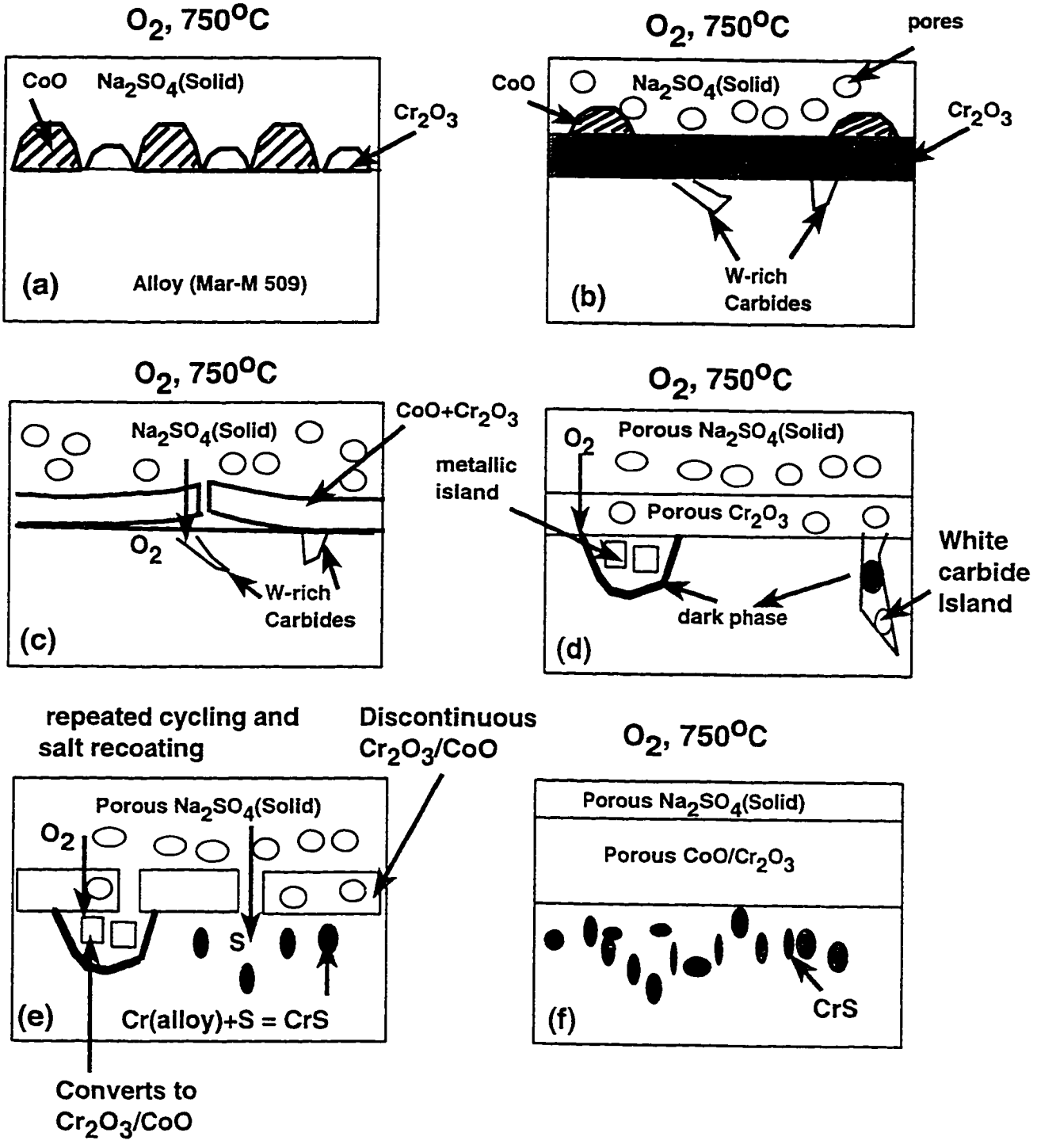

Figure 4.36: Schematic diagram illustrating the proposed mechanism of low temperature hot corrosion of Mar-M 509 in pure Na_2SO_4 at 750°C.
Initiation stage is (a) to (c): propagation stage is (d) - (e).

metal surface was exposed to the environment, the oxidation of alloy matrix (encircled by metallic fragments) allows to form a dark phase.

The formation of outer porous scale at scale/salt interface (Figure 4.25) could be attributed to the continuous cracking of scale due to thermal cycling and constant replenishment of Na_2SO_4. The continuous cracking of scale and constant re-coating of salt allows sodium sulfate to come in contact with the underlying alloy (Figure 4.36e). When Na_2SO_4 comes in contact with the metal through the cracks formed in the initially protective Cr_2O_3, then it decomposes releasing sulfur which reacts with the alloy substrate to form sulfides of Cr (Figure 4.36f). In the case of IN 738, the presence of multilayer oxides (Cr_2O_3/TiO_2), and the establishment of Al_2O_3 at metal/corrosion product interface may hinder the penetration of Na_2SO_4 even after re-coating the salt at later stages.

Effect of $NaCl$ on LTHC of Mar M 509

During the very early stages of exposure (1 cycle) of Mar-M 509 sample to $Na_2SO_4 + 25\% NaCl$ mixture, Co-oxide accompanied by the undergrowth of Cr_2O_3 nuclei form on the alloy surface (Figure 4.37 a). Eventually Cr_2O_3 will form a protective oxide layer above scale/metal interface in agreement with the simple oxidation model of Cr rich Co- base alloy (see Figure 4.27 and Figure 4.37b). Simultaneously, a low-melting eutectic of $Na_2SO_4 - NaCl$

($m.p = 625°C$) forms on the top of oxide which is liquid at the test temperature ($750°C$) [9]. Visual examination using optical microscopy indicate the wetting of the sample by this eutectic mixture. During the initial stages (20 cycles), the degradation of Mar-M 509 in sulfate/chloride mixture can be primarily attributed to the sulfidation of alloying elements Cr and Co along the boundaries between W-carbide phase and the metal substrate (Figure 4.27) , a morphology similar to some extent to the case of pure Na_2SO_4.

The major difference between this condition and the earlier condition when no $NaCl$ exist is the presence of liquid $Na_2SO_4 - NaCl$ in the present condition. Mechanical cracking of the protective scale allows the liquid salt mixture to come in direct contact with the base metal. Sodium sulfate may be decomposed upon contact with the metal according to equation (4.1). The sulfur may preferentially attack the underlying alloy along the W-carbide network to form sulfides of Cr/Co in the substrate (see Figure 4.37c) [26]. Simultaneously, chloride ion from $NaCl$ reacts Co and Cr preferentially and forms volatile chlorides ($CoCl_2$ and $CrCl_3$). These chlorides migrate outwardly and gets oxidized at salt/gas interface as mentioned earlier for IN 738 case.

During the propagation stage, further ingress of oxygen through the outer porous oxide may preferentially oxidize the chromium sulfides in the alloy (Figure 4.37 d). The sulfur released after oxidation of sulfides (which are

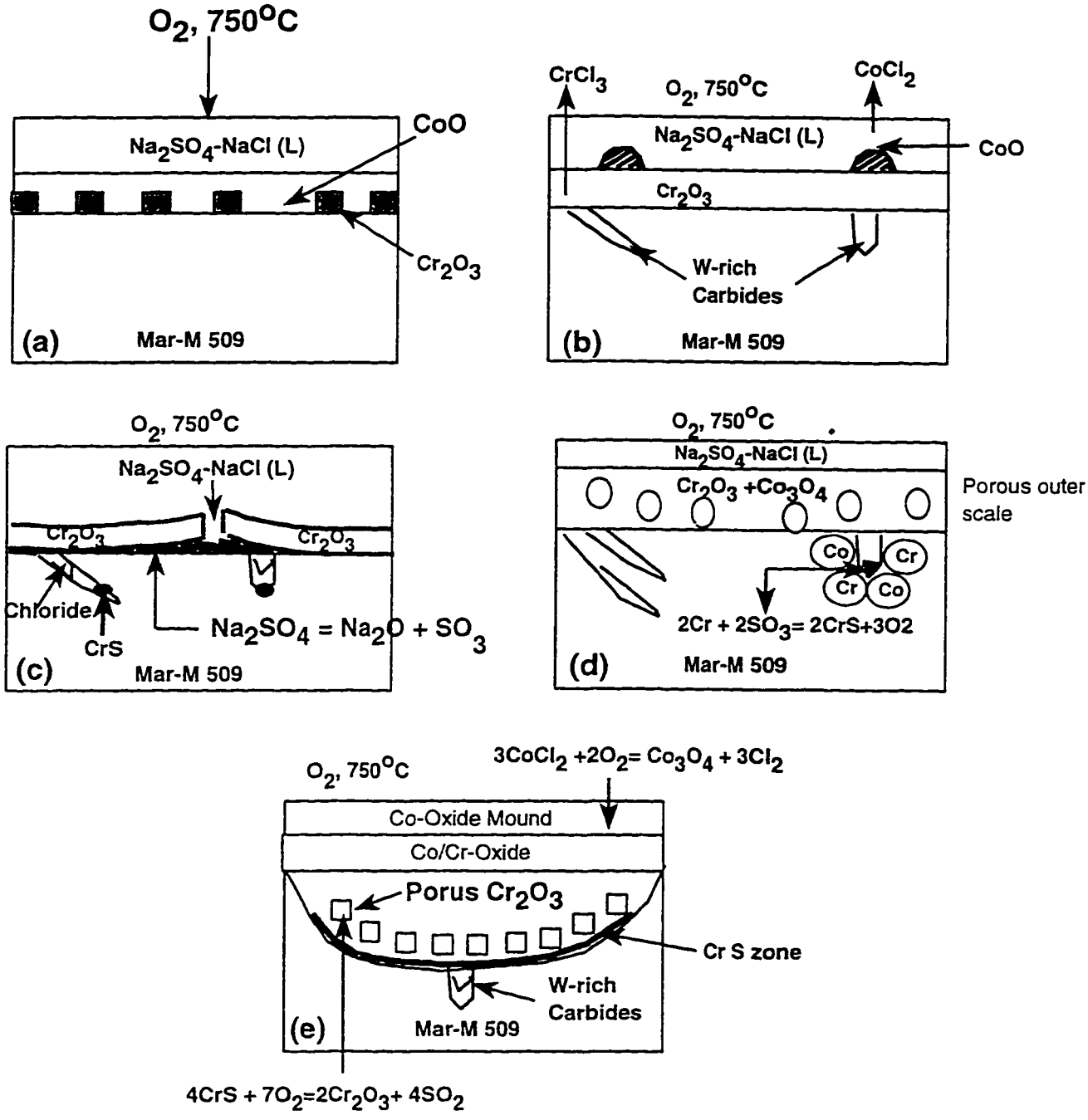

Figure 4.37: Schematic diagram illustrating the proposed mechanism of low temperature hot corrosion of Mar-M 509 in $Na_2SO_4 - NaCl$ mixtures at 750°C. Initiation stage is (a) to (c): propagation stage is (d) - (e).

previously internal oxide particles) may attack the metal ahead of corrosion front and further forms Cr- sulfides [20], a thin zone at the bottom of pit (see Figure 4.30 and Figure 4.37 e). Thus, continuous sulfidation-oxidation may inhibit the development of a protective layer of oxide. The $NaCl$ attacks the metal during the propagation stage and forms volatile metal chlorides similar to the case of initial stages. The appearance of Co– rich mound on the top of pit is a result of oxidation of $CoCl_2$ at the salt/gas interface [30].

The main role of W-carbide network is to provide an easy path for sulfidation of Cr in the alloy it self, WC seems not to undergo a reaction with either with oxygen, sulfur or chlorine. It is clearly known from the Figure 4.30 the W-rich phase is not attacked since the O and S/Cl x-ray map appear dark indicating that it is a carbide phase.

In order to confirm the attack along the W-rich phase as explained above, an alloy specimen is coated with salt mixture $Na_2SO_4 + 52w/o\%CoSO_4$ mixture then exposed for 150 hrs. The results (Figure 4.33) show the formation of pits, preferentially along the W-carbide phase. The white islands (WC phase) in the intermediate corrosion product and at pit/alloy interface are not attacked because all the X-ray maps in that particular regions indicate no enrichment of the W-rich phase.

The most important features observed during the LTHC of Mar-M 509 in

sulfate/chloride mixtures include:

1. Depletion of Cr between the pit and alloy region was not observed
2. The complete absence of internal sulfide particles ahead of corrosion front.
3. W-enriched layer at pit/alloy interface was observed.

The results of the present work are somewhat different to that Chiang et al [20], who showed that the depletion of Cr occurs in $Co-27Cr$ alloy corroded in Na_2SO_4 containing O_2+SO_3 in the environment at low temperatures. The depletion of Cr was attributed to the formation of CrS ahead of oxidation front. The initiation of LTHC was attributed to the formation of $Na_2SO_4 - CoSO_4$ rather than attack along W-rich phase, since the alloy used in their study does not contain W. The presence of a Co-rich mound on the top of pit is in agreement with the study of Chiang et al, which is attributed to the oxidation of $CoCl_2$ at the salt/gas interface [30]. The accelerated attack of Mar-M 509 in $Na_2SO_4 + 25\% NaCl$ mixtures along the W-carbide net work agrees well with mechanism proposed by Stringer[26], who attributed the formation of a loose and porous oxide scale to the attack along the Mo-carbide phase as the Co-base alloy in their study consists of high concentration of Mo strengthened by Mo-carbide phase.

From the above discussion, it can be concluded that the LTHC morphology forms only at the propagation stage when the $Na_2SO_4 + 25\% NaCl$ mixture is

continuously replenished on the alloy surface. The propagation of the LTHC is attributed to sulfidation/oxidation of *Cr*. In addition, the presence of *W*-rich phase in the alloy assists in both the initiation and propagation of low temperature hot corrosion (Figure 4.30 and Figure 4.33). The typical features of LTHC (formation of shallow pits with thin S-rich zone at pit/metal interface and a thick blister cover on the top of pit) were only seen in *NaCl* enriched salt, which is mainly due to the formation of liquid salt layer and continuous replenishment of salt.

Chapter 5

Conclusions and Recommendations

5.1 Conclusions

This study has shown that $Na_2SO_4 + 25\%NaCl$ mixture is very aggressive compared to that of pure Na_2SO_4 or $Na_2SO_4 + 1\%NaCl$ for both IN 738 and Mar-M 509. High corrosion rates were observed in $25\%NaCl$ enriched salt either at the intiation stage or at the propagation stage. Quick initiation of hot corrosion of IN 738 and Mar-M 509 in $NaCl$ enriched salt was related to the vaporization losses incurred due to the formation of volatile compounds and cracking due to thermal cycling. The degradation of IN 738 is much

more severe than Mar-M 509 in sulfate/chloride mixtures, which is due to the presence of more Cr in Mar-M 509 and due to the high melting point of Co-sulfides.

The specific conclusions may be summarized in the following:

1. The typical LTHC features (formation of shallow pits with blister cover) has been developed only when the IN 738 sample was corroded in Na_2SO_4+ 25%$NaCl$ mixture. These features were not observed either in pure Na_2SO_4 or Na_2SO_4 + 1%$NaCl$ mixtures because the solid salt layer builds upon continuous replenishment of salt.

2. The propagation of LTHC of IN 738 in Na_2SO_4 + 25%$NaCl$ was attributed to the dissolution and precipitation of Al_2O_3/Cr_2O_3 and sulfate decomposition.

3. The presence of W-carbide (probably in the form of M_7C_3) plays a minimal role in the low temperature hot corrosion of Mar-M 509. However, it provides a easy path for sulfides of Cr in the alloy.

4. The propagation stage (150 cycles exposure) of LTHC of Mar-M 509 in mixture was related to sulfidation/oxidation of Cr.

5.2 Recommendations

1. Pure Ni. Co and Ni-Cr/Co-Cr alloy containing no Al need to be studied to clarify the type of attack at the scale/metal interface in sulfate/chloride mixtures.

2. A more realistic test such as dean-rig test system need to be utilised where continuous salt arrival of salt can be closely modelled and the present results need to be compared to the results obtained from dean rig system.

3. The LTHC of $CoCrAlY$ and $NiCrAlY$ coatings need to be studied further in the sulfate/chloride mixtures.

Bibliography

[1] R.W. Fawley. "The Superalloys". (eds) Chester T. Sims and William C. Hagel. *A willey-interscience Publication.* NewYork. 1972. pp: 3.

[2] B.C. Markham. " Marine Proteus Engines for the Brave class Petrol Boats". *Trans institute of Marine Engineering.* Vol. 71. Oct. 1959.

[3] W.T. Reid. R.C. Corey and B.J. Cross. *Transactions of AIME.* Vol. 67. 1945. pp: 279.

[4] E.L. Simons. G.T. Browning and H.A. Liebhafsky. *Corrosion* . Vol. 11. 1955. pp: 505t.

[5] A.U. Seybolt. *Transactions of AIME.* Vol. 242. 1968. pp: 1955.

[6] N.S. Bronstein and M.A. Decresente. *Transactions of the Metallurgical Society of AIME.* Vol. 245. 1969. pp: 1947.

[7] J.M. Quets and W.H. Dresher. *Journal of Materials.* Vol. 4. 1965. pp: 583.

[8] J.A. Goebel and F.S. Pettit. "The Na_2SO_4-induced Accelerated Oxidation (Hot corrosion) of Ni-base Alloys" *Metallurgical Transaction*. Vol. 1. 1970. pp: 1943.

[9] J.F.G. Conde. "What are the Separate and Interacting Roles of Sulfur. Sodium and Chloride in Hot corrosion ?". *Specialist Meeting on High Temperature Corrosion of Aerospace alloys*. 36^{th} meeting of the structures and materials panel. AGARD lynby. Denmark. 1972.

[10] J.A. Goebel. F.S. Pettit and G.W. Goward. "Mechanism for the Hot corrosion of Nickel-Base Alloys. *Metallurgical Transactions*. Vol. 4. 1973. pp: 261.

[11] J. Stringer. *Annual review of Material science*, (ed) R.A. Huggins (Palo Alto. C.A : Annual Review Inc). 1977. pp: 449.

[12] R.A. Rapp and K. Goto. *Proceedings of the fused salt symposium II*, (ed) J. Bronstein. The Electrochemical Society. Princeton. 1979.

[13] J. Balakja and V. Danek. *Werkstoffe and Korrosion*. Vol. 21. 1970. pp: 254.

[14] L.F. Aprigliano. *Report No: MAT-77-78*. (ed) David. W. Taylor. Naval ship Research center. Bathesda. MD 20084. 1978.

[15] R.L. Jones and S.T. Godamski. *NRL letter Report*. Nov 1977. pp: 6170-773.

[16] C.S. Giggins and F.S. Pettit. Hot corrosion Degradation of Metals and Alloys. "*A Unified Theory*". *Pratt & Wittney Aircraft Group*. contract No. F44 620-76-C-0123. PWA report No. IR-11545. June 1979.

[17] K.L. Luthra and D.A. Shores. "Mechanisms of Na_2SO_4-induced Corrosion at $600 - 900°C$". *Journal of The Electrochemical Society*. Vol. 127. No. 11. 1980. pp: 2207.

[18] K.L. Luthra. "Mechanism of Low Temperature Hot corrosion". in "*High Temperature Corrosion*". R.A. Rapp (ed). NACE. Houston. Texas. 1983. pp: 505.

[19] R.L. Jones. "Cobalt Oxide-SO_2/SO_3 Reactions in Cobalt-Sodium Mixed Sulfate Formation and Low-Temperature Hot corrosion, in "*High Temperature Corrosion*".. R.A. Rapp (ed). NACE. Houston. Texas. 1983. pp: 507.

[20] K.T. Chiang . F.S. Pettit and G.H. Meier, in "*High Temperature Corrosion*". R.A. Rapp (ed). NACE. Houston. Texas. 1983. pp: 511.

[21] A.K. Misra and D.P.Whittle. "Effects of SO_2 and SO_3 on the Na_2SO_4 induced Corrosion of Nickel" *Oxidation of Metals*. Vol. 22. No's 1/2. 1984. pp: 1-33.

[22] D.J. Wortman. F.E. Freyxell and I.I. Bessen. "A Theory for Accelerated Turbine Corrosion at Intermediate Temperatures". *Third conference*

on Gas turbine Materials in a Marine Environment. University of Balk. England. session V. paper 11. sep 1976.

[23] J.F.G. Conde. *in Proceedings of the 1974 Gas turbine Materials in the Marine Environment Conference*. (eds) J.W. Fairbanks and I. Machlin. M.C.I.C. Report 75-27. Castine. 1974. pp: 73.

[24] R.C. Hurst. J.B. Johnson. M. Davis and P. Hancock. "Sulfate and Chloride attack of Nickel-based alloys and Mild steels". *Deposition and Corrosion in Gas turbines*. (eds) A.B. Hart and A.J.B. Cutler. Applied science publishers. London. 6-7 Dec 1972. pp: 143.

[25] D.M. Johnson. D.P. Whittle and J. Stringer. "Mechanism of Na_2SO_4-induced Accelerated Oxidation". *Corrosion Science*. Vol. 5. 1975. pp: 721-739.

[26] J. Stringer. V. Nagarajan and D.P. Whittle. " The Role of Chloride in the Hot corrosion of Cobalt-Base Alloys". in *High Temperature Metal Halide Chemistry*. (eds) D.L. Hilderbrand and C.D. Cubicciotti. Vol. 78-1. The Electrochemical Society. Princeton. 1978. pp: 617.

[27] D.W. Meckee. D.A. Shores and K.L. Luthra. *Journal of The Electrochemical Society*. Vol. 125. No. 3. 1978. pp: 411-419.

[28] R.H. Barkalow and F.S. Pettit. " The Effect of NaCl on the Na_2SO_4-induced Hot Corrosion of Alloys". in *High Temperature Metal Halide*

Chemistry, (eds) D.L. Hilderbrand and C.D. Cubicciotti. Vol. 78-1. The Electrochemical Society, Princeton, 1978.

[29] J.F.G. Conde, E.Erdos and A. Rahmel. "Mechanisms of Hot corrosion in Marine Gas turbines". *High Temperature Alloys for Gas turbines*, R. Brunetaud, D. Coutsouradis, J.B. Gibbons, Y. Lindlom, D.B. Meadowcroff and R. Sticler (eds), 1982 pp: 99-148.

[30] S. Kameshwari. "The Role of *NaCl* in the Hot corrosion Behaviour of Nimonic Alloy 90". *Oxidation of Metals*, Vol. 26, No's 1/2, 1986, pp: 39.

[31] P. Hancock, " Vanadic and Chloride attack of Superalloys", *Journal of Material science and Technology*, Vol. 3, July 1987, pp: 543.

[32] J.R. Nicholis and D.J. Stephenson, "A life prediction Model for Coatings Based on the Statistical Analysis of Hot salt corrosion Performance" *Corrosion Science*, Vol. 33, No. 8, 1992, pp: 1314.

[33] F. Umland, H.P. Voigt and F. Fechner, *Werkstoffe and Korrosion* , Vol. 21, 1970, pp: 254.

[34] A.J.B Cutler and C.J. Grant, "Electrochemical Measurement of Corrosion rates for Gas turbine Alloys", in *Deposition and Corrosion of Gas turbines*, (eds) A.B. Hart and A.J.B. Cutler, Applied Science Publishers, London, 1973, pp: 191.

[35] K.L. Luthra. "Low Temperature Hot corrosion of Cobalt-Base Alloys : Part II - Reaction Mechanism". *Metallurgical Transaction*. Vol. 13A. Oct 1982. pp: 1853-1864.

[36] K.L. Luthra. "Kinetics of the Low Temperature Hot corrosion of $Co-Cr-Al$ Alloys". *Journal of The Elecchemical Society*. Vol. 132. No. 6. 1985. pp:1298.

[37] K.L. Luthra and O.H. Leblanc. "Low Temperature Hot corrosion of $Co-Cr-Al$ Alloys". *Material Science Engineering*. Vol. 87. 1987. pp: 332.

[38] Ajay. K. Misra. *Engineering Materials*. Vol. 4. 1988. pp: 20-28.

[39] M. Levy. R.Huie and F.S. Pettit. "Oxidation and Hot corrosion of some Advanced Superalloys at $704°C$ to $1093°C$". *Corrosion*. Vol. 45. No. 8. 1989. pp: 673.

[40] V. Buscaglia. P. Nanni and C. Bottonio. "The Mechanism of Sodium sulphate-Induced Low Temperature Hot corrosion of Pure Iron". *Oxidation of Metals*. Vol. 24. 1992. pp:

[41] L.Q. Shi. Y.S. Zhang and S.T. Shih, *Oxidation of Metals*. Vol. 38. 1992, pp: 385.

[42] L.Q. Shi. Y.S. Zhang and S.T. Shih. "The Effect of K_2SO_4 Additive in Na_2SO_4 Deposit on Low Temperature Hot corrosion of Iron-Aluminium Alloys". *Corrosion Science*. Vol. 33. 1992. pp: 1427.

[43] M. Misbahl Amin. "Oxidation behaviour of AISI-304 steel in the presence of Na_2SO_4 and $Fe_2(SO_4)_3$ at 700°C". *Thin Solid Films*. Vol. 237. 1992. pp: 172-174.

[44] J.F.G. Conde. *in Proceedings of the 1974 Gas turbine Materials in the Marine Environment Conference*. (eds) J.W. Fairbanks and I. Machlin. M.C.I.C. Report 75-27. Castine. 1974, pp: 73.

[45] D.W. Meckee. D.A. Shores and K.L. Luthra. "Effect of SO_2 and $NaCl$ on High Temperature Hot corrosion ". *Journal of The Elecchemical Society*. Vol. 125. No. 3. 1978. pp: 411-419.

[46] S. Kameshwari. "Hot corrosion Behaviour of Nimonic-105 in $NaCl$ and Na_2SO_4". *Werkstoffe and Korrosion*. Vol. 40. 1989. pp: 213-218.

[47] P. Sivakumar. "On the Electrochemical nature of Hot corrosion attack in $Ni - Cr$ alloys". *Oxidation of Metals*. Vol. 24, No's 5/6, 1985.

[48] Surayanarayanan. K.J.L. Iyer and M. Radhakrishnan, "Interaction of Low Temperature Hot corrosion and Creep", *Journal of Material science and Engineering*. Vol. A 112. 1989. pp: 109.

[49] J. Stringer. *Journal of Material Science Technology*. Vol. 3, 1987. pp: 482-485.

[50] J. Stringer. "Hot Corrosion of Gas Turbines". *MCIC report*. Metals and Ceramics Information Centre. Battelle. Columbus. 1972. pp: 1-49.

[51] J. Stringer. "Role of Sulfur in Hot Corrosion. *in Proceedings of the 1974 Gas turbine Materials in the Marine Environment Conference* (eds) J.W. Fairbanks and I. Machlin. M.C.I.C. Report 75-27. Castine. 1974. pp: 167.

[52] J.F.G. Conde. G.C. Booth. A.F. Taylor. "Protection against Hot corrosion in Marine Gas turbines". *Journal of Material Science Technology.* Vol. 2. March 1986. pp: 317.

[53] J.A. Goebel. F.S. Pettit and G.W. Goward. "Hot corrosion Mechanisms in Stationary Gas Turbines". *Deposition and Corrosion in Gas turbines.* (eds) A.B. Hart and A.J.B. Cutler. Applied science publishers. London. 6-7 Dec 1972. pp: 102.

[54] W.C. Fang and R.A. Rapp. "Electrochemical Reactions in a pure Na_2SO_4 Melt". *Journal of The Electrochemical Society,* Dec 1983. pp: 2340.

[55] V. Nagarajan. J. Stringer and D.P. Whittle, "The Hot Corrosion of Cobalt-base alloys in a Modified Dean's Rig - I. Co-Cr. Co-Cr-Ta and Co-Cr-Ti alloys". *Corrosion Science.* Vol. 22, No. 5. 1982. pp: 425.

[56] J. Stringer and D.P. Whittle. "Hot corrosion of Nickel-Base super alloys: The effect of Molten Salt Chemistry". *Metal-slag-gas reactions and processes.* (eds) Z.A. Foroulis and W.W. Smeltzer. The Electrochemical Society. Princeton. 1975. pp: 666.

[57] S.R.J. Saunders. M.K. Hossain and J.M. Ferguson. "Comparison of Hot-

salt Corrosion Test procedures". in *High Temperature Alloys for Gas turbines*. R. Brunetaud. D. Coutsouradis. J.B. Gibbons. Y. Lindlom. D.B. Meadowcroff and R. Sticler (eds). 1982. pp: 184.

[58] L.Q. Shi. "Accelarated oxidation of Iron-induced by Na_2SO_4-deposits in Oxygen at 750°C - A-New-Type Low-Temperature Hot corrosion". *Oxidation of Metals*. Vol. 40. No's 1/2. 1993. pp: 210.

Vita

- S.P. Akbar Hussain
- Born in India.
- Permanent Address :

  H.No. 22/77, Gandhi Road, Proddatur 516360

  Cuddapah (Dt), A. P., INDIA, Ph +0091-8564-51162.
- Received Bachelor of Engineering (**B.E.**) degree in Mechanical Engineering from Osmania University, Hyderabad, India in July 1990.
- Worked in Larsen and Toubro LTD as Mechanical Engineer (Project) from Aug. 1990 to june. 1993
- Joined Mechanical Engineering Dept, King Fahd University of Petroleum and Minerals in october, 1993.